isvr Institute of Sound and Vibration Research

A Strategy for the Development and Standardisation of Measurement Methods for High Power/Cavitating Ultrasonic Fields: Review of Cavitation Monitoring Techniques

T.G. Leighton

ISVR Technical Report No 263

January 1997

University of Southampton

SCIENTIFIC PUBLICATIONS BY THE ISVR

Technical Reports are published to promote timely dissemination of research results by ISVR personnel. This medium permits more detailed presentation than is usually acceptable for scientific journals. Responsibility for both the content and any opinions expressed rests entirely with the author(s).

Technical Memoranda are produced to enable the early or preliminary release of information by ISVR personnel where such release is deemed to the appropriate. Information contained in these memoranda may be incomplete, or form part of a continuing programme; this should be borne in mind when using or quoting from these documents.

Contract Reports are produced to record the results of scientific work carried out for sponsors, under contract. The ISVR treats these reports as confidential to sponsors and does not make them available for general circulation. Individual sponsors may, however, authorize subsequent release of the material.

UNIVERSITY OF SOUTHAMPTON

INSTITUTE OF SOUND AND VIBRATION RESEARCH

FLUID DYNAMICS AND ACOUSTICS GROUP

A strategy for the development and standardisation of measurement methods for high power/cavitating ultrasonic fields: Review of Cavitation Monitoring Techniques

by

T G Leighton

ISVR Technical Report No. 263

January 1997

Approved: Group Chairman, P.A. Nelson
Professor of Acoustics

CONTENTS

Page No.

LIST OF FIGURES

Page No.

ABSTRACT

This report was written in a 28-day subcontract to the National Physical Laboratory, as part of their contract to the National Measurement System Policy Unit to write a *Report to Review Progress, Identify Measurement Methods and Address Implementation for Remote and Local Sensing Methods for the Measurement of High Power/Cavitating Ultrasonic Fields.* It is divided into four sections, as follows:

1. INTRODUCTION TO CAVITATION

2. TECHNIQUES FOR THE DETECTION OF STABLE BUBBLES

3. TECHNIQUES FOR THE DETECTION OF INERTIAL CAVITATION

4. DISCUSSION OF THE POSSIBILITY OF A STANDARD FOR CAVITATION

Section 1 outlines the basics of cavitation in order to give the reader an appreciation of the various features which can be important when ultrasound generates cavitation typical of that seen in many applications. Section 2 describes techniques for the detection of non-inertial cavitation and, more generally, stable bubbles.

The third section follows on from the second, and discusses in turn methods for characterising inertial cavitation. Though, with rare exceptions, individual inertial collapses are transient events, the signals characteristic of inertial cavitation which are emitted by the cloud as a whole depend on the cloud dynamics. Therefore in response to microsecond pulses of ultrasound, the signals used to detect cavitation will give a transient response (though of course a longer-lasting effect will be observed from any signals, as discussed in Section 2, capable of responding to the presence of the bubble fragments which remains after the inertial event is over). Continuous-wave insonation at the threshold for inertial cavitation can also generate transient signals in this way, depending on the nucleation. However continuous-wave insonation in well-nucleated super-threshold conditions will generate a sustained bubble clouds, and the signals characteristic of inertial cavitation may be time-averaged to give an overall impression of the cloud behaviour. Such types of cavitation, and the signals appropriate for their study, are discussed in the third section.

The fourth and final section tackles the difficult issue of whether it would be possible to define a standard for cavitation, and if so, whether sensors appropriate to use in ultrasonic systems 'in the workplace' could be calibrated against that standard. The difficulties in defining an absolute measure of cavitation, based on fundamentals, are addressed. The option of setting up a repeatable cavitation system against which calibration can be made are discussed. The options amongst the available sensors for assessing the 'standard cavitation system', if one could be produced, and for use 'in the workplace', are outlined.

Report To Review Progress, Identify Measurement Methods And Address Implementation For Remote And Local Sensing Methods For The Measurement Of Cavitating Ultrasonic Fields

1. INTRODUCTION TO CAVITATION

This report has been written for DTI National Measurement System Policy Unit as part of a study to "Review Progress, Identify Measurement Methods and Address Implementation for Remote and Local Sensing Methods for the Measurement of High Power/Cavitating Ultrasonic Fields". The report discusses cavitating fields, with the Section 1 introducing basic features of cavitation. Sections 2 and 3 outline techniques for the detection of stable bubbles and inertial cavitation respectively. Section 4 discusses whether a standard for cavitation is feasible.

1.1. Introduction: The Characterisation Of Cavitation

Acoustic cavitation has in the past been defined in various ways. It is perhaps most useful when defining the term for a given report to consider the applications for which the article is intended. The prime purpose of this report is the discussion of the cavitation which might be expected to occur in high power ultrasonic fields. Therefore it is useful to consider cavitation to be the 'activation' of a gas inclusion in a liquid by an acoustic field. In this way, such phenomena as the emission of sound from a gas bubble upon injection into a liquid can be excluded: the inclusion of such 'passive cavitation', though undoubtedly of interest in a range of applications including oceanic bubble clouds and industrial injectors, would unnecessarily lengthen and complicate a discussion of ultrasonic fields.

What remains are those phenomena which arise as a result of the pulsations or surface perturbations of the gas/liquid interface of the gas inclusion. Acoustic cavitation may be detected through the effects it generates [1.1§5]. To what extent the cavitation might subsequently be characterised via these effects is variable. Optical light scattering is perhaps the most readily interpreted to characterise some forms of cavitation, where the bubble is relatively stable. However it is inapplicable in many circumstances (e.g. optical opacity) [1.2]. Chemical, biological and erosive effects are readily observed, but characterisation of the cavitation from them is rarely either simple or real-time [1.3].

Theoretical descriptions of cavitation have been available since the start of the century. It was the presence of erosive pits in propellers which inspired Lord Rayleigh [1.4] to develop in 1917 his pioneering analysis for the collapse of an empty spherical cavity under a static pressure. Coupling this energetic collapse phase with the explosive growth phase of a sufficiently small bubble (as expounded by Blake [1.5]), Noltingk and Neppiras [1.6, 1.7] characterised a particular type of cavitation whereby appropriately small bubbles in sufficiently strong sound fields undergo growth to many times their original size and then a subsequent rapid collapse. It has since been verified that such events concentrate the acoustic energy, generating high gas temperatures [1.6, 1.7], liquid [1.4] and gas [1.8] shocks, and free radicals [1.9]. The latter may be involved in sonochemical reactions [1.9], and may generate sonoluminescence [1.1§5.2]. Flynn [1.10] distinguished the so-called "transient" cavitation (currently termed "inertial" cavitation) with which such manifestations are associated, from the less energetic "stable" cavitation, where the bubble pulsates about an equilibrium radius over many acoustic cycles.

Perhaps not surprisingly, therefore, this field which grew from the observation of erosive damage in propellers developed into a problem coupling fluid dynamics with acoustics, and indeed acoustic techniques feature amongst the most common ways in which cavitation is initiated and measured [1.11].

Though the distinction between *transient* and *stable* (or *inertial* and *non-inertial*) cavitation is inexact, many formulations have concentrated mainly on attempting to distinguish the threshold values of acoustic frequency, pressure amplitude, and initial bubble radius corresponding to the transition between the types of cavitation [1.1§4.3.1, 1.12-1.15]. However once the threshold has been exceeded, the extent to which cavitational effects are generated (the "activity" of the cavitating field) is a key parameter (see Section 1.4).

With rare exceptions [1.16]' whilst theory has tended to concentrate on the dynamics of single bubbles, in practice when cavitation causes sonochemical, biological, and erosive changes, it is generally *populations* of bubbles that are involved [1.3]. Whilst the exploitation of cavitation in many common applications (such as cell killing, ultrasonic cleaning, cavitation erosion and sonochemistry) relies upon inertial cavitation (through sonochemistry, gas and liquid shocks, and bubble jetting) [1.11], the application of these effects depends upon the characteristics of the bubble *population* and its interaction with the sound field. These two key factors may be influenced by stable cavitation, via nucleation and the relatively low-energy phenomena of bubble migration, dissolution and exsolution [1.3].

An experimental characterisation of cavitation which is to be of use to common applications must therefore account for the following problems:

- Whilst most applications involve bubble populations, the models and theories overwhelmingly rely upon single-bubble descriptors;
- These descriptors are themselves inexact;
- To *predict* the high-energy cavitation events, one must also characterise the low-energy stable bubbles which serve as nucleation site and which may modify the sound field.

1.2. Types of Cavitation

Conceptualisations of bubble dynamics begin with models of isolated spherical bubbles. These models in turn become modified to allow the incorporation of experimentally-observed phenomena. In this way have arisen the well-known classifications of transient and stable cavitation (a terminology which is currently being replaced by inertial and non-inertial cavitation) [1.1§4.2-4.3; 1.3]. An impression of the range of bubble behaviours is shown in Figure 1.1. Neither of the phenomena shown in the first two rows (a static bubble, or slow growth) will give rise to acoustic emission. However pulsation will give rise to such emission, and as such can be detected acoustically at a distance. The spherical bubble is, to a first approximation, an oscillator with a single degree of freedom, with a resonance determined by the ratio of the stiffness (determined by the compressibility of the gas content within the bubble) to the inertia (based principally in the surrounding liquid, which must move if the bubble wall does) [1.1§3.2]. The resonance frequency of the bubble is inversely proportional to its radius [1.17].

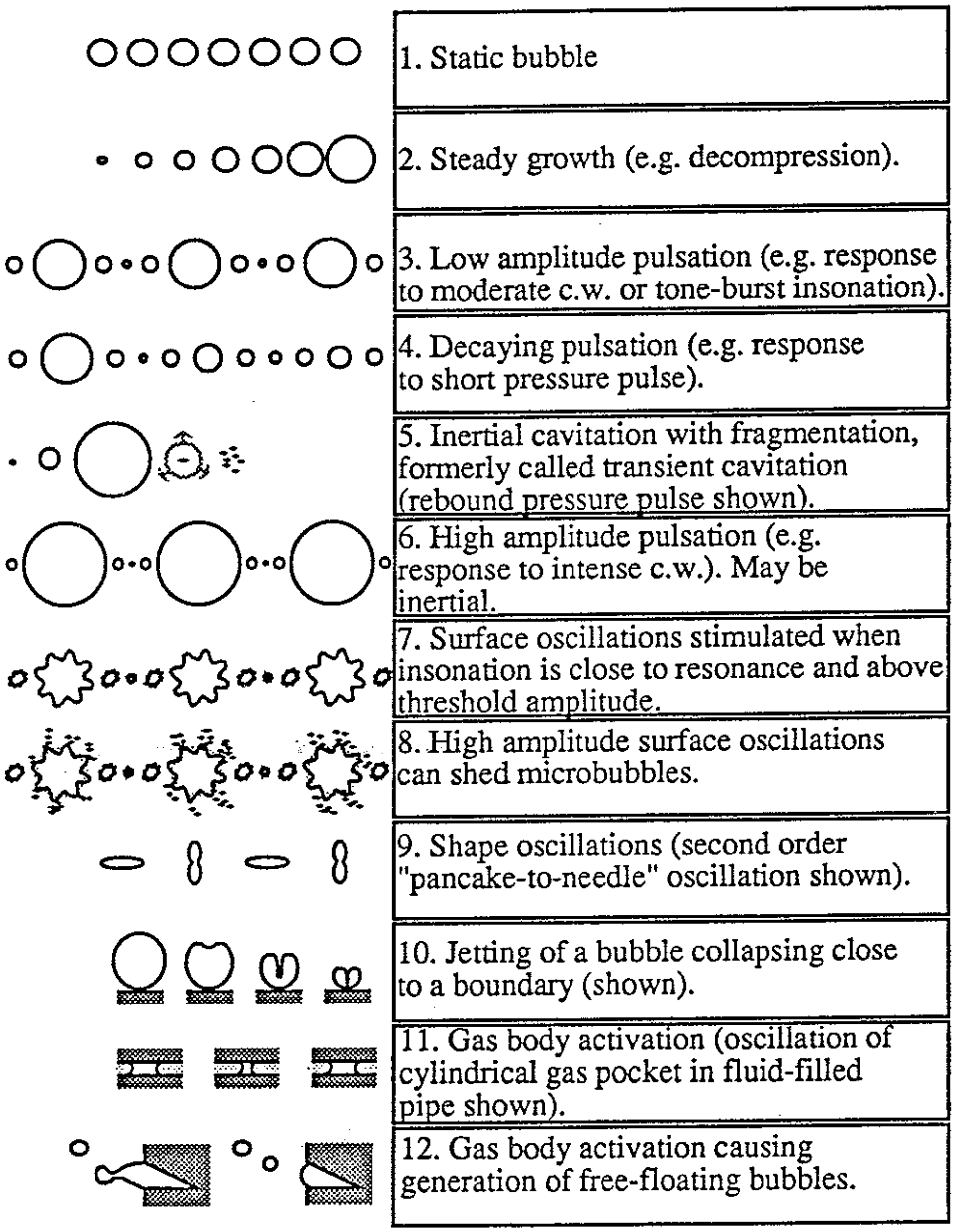

Figure 1.1. A schematic illustration of a range of bubble behaviour. Rows 3 to 11 are effects through which the bubble can be expected to be acoustically active. The expansion ratios drawn for these bubbles are exaggerated to more clearly illustrate the pulsations.

As such an oscillator, the bubble can be driven into pulsation by an incident sound field. If it is driven such that the amplitude of oscillation of the bubble wall is low (for example, the incident sound field has a low acoustic pressure amplitude, or the bubble has a size which differs greatly from that required for resonance with the driving frequency†), then the bubble will scatter the sound field. If an ultrasonic beam is incident on the bubble, acoustic energy will be converted to heat through viscous and thermal damping mechanisms associated with the bubble motion [1.18, 1.19], and scattered out of the beam (to first order as a spherical re-radiation) by the bubble. Row 3 of Figure 1.1 shows just such an oscillation. Despite damping, the illustrated bubble pulsations are shown not to decrease in amplitude, suggesting a continuous-wave or tone-burst insonation, rather than a short pulse (which is the case illustrated in Row 4). If pulsations of this type are of sufficient amplitude, cavitation of this type can strongly influence the effects of power ultrasound. First, such bubbles can directly generate physical and biological effects. These are usually associated with acoustic radiation forces, and one example is the aggregation of platelets in blood [1.20]. However cell disruption may also be brought about, as bubbles may travel rapidly through the liquid under the influence of acoustic radiation forces, and generate stresses which can, for example, produce hemolysis [1.21]. Second, such bubbles can strongly influence both the population of nuclei available to seed inertial cavitation, and the acoustic pressure amplitudes to which those nuclei are subjected (see section 3.1) [1.3].

It is well-known that when ultrasound of sufficient intensity passes through a liquid containing bubbles which have, initially, the appropriate small size, such gas inclusions may nucleate inertial cavitation [1.15; 1.22-1.24]. This is typified by the sudden expansion and then rapid collapse of the bubble (Row 5 of Figure 1.1). During the rapid collapse, the gas within the bubble is compressed. It may be heated to high temperatures [1.9, 1.24, 1.25] and gas shocks may propagate [1.1§5.2.1, 1.26]. Electrical discharge and other effects may be associated with this phenomenon [1.27, 1.28]. Mechanisms for the generation of sonoluminescence based on all these, and yet more [1.29, 1.30], processes have been proposed. Certainly the production of free radicals and electronically excited species has been associated with the extreme conditions which occur within the bubble. These can cause chemical and biological effects.

Immediately after the collapse, the bubble rebounds, emitting a pressure pulse* into the liquid [1.1§5.4; 1.4, 1.6, 1.7, 1.31, 1.32]. This may cause mechanical damage (and indeed clouds of bubbles may collapse co-operatively, enhancing this effect [1.33]). The bubble may then fragment or repeat the growth/collapse cycle a number of times. It was initially thought that in the type of bubble activity which gave rise to such phenomena as sonoluminescence, the bubble would fragment after one (as shown in Figure 1.1, Row 5) or a few cycles, and as such this type of behaviour was termed 'transient' cavitation. To contrast, less energetic bubble oscillations were termed 'stable' cavitation. Following the discovery that in specialised conditions the bubble can pulsate for thousands of cycles (in a manner similar to Row 6 of Figure 1.1), emitting as sonoluminescent flash at each collapse [1.16, 1.34], this terminology clearly needed replacing. Since models of the bubble collapse had shown that, to achieve the energy concentration expected to generate

---

† Bearing in mind that we are at present considering only models of bubbles which remain spherical at all times.

* This is shown figuratively in Figure 1.1 Row 5 by arrows.

what had been known as 'inertial cavitation' the inertial of the liquid had to play a dominant role during the collapse, the terms 'inertial' and 'non-inertial' replaced 'transient' and 'stable'.

The generic oscillation shown in Row 6 of Figure 1.1 is a high-amplitude pulsation of a spherical bubble (Figure 1.2). Depending on the amplitude, such oscillation may be inertial (as described above for specialised conditions) or non-inertial, but of high amplitude. If non-inertial, for example, it is what one would expect the activity in Row 3 would become in a higher-amplitude sound field. An increased amplitude of wall oscillation might be expected if the bubble, of course, is closer to resonance size than that shown in Row 3. However in bubbles driven close to resonance, other effects occur. Most notable of these are surface waves, which visually cause an attractive 'shimmer' to appear on the surface of the bubble (Figure 1.1 Row 7; Figure 1.3b) [1.22, 1.35]. However such surface waves can be associated with an erratic 'dancing' translational motion [1.36], and at high amplitude microbubbles might break off from the tips of the surface waves (Figure 1.1 Row 8; Figure 1.3c) [1.3].

Other departures from spherical symmetry include shape oscillations, (Figure 1.1 Row 9), found particularly in larger bubbles, where the restraining effect of surface tension (which tends to promote sphericity) is weaker [1.1§3.3; 1.37; 1.38]. If extreme, such shape oscillations can break a bubble up, usually generating a small number of fragments of roughly-similar size (in contrast to the process shown in Figure 1.1 Row 8) [1.3, 1.39]. Shape oscillations are encouraged by anisotropies, such as are caused by the presence of other bubbles, particles or walls, which occur in the environment. If such are present during bubble growth, then during the subsequent collapse the bubble may involute, one wall passing through the bubble to form a high-speed liquid jet (Figure 1.1 Row 10) [1.40-1.42]. This, like the pressure pulse emitted on rebound (Figure 1.1 Row 5), can cause mechanical damage. The bubble will fragment [1.12].

As can be seen, the model of an isolated spherical bubble in a infinite fluid is proving inadequate to describe the range of behaviours seen: Departures from spherical symmetry in both the bubble wall and the environment must be incorporated. One such environmental feature which has proved to be important is the presence of solid bodies which surround the gas pocket to a greater or lesser extent. Whilst the jetting feature, described above, is usually thought of as a modification of the spherical bubble model, a new class of gas inclusion has been introduced in recent years, the *stabilised gas body*. These are pockets of gas partially bounded by liquid, and partially by solid structures, which can stabilise them against dissolution. They might comprise, for example, approximately cylindrical pockets of gas contained within tubular vessels, such as found in biological structures (plants [1.43], insect tracheae [1.44], and, speculatively, mammalian blood vessels and ear canals [1.45]) (Figure 1.1 Row 11). If rigid (which is not always the case), the curved solid/gas walls would not move, whereas the gas/liquid interfaces which comprise the end-walls of the cylinder might oscillate in a piston-like or a membrane-like manner [1.46-1.48]. Oscillations of such gas pockets may cause the nucleation of free -floating bubbles into the liquid (Figure 1.1 Row 12; Section 1.3.2).

When considering cavitation in high power ultrasonic fields it is not sufficient to assess only the likelihood of inertial cavitation. Although in most circumstances it will be the inertial cavitation which brings about the effects (chemical, erosive etc.) of concern, inertial cavitation rarely occurs without accompanying non-inertial cavitation, which may affect it to a very great extent [1.3]. In addition, if one is to predict the likelihood of inertial cavitation prior to the application of an ultrasonic field (particularly in the MHz range), one must first characterise the population of nuclei present. If this is to be done acoustically, as many techniques promise, then non-inertial cavitation must occur.

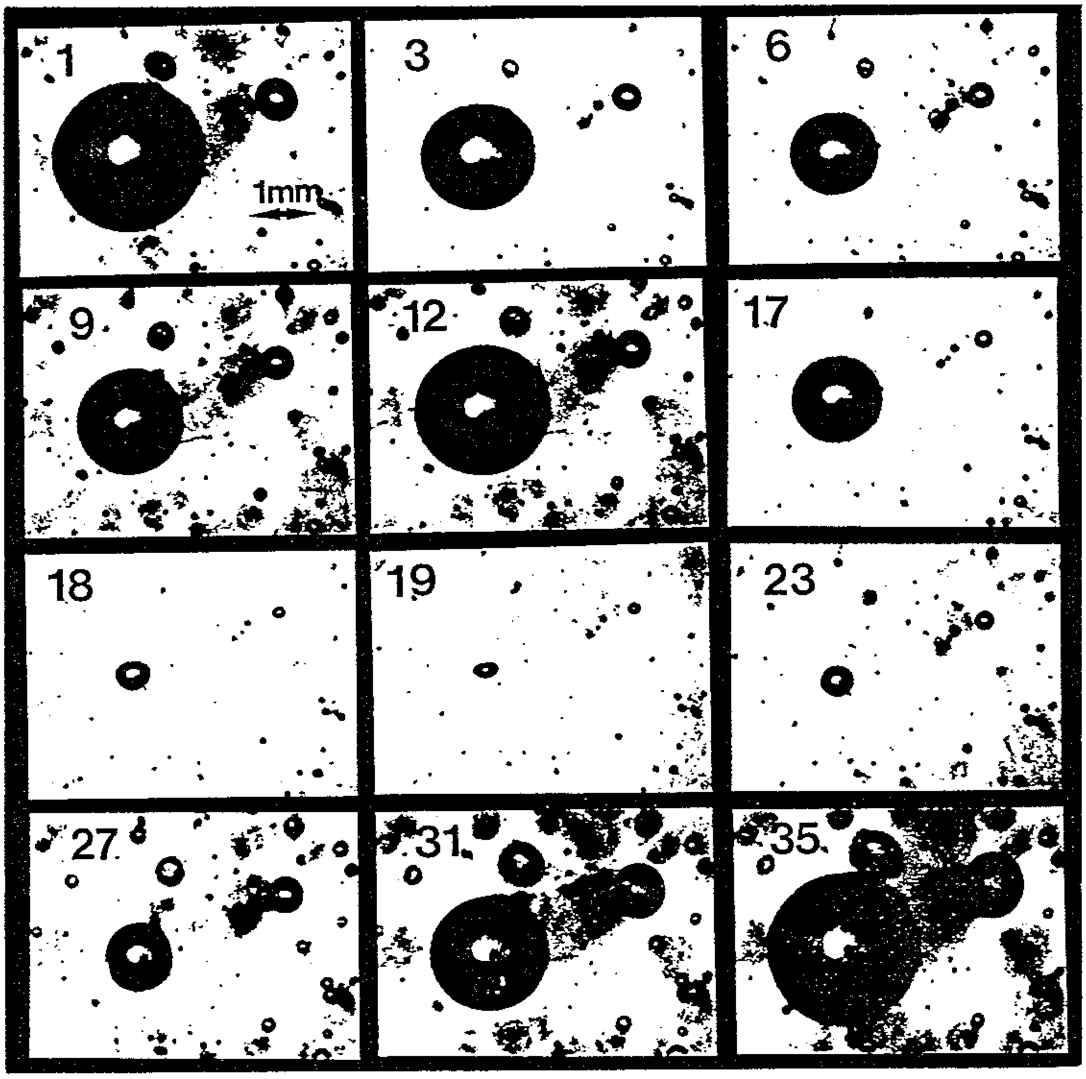

Figure 1.2. The oscillations of air bubbles in glycerol. The bubbles are driven by an inertially-generated 100 Hz pressure field, of amplitude 3900 Pa, with 600 Pa static pressure. A selection of frames is shown from a sequence of 35 consecutive frames, filmed at 2000 frames per second. They illustrate the periodic unit in the motion of the largest bubble. The bubble contracts from maximum size in frame 1 to a minimum in frame 6, before expanding again to a second maximum (frame 12), then collapsing to a second minimum (frame 19), and finally expanding to reach in frame 35 the same size as it had in frame 1. The second collapse is far more rapid than the first. After Leighton et al. [1.75]. Reprinted by permission from the European Journal of Physics, vol. 11, pp. 352-358; Copyright © 1990 IOP Publishing Ltd.

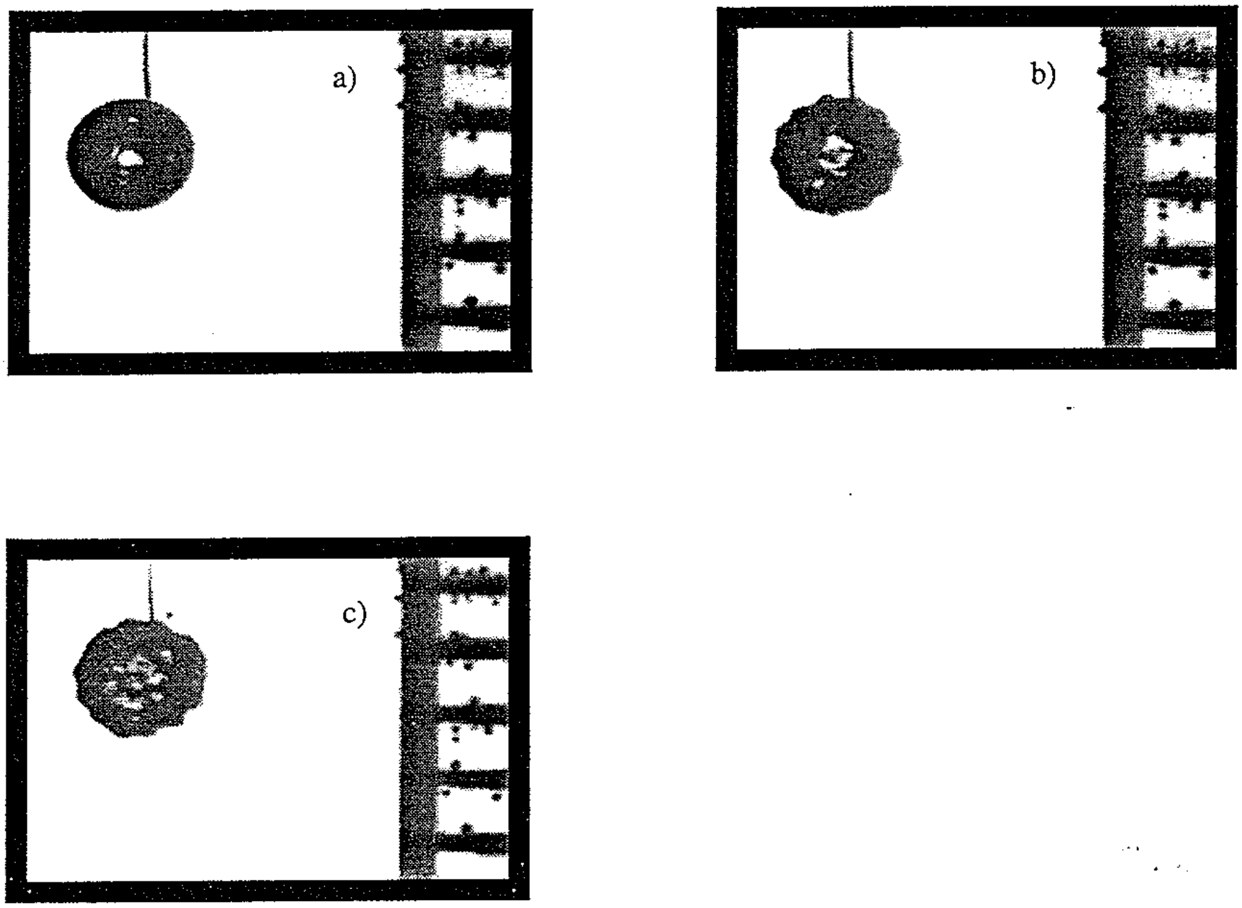

Figure 1.3 Video frames at 30 f.p.s. of *a tethered bubble driven at 4.4 kHz at resonance (a) below the amplitude threshold necessary to generate surface waves; (b) above the threshold, showing surface waves around the bubble wall; and c) showing the generation of a small bubble pinched off as a result of surface wave activity. To the right in the pictures is a mm scale (Photograph: A D Phelps, T G Leighton).*

1.3. The thresholds between inertial and non-inertial cavitation, and the importance of stable gas bodies

Inertial cavitation is a threshold phenomenon, and whether or not it occurs depends critically on a number of parameters. The acoustic frequency is one, and this can be readily controlled. The acoustic pressure amplitude of the sound field *at the bubble* is another critical threshold parameter. Whilst the operator can readily control the acoustic field emitted by the ultrasonic transducer, it is not so simple to control the field amplitude at any individual bubble. The third key parameter, the initial bubble size, is often the least controlled.

1.3.1 The effect of bubble activity on the acoustic pressure amplitude at the bubble

Even in a bubble-free container, standing waves and acoustic modal patterns can be set up, the acoustic pressure field having maximum amplitude at the pressure antinodes. However bubbles change the acoustic properties of a liquid. Individually they can increase the absorption of ultrasound through its conversion into heat (section 1.2). Collectively, the properties of bubbly liquids (density, compressibility, sound speed etc.) differ from those of bubble-free liquid [1.1§4.1.2e], so that an ultrasound beam can be reflected from a bubble cloud, which can effectively shield the medium beyond it [1.49]. Such clouds may occur because, though distributed throughout the body of a liquid sample when the ultrasonic power is low, when it is high intense cavitation may be confined to a region close to the transducer faceplate. There they may act as acoustic shields, which explains the phenomenon sometime observed, where an increase in power to a continuous-wave transducer can result in a decrease in yield [1.3, 1.24]. Bubbles may also collect in a standing-wave field, those smaller than resonance size being attracted to pressure antinodes (where, in Figure 1.4, they sonoluminesce), and those larger than resonance size aggregating at the pressure nodes (where they may form shields [1.50]). Changing the frequency of the ultrasonic field will clearly alter such spatial restriction and, for example, cause more uniform treatment by cavitation of a sample [1.3, 1.51]. If, however, small bubbles accumulate on the axis of an ultrasonic beam, they may reduce the sound speed there, and cause self-focusing: Wavefronts in the beam are slowed in regions close to the axis, causing them to curve inwards and generate a focus‡ (Figure 1.5) [1.3]. In summary, effects such as self-focusing [1.52], acoustic self-transparency [1.53], standing waves and multiple reflections, and the presence of other bubbles (including both those which undergo inertial cavitation and those which do not), can strongly affect the field amplitude at any bubble in question, and so determine whether or not it undergoes inertial

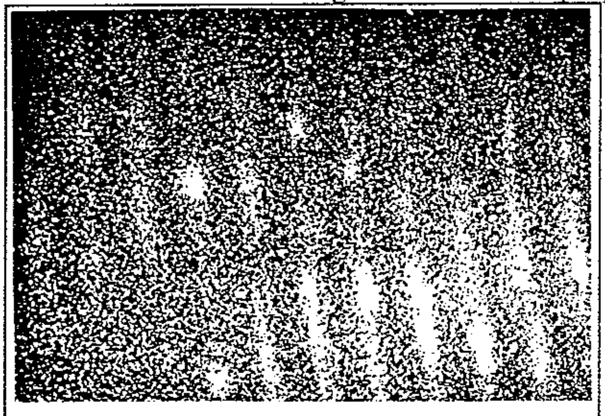

Figure 1.4. Bands of sonoluminescence generated by bubbles aggregating at the pressure antinodes in a standing wave field generated in water from a 1 MHz physiotherapeutic transducer generating a spatial-average acoustic intensity of 3 W/cm^2 (Image-intensified photograph: T G Leighton, M J W Pickworth)

‡ Both thermal self-focusing and self-defocusing can occur in liquids, and can arise through mechanisms other than bubble-mediated (e.g. thermal) [1.1§1.2.3c].

cavitation. It should be stressed that these examples simply illustrate the range of behaviour that can occur: How much each of these, or any other, effects occurs in a given cavitation field, if at all, is case-specific.

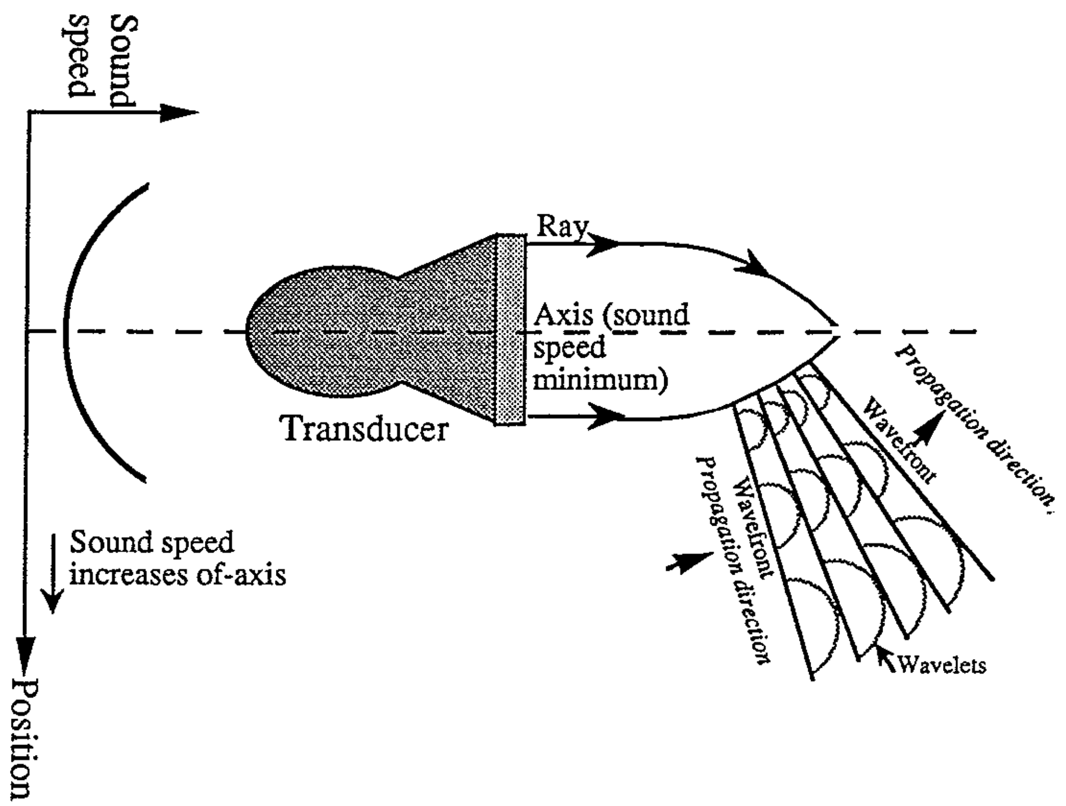

Figure 1.5. A schematic diagram using Huygens' principle to show how self-focusing can occur. The sound speed profile is shown on the left of the figure, illustrating that a minimum in the sound speed occurs on the transducer axis. As a result, successive wavefronts, as found from the envelope of the wavelets emitted from the preceding wavefront, are angled so that the rays tend to bend inwards towards the transducer axis (after Leighton, [1.03]).

1.3.2 The nucleation of inertial cavitation

The parameter which is often subject to least control is the initial size of the bubble present. If it is too small, then surface tension forces prevent the initial sudden growth, and inertial cavitation does not occur. If it is too large, then it may grow, but be too 'sluggish' to concentrate the energy sufficiently on collapse to generate free radicals etc. There is therefore a critical size range in which, for a given sound field, the initial size of the bubble must fall if it is to nucleate inertial cavitation [1.1§4.3.1; 1.10, 1.14, 1.54]. The lower the frequency, the wider this range.

This is clearly shown in Figure 1.6, where the threshold transition between inertial and non-inertial cavitation is plotted, based upon calculations by Apfel and Holland. They assumed that, in response to a single cycle of ultrasound, a bubble which is spherical at all times should grow and, upon subsequent adiabatic collapse, the gas within the bubble should attain a temperature of at least 5000 K if the collapse is to be "inertial" [1.15, 1.23]. Though there are clear approximations and the choice of such a criterion for defining inertial cavitation is not fundamental, this is nevertheless an extremely useful calculation, and illustrates that the acoustic pressure amplitude required to cause a bubble to undergo inertial cavitation is dependent upon the initial radius of that bubble. Since in most applications the frequency is the easiest of these three parameters to control, followed by the acoustic pressure amplitude *at the bubble*, with the radii of the nuclei present being the least accessible, then the graph can be interpreted in another manner. At a fixed frequency, say 10 MHz, an ultrasonic cycle with a peak negative pressure of 1.5 MPa (assumed to be constant throughout the field) will only generate inertial cavitation within a water liquid sample if, according to this model, it contains bubbles within radii between 0.03 and 0.77 μm. As the pressure amplitude decreases, so does the range of bubble sizes which can nucleate inertial cavitation. The very lowest peak negative pressure which could give rise to inertial cavitation, according to this model, is P_{opt} (around 0.84 MPa at 10 MHz): and at this pressure only bubble of a radius R_{opt} (0.2 μm at 10 MHz) could possibly nucleate inertial cavitation.

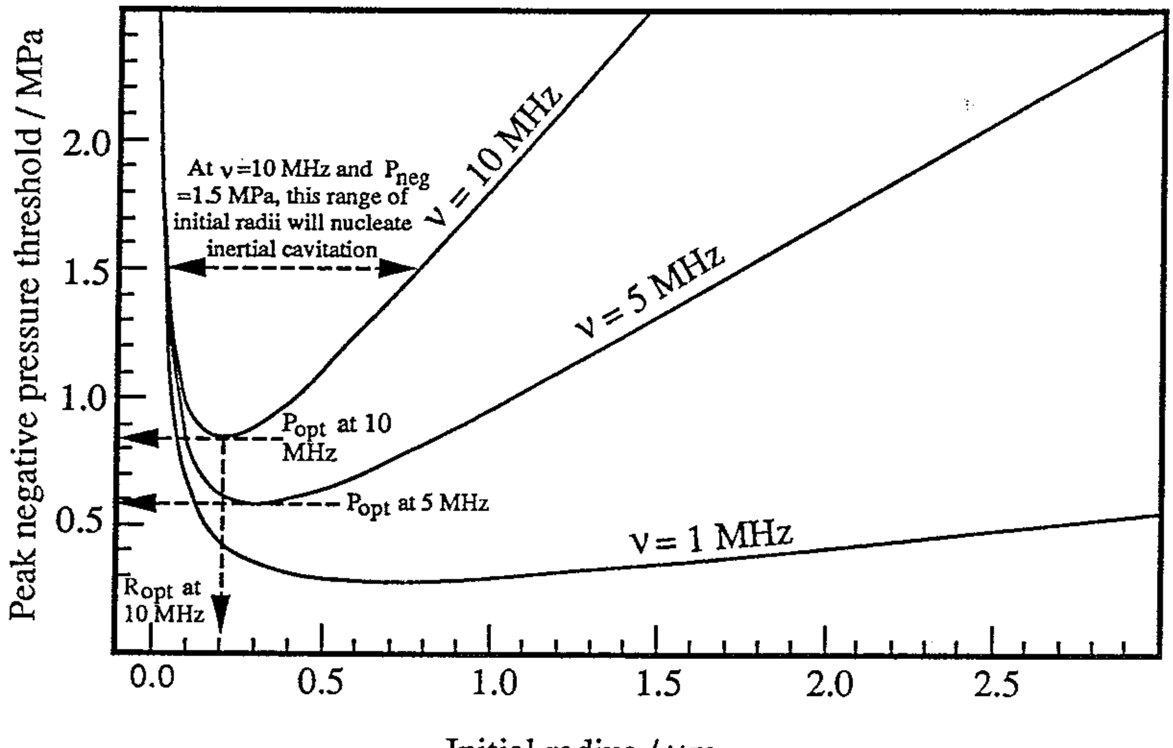

Figure 1.6 The threshold for inertial cavitation, as predicted by the theory of Apfel and Holland. For each frequency a line can be plotted: if the conditions of peak negative pressure and of the initial bubble radius are such that the point of interest on the graph lies below the line, non-inertial cavitation will occur. If the point of interest is above the line, inertial cavitation will occur (after Apfel and Holland [1.23]).

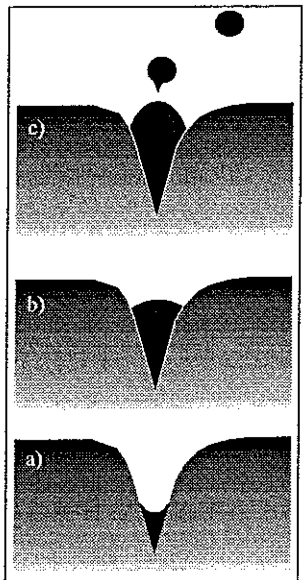

Figure 1.7. Schematic of a gas pocket (shown black) in a crevice.(a) Under atmospheric pressure the gas is stabilised against dissolution, its meniscus concave (as seen from the liquid) in contrast to the convex meniscus of a free-floating spherical bubble. (b) The volume of the gas pocket increases as the pressure in the liquid is reduced (for example, by the passage of the tensile component of an ultrasonic pressure pulse). (c) The pocket grows to such an extent that free-floating bubbles are generated within the liquid. This cycle can repeat because gas has exsolved out of solution and into the gas pocket.

The theory assumes nucleation of inertial cavitation within the first acoustic cycle, so-called "prompt cavitation", from a free-floating spherical bubble nucleus. In practice of course it is not a requirement that such nuclei be present before the start of insonation. They might be generated through bubble fragmentation (as shown in Figure 1.1 Row 8, and Figure 1.3c for example, from surface wave activity in bubbles close to resonance). Not only may bubbles initially too large to nucleate inertial cavitation enter the critical range (through, for example, dissolution, or fragmentation through a shape oscillation); Bubbles too small to nucleate cavitation may enter it through coalescence (which is promoted when radiation forces which cause bubble attraction), or through rectified diffusion [1.1§4.4.3]. Church outlines some of these possible scenarios, assessing their likelihood [1.55].

The model employed to produce Figure 1.6 is based upon the dynamics of isolated, spherical bubbles, which *de facto* must be free floating. Other possible nuclei can be found naturally as gas pockets, stabilised against dissolution in crevices and cracks (Figure 1.7) in the container wall or within free-floating particles within the liquid [1.1§2.1.2; 1.56-8]. If inertial cavitation is undesirable, then such particles can be removed by filtering (however even this will not completely remove all suitable nuclei for inertial cavitation: the passage of cosmic rays through the sample can generate them) [1.59]. High amplitude ultrasonic waves can activate such gas pockets so that they either expand out of their crevice (Figure 1.7; Figure 1.1 Row 12), or conceivably generate microbubbles through surface waves, to generate free-floating nuclei for cavitation. Such crevices are not the only mechanism through which a gas nucleus may be stabilised again dissolution: a hydrophobic 'skin' can collect on the bubble wall and cause free-floating nuclei to persist over long periods [1.60-1.64].

The theory of Apfel and Holland has given rise to a measure called the "Mechanical Index", which may be used to indicate the likelihood of exceeding the threshold required to nucleate cavitation.

1.3.3 The Mechanical Index

The model of Holland and Apfel investigates the threshold condition required to generate, within one acoustic cycle from the start of insonation, a collapse temperature of 5000 K. The threshold it predicts is relatively insensitive to the precise temperature criterion, and Holland and Apfel were able to compare their threshold predictions with those of Flynn and Church [1.13], who used a different definition* for the onset of inertial cavitation, equivalent to the bubble achieving a maximum temperature of 960 K.

Apfel and Holland [1.23] derive a *mechanical index*, which represents the likelihood that inertial cavitation will be nucleated, applicable (because of the assumption of 'prompt' cavitation) to microbubble growth in the limit of short-pulse, low duty cycle insonation. Clearly effects relating to longer insonation periods, such as the growth by rectified diffusion, are not covered. However the index can be used to gauge the probability of inertial cavitation resulting from diagnostic ultrasound fields.

As described for Figure 1.6, the model demonstrates that for a given acoustic frequency there is a minimum in the curve. If the whole range of bubble size classes are present, then there is a specific initial bubble size for which the threshold acoustic pressure required to nucleate inertial cavitation is a minimum. As the insonation frequency increases, the bubble radius which requires minimum pressure to nucleate inertial cavitation decreases, since inertial and viscous forces increase with increasing frequency, and there is insufficient time to bring about the required amount of bubble growth. For the same reason the acoustic pressure required to nucleate inertial cavitation in all but the smallest bubbles increases with increasing frequency. Surface tension dominates the response of the smallest bubbles.

If one is interested in a worst-case assessment of the likelihood that inertial cavitation will occur when a liquid is insonated, clearly one must assume that the bubble population contains bubbles at the radius corresponding to the minimum in the threshold curve. At a given frequency, it is bubbles of this radius, R_{opt}, which the analysis predicts will require the smallest peak negative pressure, P_{opt}, to undergo prompt inertial cavitation in response to a single acoustic cycle. Apfel and Holland [1.23] generate a plot of P_{opt} against frequency for water and whole blood, using pure fluid bulk property values for the σ, ρ and η relevant to the two fluids. The liquids are assumed to contain the relevant nuclei at size R_{opt}. Apfel and Holland employ a two parameter least-squares fit to these plots in order to obtain a relationship between P_{opt} and insonation frequency $\nu=\omega/2\pi$. They find that

$$\frac{(P_{opt})^{a_1}}{\nu} = a_2, \qquad (1)$$

where if P_{opt} is measured in MPa and ν in MHz, the constant a_1 takes values of 2.10 for water and 1.67 for blood, and a_2 has values 0.06 for water and 0.13 for blood. For a given sound field with a maximum negative pressure of P_{neg}, then by taking a value of $a_1 \approx 2$ to approximate the appropriate physiologically-relevant liquid, a mechanical index MI can be defined for the sound in that liquid:

$$MI = \frac{\left[\frac{P_{neg}}{MPa}\right]}{\left[\sqrt{\frac{\nu}{MHz}}\right]}, \qquad (2)$$

* based on the bubble achieving on expansion a maximum radius of at least twice its initial radius. A critical threshold for sonoluminescence of 1550 K has also been proposed [1.65-7].

The mechanical index I_{index} for prompt cavitation represents an approximate measure of the worst-case likelihood of nucleating inertial cavitation. As such it can be used to estimate the potential for nucleating inertial cavitation resulting from insonation by diagnostic ultrasound. Clearly it would be less appropriate to apply this index to tone-burst or continuous-wave insonations (during which a range of complicated processes, including rectified diffusion and enhancement of the cavitation by ultrasonic pulsing, can occur [1.1§5.3.1]). Holland and Apfel recommend that the pulse length should not exceed 10 cycles, nor the duty cycle 1:100. The peak negative pressure output from the device, as measured in water, must be derated to give the appropriate peak negative pressure that would be attained *in vivo* at the location of the maximum pulse intensity integral [1.68]. The centre frequency (which for accuracy is expected to be of the order MHz) is used for ν. Apfel and Holland [1.23] suggest that a mechanical index value below $\sqrt{0.5} \approx 0.7$ would indicate that, even in the presence of a broad size distribution of nuclei, the conditions are not sufficient to allow significant bubble expansion. If MI $\geq \sqrt{0.5}$, Apfel and Holland suggest that "the user should be advised of the potential for bubble activity". The AIUM, NEMA and FDA have adopted the mechanical index as a real-time output display to estimate the potential for cavitation *in vivo* during diagnostic ultrasound scanning [1.76].

Key points should be noted. First, the mechanical index gauges the likelihood of prompt cavitation, and nothing more: the effect of interest (e.g. a bioeffect) may be related to some other mechanism. Second, the model for the index is based on the assumption of a free-floating spherical nucleus of optimum size. In certain circumstances it may be that the nucleus is of a different type. Third, the current definition of the mechanical index does not account for the effects of nonlinear propagation, and hence might underestimate conditions *in situ* [1.69]. Fourth, when applied to diagnostic ultrasound instruments, the mechanical index describes conditions only at the focus, which is not necessarily the point of interest [1.69]. Fifth, the mechanical index has arisen from a theory which gives smooth curves of the form shown in Figure 1.6: such curves may in fact show peaks when other effects are incorporated [1.70].

Lastly, the underlying theory is applied to derive the mechanical index in a way intended to elucidate the conditions which attain the threshold for nucleating inertial cavitation. The amount by which the mechanical index is exceeded is therefore only a guide to the degree of cavitational activity, and by no means an exact predictor. Consider the MHz range illustrated in Figure 1.6, where the range of nuclei size which can seed inertial cavitation is relatively narrow. In such a sound field of fixed frequency and increasing acoustic pressure, as one exceeds the threshold in Figure 1.6, the range of nuclei which may nucleate inertial cavitation increases. In a field containing a broad range of bubble sizes, with a uniform number of bubbles in each size class, the total number of nucleated events would be expected to increase. However if there is only a narrow distribution of bubble sizes, exceeding the threshold by increasing amounts in this manner would, to first order, have little effect on the *number* of inertial events which are nucleated. What might be expected to increase is the energy associated with each collapse. Similarly as, say, the acoustic frequency changes, it is no simple matter to predict how the mechanical index might correlate with the 'degree' to which a given cavitational effect occurs.

1.4. Conclusions: The 'degree' of cavitation

Whether a particular type of cavitation is desirable or undesirable in a given circumstance, or whether or not it is amenable to control, if cavitation does occur then the question of degree becomes important.

Consider inertial cavitation. In the often complicated sound field the acoustic conditions (usually acoustic pressure and frequency) may be such that at any point within the sample there is no possibility of inertial cavitation occurring (within the limits of the Apfel-Holland model [1.15, 1.23] described in section 1.3.2) because the magnitude of the peak negative acoustic pressure is everywhere less than P_{opt}. If it is greater or equal to P_{opt}, then inertial cavitation will only occur if suitable nuclei (i.e. having radii within the appropriate range are present): if they are not initially present, they may be generated through the action of the sound (through fragmentation of larger bubbles, for example) for subsequent nucleation. Therefore knowledge of the sound field and the nuclei distribution can enable predictions of whether or not cavitation will occur, to within the accuracy of the model.

Such threshold predictions are based on whether a given bubble will undergo inertial cavitation. However what is more difficult to predict is the "amount of cavitation" that will occur if the threshold is exceeded, since this is clearly not amenable to models of single bubbles. This is partly because in referring to "the amount of cavitation" what is actually observed is the magnitude of some effect which is brought about through inertial cavitation. The relationship between the "amount of cavitation" and the ambient pressure illustrates this well.

Inertial cavitation, as described in section 1.3.2, involves two key phases: extensive initial growth, followed by a sudden, rapid collapse. Assuming that a bubble is to undergo inertial cavitation, increasing the static pressure will tend to affect a single bubble's inertial cavitation event in two ways [1.25]: First, it makes it more difficult for the bubble to expand; and second, it increases the compressive forces that drive the bubble to collapse. The first would tend to decrease, and the second to increase, the energetics of the cavitation undergone by a single bubble. Whether the magnitude of the resulting effect (erosion, sonoluminescence etc.) generated by the inertial cavitation of this bubble, and which interpreted in terms of the energetics of the cavitation, increases or decreases depends on which effect has the greater influence. However there is a second factor to consider. The preceding discussion has been limited to the effect on a single bubble, which is in practice rarely the issue. In addition to altering the energy of each individual collapse, changes in the ambient pressure will alter the range of bubble nuclei that may seed inertial cavitation, and so affect the total number of collapses. It does this, not only through physically changing the size distribution of all bubbles present in the liquid, but also by altering the forms of the curves shown in Figure 1.6: In general an increase in static pressure would make the minima in the curves sharper, reducing the range of bubbles in the population that can nucleate inertial cavitation, primarily through inhibiting the growth phase.

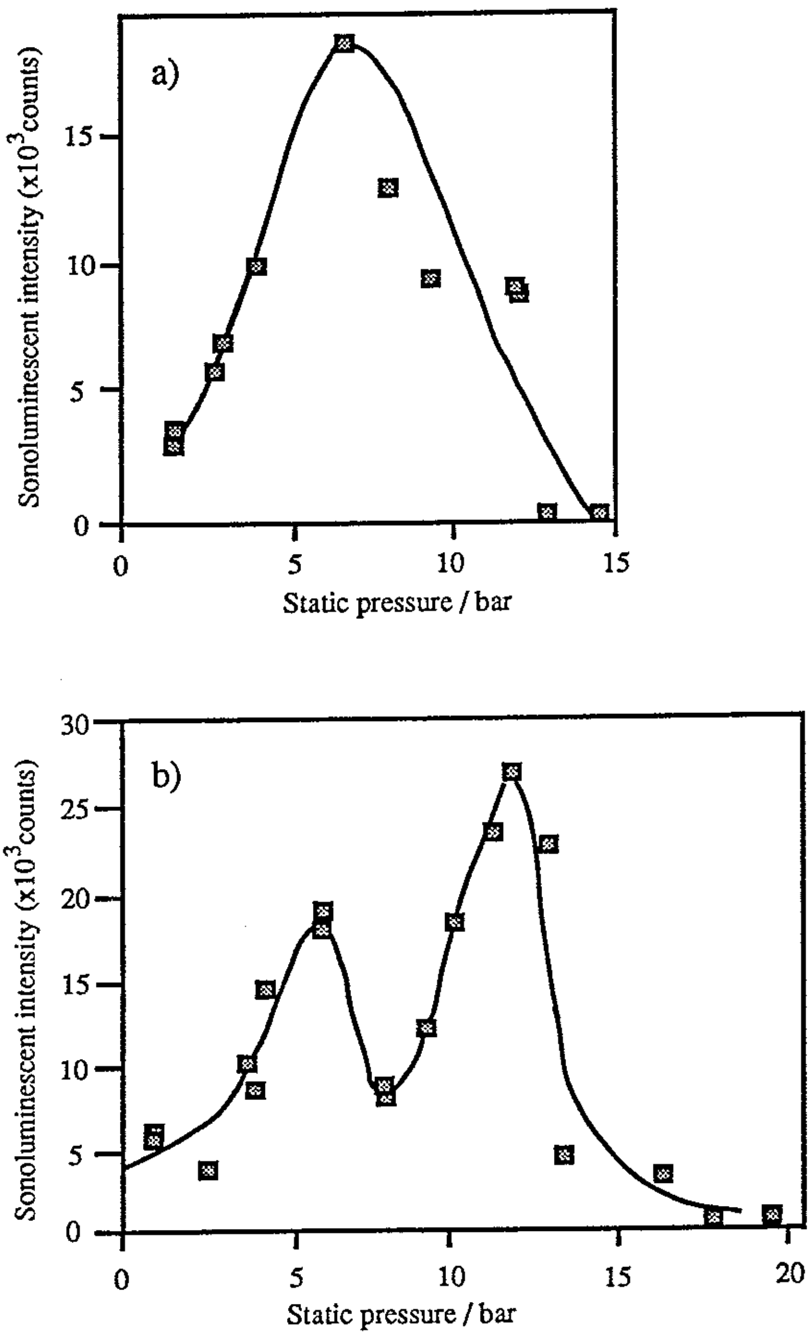

Figure 1.8 Variation of sonoluminescence with static pressure (hydraulically increased) at acoustic frequency of 20 kHz for (a) nitrogen-saturated water, and (b) a saturated solution of water in carbon tetrachloride, containing dissolved nitrogen (after Chendke and Fogler [1.71]).

Figure 1.8 shows the sonoluminescence measurements of Chendke and Fogler [1.71] at v=20 kHz for (a) nitrogen-saturated water, and (b) a saturated solution of water in carbon tetrachloride, containing dissolved nitrogen, for hydraulically-increased pressures. The general trend is that small increases in static pressure (up to 7 bar) increase the violence of each collapse, which offsets the reduction in their number: as the pressure is increased further, the latter effect dominates, until the cavitation is suppressed. It has, as an aside, long been known that by submariners that submerging the vessel will tend to reduce the noise emitted by flow-induced inertial at the propellers. However when the cavitation is strong and the vessel is at high speed, increasing the depth of the vessel will initially cause an increase in the cavitation noise, before suppression occurs [1.72]. This so-called "anomalous depth effect" is due to the fact that, before the increasing pressure suppresses the growth phase, it first increases the violence of each collapse.

In Figure 1.8 the static pressure was increased hydraulically. If the pressure is increased by increasing a gas head, it will tend to increase the concentration of dissolved gas in the liquid. This will affect the cavitation further, as can be seen when the effect of increasing the gas concentration dissolved in the liquid (which can, of course, be achieved without increasing the ambient pressure) is considered in isolation. When the bubble expands, gas previously dissolved in the liquid will exsolve into the bubble [1.73]: the greater the concentration of dissolved gas, the greater the exsolution for a given degree of expansion. This exsolution decreases the pressure reduction within the bubble which occurs just prior to collapse. The presence of a permanent gas component will tend to 'cushion' the collapse†. However the concentration of available nuclei is likely to have increased. Similarly degassing the liquid will tend to increase the violence of each individual collapse; However there will be fewer appropriate bubble nuclei, and therefore probably fewer inertial collapses [1.10].

The above discussion therefore illustrates that when the effects of ultrasonically-induced inertial cavitation are important, not only must the energetics of the individual collapses be considered, but also the number of collapses, feature which may be interdependent. In addition, from section 1.3, it is important to characterise the non-inertial cavitation which may affect both the local sound field and the nuclei distribution.

In summary therefore, there are two questions which need answering in determining the "amount of cavitation" in liquids:

(i) Will inertial cavitation occur or not? This is amenable to calculation through the use of models of single-bubble dynamics, which can predict the dependence of the threshold on acoustic pressure amplitude, nuclei availability, and acoustic frequency (less often altered variables, such as ambient pressure, can also be incorporated). However, knowledge of these parameter values within the insonated sample are required to make use of this model. Not only are values (e.g. of the local acoustic pressure at each bubble, and the population of nuclei present) required for direct input into the model, they may also be interdependent, as discussed in section 1.3, and time-dependent. Section 2 therefore

† Therefore dissolving a gas such a carbon dioxide, which will readily come out of solution during the growth phase, will again cause a reduction in the violence of individual collapses. This is a technique often used to reduce the effects of inertial cavitation. Clearly changing the gas content of the bubble will have other effects too, changing the acoustic, thermal and chemical properties of the gas contents, though such effects will not be considered here.

discusses techniques for the measurement of the population of stable bubbles, which are required to determine the availability of nuclei and the local pressure field at the bubble. Knowledge of such parameters in turn allows *predictions* of whether or not, and over what number of bubbles, the threshold is exceeded.

(ii) If inertial cavitation occurs, to what 'degree' does it occur? Not only is this an issue of the energetics of each collapse in question, but also the number of collapses. However in practice such questions may be somewhat academic, since it is the *effects* of inertial cavitation that are usually of primary interest. These may be positively or negatively affecting the ultrasonic process under consideration, and therefore important to measure in their own right. Alternatively such effects may indeed be the way in which the cavitation is being monitored and characterised. In either case interpretation back from the observed effect to the characteristics of the cavitation which gave rise to them allows investigation of controlling the cavitation to change or optimise the ultrasonic process under consideration. Such effects and their interpretation is the topic of Section 3.

To investigate these, the relative importance of nucleation and activity, with respect to inertial cavitation, need clarifying. If, for example, no free-floating spherical nuclei exist, then one must look to stabilised gas bodies to seed cavitation (see Figure 1.7). If the threshold for the seeding from gas bodies is greater than the mechanical index for the free-floating bubbles generated from such gas bodies, then the key threshold to be exceeded to generate inertial cavitation is that seeding threshold, not the mechanical index. Once seeding has occurred, cavitation will occur; and once cavitation has occurred, it will through bubble fragmentation generate the free-floating nuclei for the next generation of inertial cavitation (providing off-times in the sound field are not too long). Indeed some workers has described the observation of two distinct thresholds: a 'nucleation' threshold, which indicates when cavitation first starts; and an 'activity' threshold, which indicates the onset of enhanced cavitational activity [1.77]. For many industrial applications of power ultrasound, it is likely to be the latter, and not the former, which is critical.

Apfel [1.74] summarised the key features for the generation and detection of cavitation in his three rules: *Know thy liquid*; *know thy sound field; know when something happens.* The reasons behind the first and second rules have been discussed in this chapter. Clearly characterisation of the liquid, including its stabilised nuclei, will rely on techniques for the detection of stable bubbles (outlined in Section 2). The third rule most often relates to the techniques of Section 3, where the effect of inertial cavitation on some sensor is the issue. However when such techniques are applied, it is necessary to understand whether one is monitoring the level of activity, or the threshold; and if the threshold, whether it refers to cavitation nucleation, sustained cavitational activity, or the detection threshold of the sensor itself.

References

1.1 Leighton TG. The Acoustic Bubble (Academic Press, 1994)

1.2 Leighton TG. 1994. Acoustic Bubble Detection. I. The detection of stable gas bodies. Environmental Engineering, **7**, 9-16

1.3 Leighton TG. 1995. Bubble population phenomena in acoustic cavitation. Ultrasonics Sonochemistry, **2**, S123-136

1.4 Rayleigh, Lord. On the pressure developed in a liquid during the collapse of a spherical cavity. Phil. Mag.1917; **34**: 94-98

1.5 Blake F.G. 1949. Technical Memo No. 12, Acoustics Research Laboratory, Harvard University, Cambridge, Massachusetts, USA. (September 1949).
1.6 Noltingk B.E., Neppiras E.A. Cavitation produced by ultrasonics. 1950. Proc. Phys. Soc. 1950; B, **63**: 674-685.
1.7 Neppiras E.A., Noltingk B.E. Cavitation produced by ultrasonics: Theoretical conditions for the onset of cavitation. Proc. Phys. Soc. 1951;B, **64**: 1032-1038.
1.8 Vaughan, P.W., Leeman, S. Some comments on mechanisms of sonoluminescence. Acustica 1986; **59**: 279-281.
1.9 Suslick K.S., Hammerton D.A., Cline R.E. Jr. The sonochemical hot-spot. J Am Chem Soc 1986; **108**: 5641-5642.
1.10 Flynn H.G. *Physics of acoustic cavitation in liquids.* In: Physical Acoustics. Mason WP, ed. (New York: Academic Press) 1964; vol. 1 part B: 57-172.
1.11 Leighton TG., 1995. Acoustic Bubble Detection. II. The detection of transient cavitation. Environmental Engineering, **8**, 16-25.
1.12 Neppiras E.A. Acoustic cavitation. Phys. Rep. 1980; **61**: 159-251.
1.13 Flynn H.G., Church C.C. Transient pulsations of small gas bubbles in water. J Acoust Soc Am 1988; **84**: 985-998.
1.14 Holland C.K., Apfel R.E. An improved theory for the prediction of microcavitation thresholds. IEEE transactions on ultrasonics, Ferroelectrics, and Frequency control 1989; **36**: 204-208.
1.15 Apfel R.E. Methods in Experimental Physics Vol. 19 (Ed. Edmonds, P.D.) Academic Press, New York 1981; 355-413.
1.16 Gaitan D.F., Crum L.A. Observation of sonoluminescence from a single cavitation bubble in a water/glycerine mixture. In: Frontiers of Nonlinear Acoustics, 12th ISNA. Hamilton MF, Blackstock DT, eds. (Elsevier, New York) 1990, p. 459.
1.17 Minnaert, M. On musical air-bubbles and sounds of running water, Phil. Mag. 1933; **16**: 235-248.
1.18 Eller, A. I. Damping constants of pulsating bubbles. J. Acoust. Soc. Am. 1970; **47**: 1469-1470.
1.19 Devin, C. Jr., Survey of Thermal, Radiation, and Viscous Damping of Pulsating Air Bubbes in Water. J. Acoust. Soc. Am. 1959; **31**: 1654
1.20 Miller, D.L., Nyborg, W.L., Whitcomb, C.C. Platelet aggregation induced by ultrasound under specialized condition in vitro. Science 1979; **205**: 505.
1.21 Miller DL, Williams AR. Bubble cycling as the explanation of the promotion of ultrasonic cxavitation in a rotating tube exposure system. Ultrasound Med Biol 1989; **15**: 641-648
1.22 Neppiras, E. A. Acoustic cavitation. Phys. Rep. 1980; **61**: 159-251.
1.23 Apfel, R.E., Holland, C.K. Gauging the likelihood of cavitation from short-pulse, low-duty cycle diagnostic ultrasound. Ultrasound in Med. & Biol. 1991; **17**: 179-185.
1.24 Walton, A.J., Reynolds, G.T. Sonoluminescence. Advances in Physics 1984; **33**: 595-660.
1.25 Kamath V, Prosperetti A and Egolfopoulos FN. A theoretical study of sonoluminescence. J. Acoust. Soc. Am. 1993; **94**: 248-260
1.26 Wu, C.C. and Roberts, P. H. Shock-wave propagation in a sonoluminescing gas bubble. Phys. Rev. Lett. 1993; **70**(22): 3424-3427
1.27 Margulis, M.A. Sonoluminescence and sonochemical reactions in cavitation fields. A review. Ultrasonics, 1985; **23**: 157-169
1.28 Lepoint, T., Voglet, N., Faille, L. and Mullie, F. Bubbles deformation and interface distortion as a source of sonochemical and sonoluminescent activity. Proc. IUTAM Symposium on *Bubble Dynamics and Interface Phenomena* (Birmingham, UK, 6-9 Sept. 1993), Blake, J.R., Boulton-Stone, J.M. and Thomas, N.H. eds. Kluwer Academic Publishers, pp. 321-333
1.29 Crum, L.A. and Cordry, S. Single-bubble sonoluminescence. Proc. IUTAM Symposium on *Bubble Dynamics and Interface Phenomena* (Birmingham, UK, 6-9 Sept. 1993), Blake, J.R., Boulton-Stone, J.M. and Thomas, N.H. eds. Kluwer Academic Publishers, pp. 287-297
1.30 Eberlein C. Sonoluminescence as quantum vacuum radiation. Physics Review Letters 1996; **76**: 3842
1.31 Plesset MS, Prosperetti A. Bubble dynamics and cavitation. Ann Rev Fluid Mech, 1977; **9**: 145-185
1.32 Mørch KA. 1979. Erosion, (ed. C. M. Preece), pp. 309-353. Academic
1.33 Vyas B, Preece CM. Stress produced in a solid by cavitation. J. Appl. Phys., 1976; **47**: 5133-5138

1.34 Barber, B.P., Hiller, R., Arisaka, K., Fetterman, H., Putterman, S. Resolving the picosecond characteristics of synchronous sonoluminescence. J Acoust Soc Am 1992; **91:** 3061-3063
1.35 Kornfeld, M., Suvorov, L. On the destructive action of cavitation. J. appl. Phys. 1944; **15**: 495-506
1.36 Crum LA, Eller, AI. Motion of bubbles in a stationary sound field. J Acoust Soc Am 1969; **48**: 181-189
1.37 Strasberg M . Gas bubbles as sources of sound in liquids. J Acoust Soc Am 1956; **28**: 20-26
1.38 Longuet-Higgins MS. Nonlinear damping of bubble oscillations by resonant interaction. J Acoust Soc Am 1992; **91**: 1414-1422
1.39 Leighton TG, Schneider MF and White PR. 1995. Study of bubble fragmentation using optical and acoustic techniques. Sea Surface Sound '94. Proc. 3rd Meeting on Natural Physical Processes related to Sea Surface Sound, MJ Buckingham, JR Potter, eds., (World Scientific Publishing Ltd., Singapore) 414-428
1.40 Lauterborn W, Bolle H. Experimental investigations of cavitation-bubble collapse in the neighbourhood of a solid boundary. J Fluid Mech 1975; **72**: 391-399
1.41 Plesset, M.S., Chapman, R.B. Collapse of an initially spherical vapour cavity in the neighbourhood of a solid boundary. J. Fluid Mech. 1971; **47**: 283-290
1.42 Prosperetti A. Bubble phenomena in sound fields: part 2. Ultrasonics 1984; **22**: 115-124
1.43 Miller, D.L. (1979) "A cylindrical bubble model for the response of plant-tissue gas-bodies to ultrasound", J. Acoust. Soc. Am., **65**, 1313-1321.
1.44 Child, S.Z., Carstensen, E.L., Lam SK.. Effects of ultrasound on *Drosophila*–III. Exposure of larvae to low-temporal-average-intensity, pulsed irradiation. Ultrasound in Med. & Biol. 1981; **7**: 167-173
1.45 Leighton, T.G., White P.R and Marsden, M.A. (1995) "Applications of one-dimensional bubbles to lithotripsy, and to diver response to low frequency sound", Acta Acustica, **3**, 517-529
1.46 Miller, D.L. (1984) "Gas body activation", Ultrasonics, **22**, 261-269
1.47 Miller, D.L. and Neppiras, E.A. (1985) "On the oscillation mode of gas-filled micropores.", J. Acoust. Soc. Am., **77**, 946-953
1.48 Miller, D.L. and Nyborg, W.L. (1983) "Theoretical explanation of the response of gas-filled micropores and cavitation nuclei to ultrasound", J. Acoust. Soc. Am., **73**, 1537-1544
1.49 Pickworth M J W, Dendy P P, Leighton T G and Walton A J. 1988. Studies of the cavitational effects of clinical ultrasound by sonoluminescence: 2. Thresholds for sonoluminescence from a therapeutic ultrasound beam and the effect of temperature and duty cycle. Phys. Med. Biol., **33** (11), 1249-60
1.50 Leighton T G, Pickworth M J W, Walton A J and Dendy P P. 1989. The pulse enhancement of unstable cavitation by mechanisms of bubble migration. Proc. I.O.A., **11** (5), 461-469
1.51 Crum, LA. Personal communication.
1.52 Ciuti P, Iernetti G, Sagoo MS. Optical visualisation of non-linear acoustic propagation in cavitating liquids. Ultrasonics 1980; **18**: 111-114
1.53 Yu, Kobelev A, Ostrovskii LA, Sutin AM. Self-illumination effect for acoustic waves in a liquid with gas bubbles. JETP Lett 1979; **30**: 395-398 (Pis'ma Zh. Eksp. Teor. Fiz. 1979; **30**: 423)
1.54 Flynn HG, Church CC. A mechanism for the generation of cavitation maxima by pulsed ultrasound. J. Acoust. Soc. Am., 1984; **76**: 505-512
1.55 Church C C. Prediction of rectified diffusion during nonlinear bubble pulsations at biomedical frequencies. J. Acoust. Soc. Am. 1988; **83**: 2210-2217
1.56 Harvey EN, Barnes DK, McElroy WD, Whiteley AH, Pease DC, Cooper KW. Bubble formation in animals. J Cell Comp Physiol 1944; **24**: 1-22
1.57 Trevena DH. Cavitation and Tension in Liquids. Adam Hilger, Bristol and Philadelphia, 1987.
1.58 Atchley AA, Prosperetti A. The crevice model of bubble nucleation. J Acoust Soc Am 1989; **86**:1065-1084
1.59 Greenspan M, Tschiegg CE. Radiation-induced acoustic cavitation; apparatus and some results. J. Res. natl. Bur. Stand. 1967; Section C, **71**: 299-311
1.60 Sirotyuk MG. Stabilisation of gas bubbles in water. Sov Phys Acoustics 1970; **16**: 237-240
1.61 Akulichev VA. Hydration of ions and the cavitation resistance of water. Sov Phys Acoust 1966; **12**: 144-149
1.62 Yount DE. Skins of varying permeability: a stabilisation mechanism for gas cavitation nuclei. J Acoust Soc Am 1979; **65**: 1429-39
1.63 Yount DE. On the evolution, generation, and regeneration of gas cavitation nuclei. J Acoust Soc Am 1982; **71**: 1473-81

1.64 Yount D E, Gillary E W, Hoffman D C. A microscopic investigation of bubble formation nuclei. J Acoust Soc Am 1984; **76**: 1511-1521
1.65 Sponer J. Theoretical estimation of the cavitation threshold for very short pulses of ultrasound. Ultrasonics 1991; **29**: 376-380
1.66 Sponer J. Dependence of ultrasonic cavitation threshold on the ultrasonic frequency. Czech J Phys B 1990; **40**: 1123-1132
1.67 Sponer J, Davadorzh C, Mornstein V. The influence of viscosity on ultrasonic cavitation threshold for sonoluminescence at low megahertz region. Studia Biohys 1990; **137**: 81-89
1.68 American Institute of Ultrasound in Medicine/National Electrical Manufacturers Association (AIUM/NEMA). "Standard for real-time display of thermal and mechanical indices on diagnostic ultrasound equipment", 1992.
1.69 Carstensen E, Kossof G, Preston R, and Hogaki M. Thresholds for non thermal bioeffects: Theoretical and experimental basis for a threshold index. Chapter 6 in World Federation for Ultrasound In Medicine and Biology task group draft report from WFUMB symposia on "Safety of Ultrasound in Medicine: Emphasis on non-thermal mechanisms" (Utsinomiya, Japan, July 1994; Koster Banz, Germany, April 1996).
1.70 Roy R . The demographics of cavitation produced by medical ultrasound. J. Acoust. Soc. Am. 1996; **99**: 2485 (abstract).
1.71 Chendke, P.K., Fogler, H.S. Sonoluminescence and sonochemical reactions of aqueous carbon-tetrachloride solutions. J. phys. Chem.,1983; **87**: 1362
1.72 Urick RJ. Principles of underwater sound, 3rd edn. McGraw-Hill, New York 1983; p. 337
1.73 Church, C.C. A theoretical study of cavitation generated by an extracorporeal shock wave lithotripter. J. Acoust. Soc. Am. 1989; **86**: 215-227
1.74 Apfel RE. Acoustic Cavitation Inception. Ultrasonics 1984; **22**: 167-173
1.75 Leighton T G, Wilkinson M, Walton A J and Field J E. 1990. The forced oscillations of bubbles in a simulated acoustic field. Eur. J. Phys., **11**, 352-358.
1.76 American Institute of Ultrasound in Medicine (1992). Standards for real-time display od thermal and mechanical acoustic indices on diagnostic ultrasound equipment. Laurel, MN, AIUM.
1.77 Calabrese AM. Threshold measurements and production rates for inertial cavitation due to pulsed, megahertz-frequency ultrasound. PhD dissertation, University of Mississippi, 1996.

2. TECHNIQUES FOR THE DETECTION OF STABLE BUBBLES

2.1 Applications

As stated in section 1.4, the ability to characterise non-inertial cavitation is important in assessing cavitation in high-power ultrasonic fields, despite the fact that the first impression is usually that it is of secondary importance when compared with inertial cavitation (which can produce such obvious chemical, biological, erosive effects, and luminescent and acoustic emissions). This importance arises because: first, inertial cavitation rarely occurs without accompanying non-inertial cavitation; and second, the techniques for monitoring non-inertial cavitation are in general the same as those used to detect pre-existing stable gas bodies. The implications are as follows:

• High-amplitude non-inertial cavitation can produce effects in common with inertial cavitation. Some of these (bio-effects being perhaps the most obvious examples) may be desirable or not in a given application of high-power ultrasound, and knowledge of the non-inertial cavitation is necessary to promote or inhibit the effects. Certain effects (such as emission of a subharmonic) can be generated by either inertial or non-inertial cavitation [1.1§4.4.7], and if such a phenomenon is being used to monitor the cavitation, the relative contributions from both types of cavitation should be known.

• Non-inertial cavitation can affect the local pressure field at a bubble, and the nuclei population (through fragmentation, coalescence, rectified diffusion etc.) [1.3]. The prediction of inertial cavitation requires knowledge of both those bubbles undergoing non-inertial cavitation, and those which are pre-existing prior to insonation.

Of relevance to the last point, many techniques for the detection of non-inertial cavitation are appropriate for the detection of stable bubbles, as stated above. Application of any active acoustic techniques for the detection of pre-existing stable bubbles, bar geometrical scattering (section 2.3.1), will drive the bubble into (usually) non-inertial pulsations. Therefore the act of detection using such a technique, for example to characterise the nuclei present to predict the likelihood of inertial cavitation (section 1.3.2), will be invasive (section 2.3.6).

Such methods are desirable in many applications, for reasons other than the characterisation of cavitation in high-power ultrasonic fields, and have therefore been the subject of considerable study. Even so there is as yet no wholly comprehensive detector. These applications include the preparation of molten glass or polymer solutions [2.1], and filling operations in the paint, food, detergent, cosmetics and pharmaceutical industries where bubbles may degrade the product [2.2]. In the petrochemical industry alone, bubbles detection is required to optimise harvesting and transportation. Gas which had dissolved into the crude in the high pressures at the well base exsolves as the crude is brought up to surface pressures. Bubble detection in the bore may warn of high-pressure gas pockets.

Ultrasonic probes will interact with bubbles, and can be found in the nuclear power industry [2.3-2.7], where passive acoustic emissions can be used for monitoring [2.8]. Ultrasonic bubble detection has other industrial applications, including fluid processing [2.9], pressure measurement [2.10], and pressure vessel monitoring [2.11]. Medical applications include studies of decompression sickness [2.12, 2.13], and contrast echocardiography [2.14]. Bubbles *in vivo* can be detected actively [2.15] and passively [2.16-2.18].

Bubbles in the ocean have applications for underwater communications (e.g. background noise [2.19], signal channelling [2.20], and sensing [2.21]); and monitoring of methane seeps, rainfall [2.22§3.7.2] and gas flux between ocean and atmosphere. More than 1000 million tonnes of atmospheric carbon dissolve into the seas each year [2.23]. Fluxes of carbon dioxide [2.24] and dimethylsulphide [2.25] have climatic significance [2.26].

2.2 "Cavitation Detection and Monitoring": A report by Work Group 22 of Accredited Standards Committee S1 of the Acoustical Society of America.

As stated at the end of section 1, this section will discuss techniques for the detection of stable bubbles, and section 3 will outline methods for the characterisation of inertial cavitation. Concurrent with the writing of this report, a document [2.27] is being prepared under the chairmanship of Prof. Wesley Nyborg, on behalf of Working Group 22 of Accredited Standards Committee S1 of the Acoustical Society of America, entitled "Cavitation Detection and Monitoring".

It is intended that the two reports will be complimentary. Both will discuss techniques for the characterisation of inertial and non-inertial (stable-bubble) cavitation. However there are important differences. This report is intended to examine the methods of characterising cavitation in high-power ultrasonic fields. It introduces techniques for the detection of stable bubbles only in as much as such methods are needed to completely characterise the nuclei population, or determine how non-inertial cavitation in the field will influence the effects of high-power ultrasound. The ASA report in contrast introduces each technique as a method in its own right, with each one described in detail by an expert. Therefore the ASA report has the opportunity for greater specialist input, with for example numerical quantification of the limitations of each method. For specific techniques the report will quantify the sensitivity, the bubble size resolution, the spatial and temporal resolution, and outline the significance of each technique, the advantages and disadvantages, applications and apparatus. This report does not include such detail, but rather gives a narrative overview of the range of techniques from the perspective of a single author. Non-experts might, for example, benefit from first reading this report, to obtain familiarity of how the various signals used arise from increasingly complex forms of bubble behaviour (low-amplitude linear pulsations, nonlinear pulsations, surface wave activity, inertial cavitation, etc.), and therefore gain an appreciation of the nature of the assumptions inherent in description of the bubble dynamics associated with a given technique. Inspection of the ASA would then be strongly recommend for details on individual methods. The author would like to express his gratitude and indebtedness to Prof. Nyborg and the other authors of "Cavitation Detection and Monitoring" for the benefits he obtained in reading that report whilst writing this one.

2.3 Acoustic detection techniques

These will be discussed in order of the complexity of the interaction between the bubble and the sound field (as illustrated in Figure 1.1). Simple geometrical shadowing requires no bubble pulsation, but as such is insensitive to bubble size and on its own cannot distinguish from a bubble or a particle. Size resolution is instead usually achieved through exploiting the resonator characteristics of the bubble. The pulsation resonance frequency reflects the bubble volume, and therefore is not greatly influenced by departures from sphericity, which can greatly affect optical measurements. Also, it varies roughly inversely with the equilibrium radius (R_O), making it suitable for sizing small bubbles.

Upon entrainment, for example by injection, the bubble will emit a decaying signal at its natural frequency (section 2.3.2). An imposed sound field will drive the bubble to pulsate, the oscillation tending to be linear the smaller the pulsation amplitude. Larger amplitude pulsations generate increasingly non-linear signals: these occur if the amplitude of the imposed sound field is increased, or becomes closer to resonance (section 2.3.3i). In the latter condition, surface waves can be generated on the bubble, and whilst these do not in general emit an acoustic signal to a distance, they can be exploited (section 2.3.3ii). A summary of various acoustic methods is given in Table 2.1. All such techniques are limited in one way or another. Recent studies have investigated their simultaneous use so that the limitations of one might find compensation in the deployment of another (section 2.3.4).

Scatters	**Advantage**	**Disadvantage**	**Example prior deployments**	**Bubble sizes investigated in 1 expt.**
Geometric	Rapidly obtains images with high spatial (location) resolution	Cannot distinguish between bubbles and solid particles	Laboratory [2.29, 2.31, , 2.31, 2.33]	Distribution (low radius resolution).
Fundamental	Apparatus simple	Large bubbles and bubble clouds may falsely register as resonant bubble (geometric scattering). Low spatial resolution. False triggering and off-resonance scattering may occur. High number densities only are valid if 'bulk properties' are assigned to the liquid.	Resonator [2.67] Attenuation [2.99] Backscatter [2.105]	Four [2.104]; ~nine [2.67] ~seventy [2.33] (7 kHz span with 98 Hz resolution).
Second harmonic	Little contribution from geometric scattering.	Low spatial resolution. False triggering and off-resonance scattering may occur.	Clinical, detecting ≈μm radius bubbles [2.72-3]	One [2.72] or two [2.73] per trial. Forty [2.33] (i.e. 2 kHz range with 50 Hz resolution)
$\omega_i \pm \omega_p$	No threshold.	False triggering and off-resonance scattering may occur.	Lab. [2.101, 2.106], field [2.106, 2.109, 2.111]	Distribution
$\omega_i \pm \omega_p/2$	Minimal false triggering or, at threshold, off-resonance scattering.	Threshold acoustic pressure required for fine radius resolution.	Laboratory [2.102, 2.33]	Distribution @ 25 Hz resolution [2.102]

Table 2.1: The various acoustic techniques available for bubble detection. Numerals in cols. 4 and 5 are references.

2.3.1 Geometrical scattering

As the dimension of a body becomes significantly greater than the wavelength of the radiation it scatters, the regime more closely approaches that of geometric scattering. Though in general the size of a bubble is at best of comparable scale with the wavelength, the phrase 'geometrical scattering' nevertheless is useful to distinguish from resonant or just off-resonant scattering. If MHz sound is, for example, employed to detect mm-sized bubbles, the small wavelengths involved (≈0.4 mm in water at 3.5 MHz) allow the bubble to be located, but do not accurately give bubble size [2.29-2.33].

This ultrasonic shadowing is the only acoustic technique which does not require a bubble volume change. Geometric scattering relies on the acoustic impedance mismatch between the inhomogeneity and the surrounding liquid, and so is insensitive to the nature of the inhomogeneity, and in practice may not distinguish between bubbles and solid bodies of a similar size.

In addition it may not distinguish between resonant bubbles, and bubbles which are large compared with the wavelength. Simple linear theory demonstrates that the variation of the acoustic scattering cross-section of a given frequency, as a function of the radius of the bubble in question, is only a local, and not a global, maximum at resonance (section 2.3.2ii): bubbles very much larger than resonance size can geometrically scatter sound to a greater degree than can smaller, resonant bubbles.

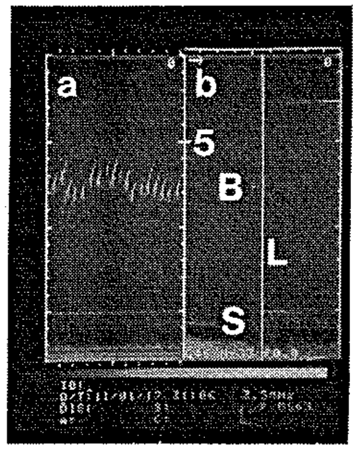

Fig. 2.1. a) M-mode (1 s sweep) and b) B-mode images from Hitachi ultrasound scanner. In 'b' a bubble (B), loudspeaker (S), the 5 cm marker from transducer faceplate (at top of image) and the line (L, occurrence of an image in which defines the M-mode image) are indicated.

Fig. 2.1 shows both the a) M- and b) B-mode images obtained using the Hitachi ultrasound scanner, the section shown being a slice at 45° to vertical through which rising bubbles pass (Figure 1b). The bubble (labelled B) can be located in Fig. 2.1b (near-field is at top of image), which also images the loudspeaker (S) and part of the cage. The images which intersect the vertical line (L) in 1 s are plotted in Fig. 2.1a: almost 19 bubbles pass through the beam in that time, with rise speed (from the image, within the limits of the rectilinear bubble motion, adjusting for the 45° orientation) of 20±2 cm/s. Comparison of 'a' with 'b' allows the transient features (e.g. bubbles) to be distinguished from the time-invariant ones (the label 'S' refers to the ultrasonic image of the loudspeaker shown in Figure 2.1b). The application of such scattering to bubble detection will be discussed further in section 2.3.2(ii)

2.3.2 Detection through 'linear' oscillations

Whilst the oscillating bubble is inherently non-linear (the stiffness of the gas, for example, is a function of the wall displacement†), so that in theory no bubble oscillation will be wholly linear, in practice at small pulsation amplitudes the assumption of linearity is often justified. Certainly there are a range of techniques which interpret the acoustic signal detected in terms of linear oscillations. The efficacy of these acoustic techniques for detection of 'stable' bubbles relies on three factors: (i) the ability of the bubble to act as an oscillator which approximates to linearity at small amplitude with a well-defined resonance; (ii) the excellent coupling between the sound field and the bubble, as evidenced by the high values taken by the acoustic scattering cross section at resonance; and (iii) the ability of a bubble population to impart equivalent acoustic bulk properties to a medium. These properties are employed in most experiments which exploit the oscillator properties of the bubble ((ii) and (iii) require (i) as prerequisite).

† On a more simplistic level, the basic asymmetry of the wall oscillation would suggest a degree of non-linearity. In an extreme example, the bubble wall can on contraction be displaced no more than the equilibrium radius (at which point the buble has zero volume), whilst there is no such limit on expansion.

(i) The bubble as an oscillator

The natural frequency ν_o of a spherical bubble pulsating in an inviscid liquid can be expressed as:

$$\nu_o = \frac{\omega_o}{2\pi} = \frac{1}{2\pi R_o}\sqrt{\frac{3\kappa p_o}{\rho}\left(1+\frac{2\sigma}{p_o R_o}\right) - \frac{2\sigma}{\rho R_o}} \qquad (2.1)$$

[2.22§3.4.2b] where ρ is the liquid density, σ the surface tension, and p_o the static pressure (first derived neglecting surface tension [2.34]). The polytropic index κ varies between γ (for the adiabatic case) and unity (isothermal processes). For macroscopic air bubbles in water under one atmosphere, equation 2.1 reduces [2.35] to:

$$\nu_o R_o \approx 3\ s^{-1}.\ m \qquad (R_o > \sim 10\ \mu m) \quad (2.2)$$

Studies on injected bubbles [2.34, 2.36-2.39] showed the underwater acoustic emission to approximate to an exponentially-decaying sinusoid typical of a lightly-damped oscillator. Such bubble signatures can be used to detect and size bubbles under waterfalls [2.38, 2.40], rainfall [2.41-2.44], and breaking waves [2.45, 2.46]. Since the freely oscillating bubble must first be excited in order to emit in this manner when passive emissions are used for bubble detection, the signal samples not the whole population, but only those bubbles entrained during the period of observation. The acoustic detection of older bubbles, which persist but whose entrainment emissions have ceased, requires those bubbles to be further excited to radiate or scatter sound. An example of this is the exploitation of the Doppler shift on signals from the moving bubbles in blood [2.47], which can distinguish them from reflections from static objects. However Doppler techniques may be unable to distinguish between a single large bubble and a cluster of smaller ones [2.10]. Formulation of the ability of bubbles to scatter sound is most usually done using the concept of the acoustic cross-section. In the next section, such resonance scatter is examined.

(ii) Acoustic scatter from bubbles

The acoustic scattering cross-section, Ω_b^{scat}, is defined as the ratio of the time-averaged power scatter by the bubble from the a plane wave to the intensity of that plane wave. If the bubble is assumed to be a linear oscillator, it is given by

$$\Omega_b^{scat} = \frac{4\pi R_o^2}{((\omega_o/\omega)^2 - 1)^2 + (2\beta_{tot}/\omega)^2} \qquad (2.3)$$

in the limit $kR_o \ll 1$, where k is the wavenumber, c the sound speed, and where ω_o and $\omega = ck$ are the radian frequencies of the bubble resonance and the insonating frequency respectively, and β_{tot} is a parameter associated with the damping of the bubble [2.22 §4.1.2d]. For a fixed insonation frequency, this quantity is locally a sharp maximum at resonance for lightly-damped bubbles (Figure 2.2). Medwin [2.48] noted two facts which make the technique very suitable for bubble counting, provided that much larger scatterers are not present: Firstly, the scattering cross-section of a bubble is about 1000 times its geometrical cross-section at resonance, and about 10^{10} times that of a rigid sphere; and secondly the resonance frequency varies inversely with the radius if surface tension effects are negligible (equation 2.1), thereby facilitating the observation of small bubbles. However the approximation which is often employed, namely that *only* resonant bubbles scatter a given sound field, is not rigorous: There are two counter indications (Figure 2.2). Firstly, in conditions of finite damping, bubbles close to resonance size will contribute. Secondly, the peak at resonance is only a local minimum, and that bubbles much larger than resonance can scatter to a greater degree than those at resonance. The scattering by resonant bubbles is due to the strong coupling with the incident wave, as manifested by the large amplitude of wall pulsation. Much larger bubbles in contrast pulsate to a negligible degree: in the limit of the bubble size being much larger than the acoustic wavelength, the process is geometric, the bubbles generating acoustic shadows. Large bubbles create large shadows. It should be remembered that the formulation of equation 2.3 is for the linear limit: in many cases where acoustic techniques are deployed in this manner, in order to generate a sufficiently high signal-to-noise ratio the sound field is strong enough to impart a degree of nonlinearity into the bubble oscillation.

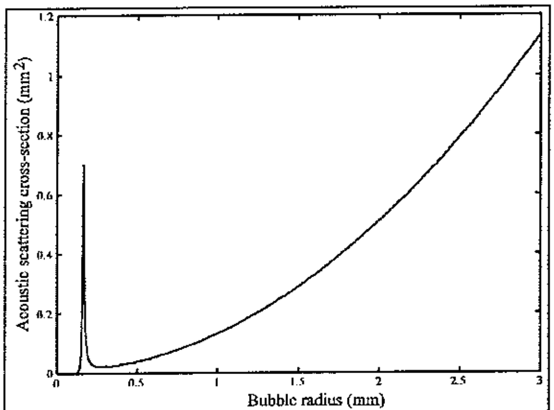

Figure 2.2 The acoustic scattering cross-section of a spherical bubble insonated at 20 kHz, pulsating in steady-state in the limit of linear oscillations. The damping is assumed to be constant (Q=15) over the radius range presented. Resonance occurs around R_o~0.2 mm [2.113].

Studies which have exploited the enhanced scattering from resonant bubbles include both oceanic sonar studies [2.49, 2.50] employing frequencies up to about 200 kHz, and medical studies involving ultrasound of higher frequency. Decompression bubbles have been imaged [2.51]; the returning echo strength at 7.5 MHz *in vivo* in humans, fish, and guinea pigs has been taken to be a measure of the bubble size (calibrated through comparison of microscopic and ultrasonic measurements on bubbles in water, gelatine, and transparent fish) [2.52]. However small bubbles close together scattered such that they could not be distinguished from single, larger bubbles.

By the early 1980's there was evidence using such techniques of ultrasonically-generated cavitation effects *in vivo* [2.53-2.55]. ter Haar et al. [2.56-2.58] employed a pulse-echo ultrasonic B-scan system to detect bubbles generated *in vivo* in the hind limbs of guinea pigs in response to 0.75 MHz insonation by continuous-wave or 1:1 duty cycle pulsed ultrasound from a commercial therapy device. The minimum detectable bubble radius of this system was about 5 μm [2.59]. It was not able to distinguish between individual large bubbles and tight clusters of smaller bubbles separated by less than the resolution of the system [2.56], and no accurate measurements of bubble size could be made [2.59].

Fowlkes et al. [2.60] generated bubbles in excised canine urinary bladders which were sealed within a bag of degassed saline solution and then placed in a bath of degassed water at the common focus of a 555 kHz transducer and a brass reflector. The bubbles were visualised on a diagnostic ultrasound scanner with a 5 MHz in-line mechanical scanhead. Pressure amplitudes as great as 10-20 bars were used to generate the largest bubbles detected which, from their rise times, had estimated radii of 50-70 μm. These bubbles, being very much larger than resonance, were probably generated through coalescence in the standing-wave field in the bladder. As regards detection of the smaller bubbles, the inability to distinguish bubble echoes from artefacts caused by the reverberant field within the bladder set resolution limits.

Exploitation of the resonance featured explicitly in the 1977 study of Fairbank and Scully [2.61], who examined the emitted scattered signal from bubbles, assumed to be at resonance, subjected to broad band ultrasound (from 100 kHz to 1 MHz). They proposed using this technique in order to measure blood pressure changes in inaccessible regions of the heart through the resulting changes in the equilibrium volumes of injected bubbles. However resonance techniques are not ideal. Simulations of common methods of bubble sizing through resonance techniques for hypothetical bubbles size distributions by Commander and Moritz [2.62] suggests that the number of bubbles having R_0<50 μm can be significantly overestimated. More thorough analyses of data are required to compensate (see, for example, Commander et al. [2.63]).

(iii) Equivalent bulk properties

Techniques which exploit the ability of a bubble population to impart equivalent bulk properties to a volume of the medium through which it is evenly-distributed are generally interpreted through an analysis which suffers the same inherent limitations as the above technique, in that linear theory is employed in the interpretation, and that it is assumed that only resonant bubbles contribute. However they enable measurements to be made in the limit of high population densities, where most other techniques are inapplicable. An example of such a bulk parameter is the sound speed, which for longitudinal waves in a continuum depends on the square root of the ratio of the bulk modulus and the density. The addition of resonant bubbles to a liquid reduces the bulk modulus (or, equivalently, increases the compressibility) of the resulting mixture when it in turn is viewed as a continuum, to a far greater extent than it reduces the density. Therefore the sound speed falls to less than that of the bubble-free liquid, and in a sufficiently bubbly mixture at frequencies less than resonance can be less than that of the gas phase alone (owing to the contribution of the liquid phase to the density). If there is a distribution of bubble sizes within a bubble cloud, such that $n^{gr}(z,R_0)dR_0$ is the number of bubbles per unit volume at depth z having radii between R_0 and R_0+dR_0, the speed of sound c_C is a function of both the depth and the acoustic frequency:

$$c_C(z,\omega)=c\left\{1-(2\pi c^2)\int_{R_0=0}^{\infty}\frac{R_0}{\omega^2}\left(\frac{(\omega_0/\omega)^2-1}{\{(\omega_0/\omega)^2-1\}^2+d^2}\right)n^{gr}(z,R_0)\,dR_0\right\}, \quad (2.4)$$

where d is a dimensionless damping parameter [2.22 §4.1.2e; 2.64], and c the sound speed in bubble-free water. The results of resonators of the type developed by Medwin and Breitz [2.65] can be interpreted in terms of bulk properties. The resonance frequencies of the device when it is filled with bubbly liquid are less than that when it is bubble-free as a result of the reduced sound speed; similarly the widths of the resonances are broadened since the bubbles introduce greater dissipation. The exploitation of this effect to examine bubble populations using acoustic attenuation will be discussed in the next section *(iv) Attenuation*

As well as scattering sound from an incident beam, bubble pulsations, being damped, can convert acoustic energy to heat through loss mechanisms. Acoustic cross-sections for these thermal and viscous absorption processes can readily be defined [2.22§4.1.2d]. The loss of acoustic energy from a beam through scatter and absorption by a pulsating bubble can be formulated, and is a maximum at resonance. Therefore the additional attenuation which results from a bubble population can be used to measure that population, and this has been used to monitor ocean bubble population *in situ* measuring bubbles in the radius range 15 to 300 μm [2.48]. The study included measurements of scattering and phase velocity, though dispersion was too small to measure accurately. The effect on dispersion and attenuation of multiple scattering in bubble populations has been analysed [2.66]. Bleeker et al. [2.67] used the attenuation coefficient, sound speed and backscatter coefficients at 5 and 7.5 MHz to examine a controlled population of Albunex™ spheres, a commercial echo-contrast agent for clinical applications, which consists of microbubbles in the size range $0.5\ \mu m \lesssim R_0 \lesssim 5\ \mu m$ stabilised against dissolution by a shell approximately 28 nm thick made of coagulated human serum albumin.

In summary, to insonate a sample of bubbly liquid at a frequency ω, and assume that variations in the signal at ω are caused by bubbles resonant with the frequency ω, is to assume that the ω signal is yielding information about resonant bubbles only. However the resonance peak is only a *local*, and not a global, maximum (Figure 2.2): The signal at ω may be affected by bodies other than resonant bubbles, and interpretation in terms of resonant bubbles alone may be incorrect. This problem will not occur if the monitored signal is a global maximum at resonance, as occurs with certain signals that arise through nonlinear interactions. These will be discussed in the following section.

2.3.3 Detection through nonlinear oscillations

(i) Detection through the second harmonic emission

As discussed in section 1.2, the bubble is, at finite amplitude, a nonlinear oscillator [2.68-2.70], and at low insonation powers generation of the second harmonic signal gives a global maximum at resonance [2.71]. This generation is illustrated through a simple power series expansion of the force/response relationship in the bubble oscillator. The general response Y of a bubble (which may correspond to the wall motion) is then a power series of the driving force f, for example,

$$Y(t) = s_0 + s_1.f(t) + s_2.f^2(t) + s_3.\,f^3(t) + s_4.\,f^4(t) + \ldots \quad , \qquad (2.4)$$

Substitution of a single-frequency driving force (the acoustic pressure) of $f \equiv P(t) = P_A \cos\omega t$ into equation 2.4 will produce a harmonic at twice the driving frequency through the quadratic term, since $2\cos^2 \omega t = 1 + \cos 2\omega t$. On the assumption that, the closer to resonance, the higher the amplitude of oscillation, and so the stronger the output of the second harmonic, detection of this signal indicates the presence of a resonant bubble.

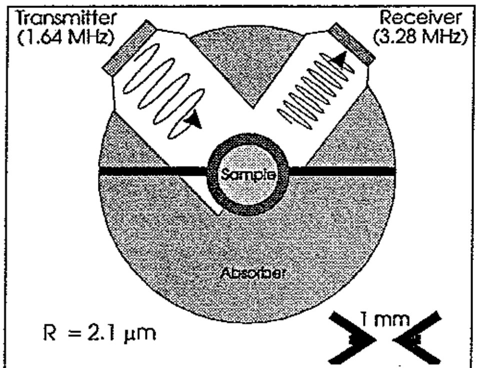

Figure 2.3 The resonant bubble detector, as developed by Miller et al. [2.64].

Figure 2.3 illustrates the "resonant bubble detector" (RBD) [2.72]. This used two transducers, a 1.64 MHz emitter (0.12 W cm^{-2}) and a 3.28 MHz receiver, mounted with suitable acoustic absorber, their axes perpendicular to each other and to the 4 mm diameter tube containing the flowing liquid that was to be investigated. The detector, tuned to twice the emitter frequency, was sensitive to bubbles sizes resonant with the emitter (R_0~2.1 μm for 1.64 MHz). Miller et al. [2.73] used a larger, modified detector such that the interrogated region was 7.4 mm from each transducer, with the emitter operating at 0.89 or 1.7 MHz. Miller [2.72] tested the device for two bubble sizes in water: the second harmonic emitted by resonant bubbles (produced by electrolysis) was 43 times stronger than that produced by injected bubbles of 250 μm radius. By comparison the fundamental emission from the resonant bubbles was 0.02 times that from the larger bubbles. Miller et al. [2.73] were able to semi-quantitatively detect bubbles produced by upstream ultrasonic cavitation, and by hydrodynamic cavitation at a detector tip, though they speculate that coalescence and radiation forces may have affected the population, and the detector responded to some bubbles which were up to 25% larger or smaller than resonance. In 1985 Gross et al. [2.18] were unable to detect bubbles downstream from the aorta when canine hearts were and were not insonated. In 1984 Vacher et al. [2.74] produced a similar bubble detector, though the frequency of interrogation (and therefore the size of bubble that was resonant) could be swept, the detector frequency being constantly twice that of the emitter. Relative to some other techniques (see section 2.3.3(iii)) spatial resolution is poor with the second harmonic technique [2.10]. Another drawback is that the second harmonic may arise through nonlinear effects when sound propagates through even bubble-free water [2.75, 2.76], and this must be avoided or corrected for. Even so the second harmonic technique has been successfully deployed in a range of applications and commercial systems are available.

(ii) Detection through the other harmonics, ultraharmonics, and the subharmonic of the bubble resonance.

The resonant bubble in fact produces, not just the second harmonic, but a range of emissions at resonance, as shown from Figure 2.4. For these to be useful tools for bubble detection and sizing, they must be generated only by resonant bubbles. If there are contributions from off-resonant bubbles, or from nonlinearities in the system (such as the detector electronics, turbulence, or the propagation of finite-amplitude waves), then these must be removed from the algorithm which converts the detected signal into bubble information: the greater the contribution from these non-bubble sources, the more difficult it is in general to do this.

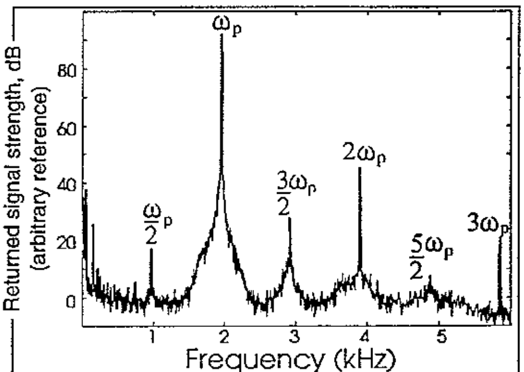

Figure 2.4 The acoustic emissions detected 1 cm from a single bubble, held on a wire and insonated at its 1950 Hz resonance with a signal of amplitude 150 Pa 0-peak. Vertical axis shows the signal strength in dB (arbitrary reference) [2.113].

Figure 2.5a shows a contour plot of the signal detected when the single tethered bubble of Figure 2.4 is insonated by a series of pump frequency tones (ω_p), incremented in 25 Hz steps from 1700 to 2200 Hz (pump signal amplitude=150 Pa 0-peak). The scattering of the fundamental (ω_p), second ($2\omega_p$) and third ($3\omega_p$) harmonics are visible, the first two suggesting an increase at the bubble resonance (1950 Hz). The subharmonic ($\omega_p/2$), and ultraharmonics at $3\omega_p/2$ and $5\omega_p/2$ also are confined to the region of the resonance. However in these circumstances (e.g. with such a low pump signal amplitude) none of these signals is ideal for bubble detection. When the bubble is removed and the experiment repeated, signals at ω_p, $2\omega_p$ and $3\omega_p$ are still detected, indicating a non-bubble contribution, as can be seen from Figure 2.5b. Though the figure shows that the signals at $\omega_p/2$, $3\omega_p/2$ and $5\omega_p/2$ are not present when the bubble is removed, these signals suffer from the disadvantage that they do not propagate well, and so cannot be used for remote detection of a stable bubble. This is because, though at resonance there are a number of mechanisms by which a stable bubble might emit a subharmonic of the driving frequency, at resonance the mechanism with by far the lowest threshold involves the stimulation of Faraday waves on the bubble wall [2.102]. It is however possible to 'image' these surface waves using a high frequency ultrasonic beam, which will propagate. This, and related techniques, will be discussed in the following section.

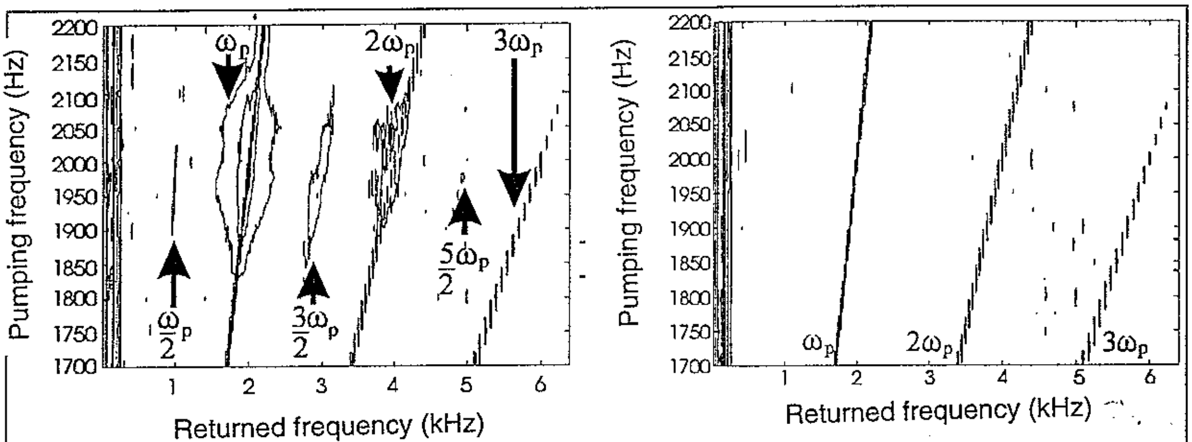

Figure 2.5 Contour plots of the signal detected when: (a) the single tethered bubble of Figure 2.4 is insonated by a series of pump frequency tones (ω_p), incremented in 25 Hz steps from 1700 to 2200 Hz (pump signal amplitude=150 Pa 0-peak); (b) the experiment is repeated with the bubble absent. Vertical axis shows the setting of the pump frequency in Hz [2.113]. Horizontal axis shows, in kHz, the scattered spectrum detected by the receiver.

(iii) Detection through combination frequencies

The power series model of the bubbles as a nonlinear oscillator (equation 2.4) can be used to illustrate how the use of two insonating frequencies can detect and size bubbles. If the driving force consists of the sum of two coherent forces of different frequency, i.e.

$$f \equiv P(t) = P_1 \cos\omega_1 t + P_2 \cos\omega_2 t \ , \qquad (2.5)$$

where $\omega_2 > \omega_1$ (the presence of phase constants would not alter the general result). The quadratic component contains a term which can be expanded to generate the sum and difference frequencies:

$$2P_2P_1 \cos\omega_1 t \,.\cos\omega_2 t = P_2P_1\{\cos(\omega_1+\omega_2)t + \cos(\omega_2-\omega_1)t\} \ . \qquad (2.6)$$

Newhouse and Shankar [2.77] describe the sizing process using the scattered signals generated when a bubble is insonated with a 'pump' frequency ω_p and an 'imaging' frequency ω_i. Experimentally, Shankar et al. [2.10] used a 2.25 MHz 'imaging' beam, the pump signal being scanned across the frequency domain where the bubble resonance could reasonably be expected to lie. When the pump frequency is far from the bubble resonance, the bubble response is of small amplitude and it approximates to a linear oscillator. In that situation, therefore, no sum- and difference-frequencies are detected. When ω_p is near the bubble resonance, the amplitude of oscillation of the bubble wall is large. The bubble oscillations are nonlinear, and they scatter sound nonlinearly. As with the second harmonic, these combination frequencies exhibit a global maximum at resonance, and Shankar et al. [2.10] therefore took the frequency of the pump signal when the sum- and difference-frequencies ($\omega_i \pm \omega_p$) are detected to be the bubble resonance, and so had a measure of the bubble size. Geometrical screening of smaller bubbles by larger ones may occur [2.78]. One advantage of combination-frequency methods is that the bubble resonance generates a signal in the MHz range (close to ω_i), removing it from 'masking' signals such as the acoustic input and ambient noise.

Clinical echocontrast bubbles [2.79, 2.80] and cylindrical gas pockets trapped in hydrophobic pores [2.81-2.84] of μm size have been sized. The fractional Doppler shift, f_{Dop}, in the received signal (the detected frequencies including ω_i, $\omega_i \pm \omega_p$, $(1+f_{Dop})\omega_i$, and $(1+f_{Dop})\omega_i \pm \omega_p$) yielded bubbles size, direction, number density and speed information [2.85], and ranges when pulsed [2.86], giving lateral and longitudinal resolution of better than 1 mm. Bubbles acting in structured populations may give rise to combination frequencies [2.69, 2.87].

There is a simpler explanation of the production of signals at ($\omega_i \pm \omega_p$) [2.89]. The imaging beam scatters from the bubble, and the acoustic scattering cross-section presented to this bubble varies periodically as the bubble pulsates. Therefore the scattered imaging signal is modulated by the bubble pulsation at the driving frequency ω_p, such that signals at $\omega_i \pm \omega_p$ are detected in the received spectrum. The closer ω_p is to the bubble resonance, the greater the amplitude of pulsation, and so the stronger the spectral components at $\omega_i \pm \omega_p$.

As discussed earlier, the nonlinear oscillations of strongly-driven bubbles can give rise to subharmonic emissions (Figure 2.4). Though the power series expansion given in equation 2.4 will not predict subharmonics, an expansion based on Fourier series expansion or perturbation methods will do so [2.88]. Since subharmonic emissions which are produced by resonant bubbles undergoing non-inertial cavitation are associated with surface waves on the bubble surface, unlike the scattering associated with bubble pulsations they do not propagate to distance (see the preceding section). Consequently they are in generate difficult to use for remote sensing. However the stimulation of Faraday waves on the wall of a bubble being driven close to resonance, oscillating as they do at half the driving frequency, will modulate the imaging frequency at $\omega_p/2$, and the received spectrum from resonant bubbles will contain additional components at $\omega_i \pm \omega_p/2$. Since the generation of Faraday waves is a threshold phenomenon, requiring a critical meniscus amplitude of oscillation to be exceeded, the generation of signals at $\omega_i \pm \omega_p/2$ will have a threshold depending on the amplitude of the pump signal [2.89-92].

This explanation of the generation of combination frequencies is reflected in the form of the time-series data from a single tethered bubble insonated at resonance ($\omega_p/2\pi$=2160 Hz) by a pump signal, and an imaging signal resonance ($\omega_i/2\pi$=1.1 MHz), shown in Figure 2.6. The data is sampled at 10 MHz, and the amplitude-modulated 1.1 MHz scattered signal plots so densely as to appear continuously black. In Figure 2.6a the bubble is insonated below threshold, the pump signal amplitude being 25 Pa 0-peak. The amplitude modulation reflects the bubble pulsation frequency. However at a greater amplitude (40 Pa 0-peak) the subharmonic component in the amplitude modulation, caused by the generation of Faraday waves on the bubble wall, is clear (Figure 2.6b).

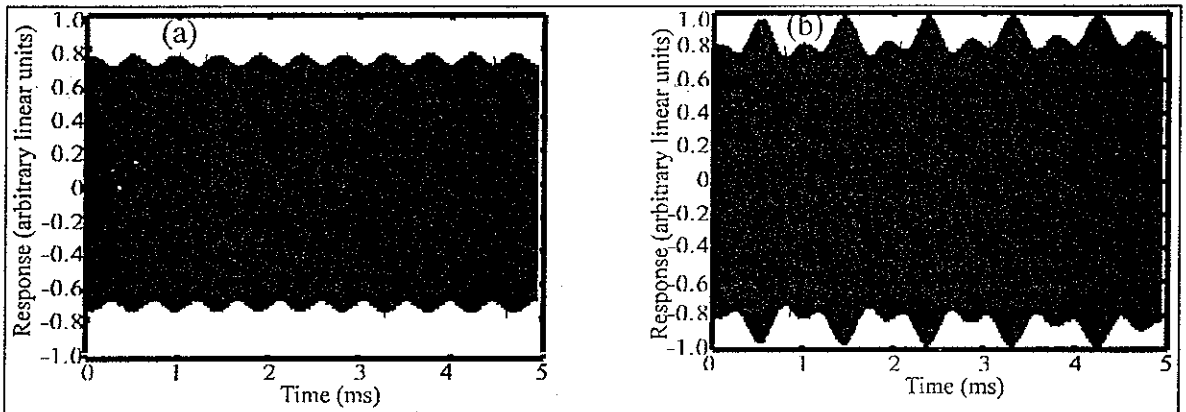

Figure 2.6 The signals, detected by a remote hydrophone which is resonant at 1 MHz and has a half power bandwidth of 450 kHz, scattered from a single tethered bubble which is insonated with a 1.1 MHz imaging signal and a pump signal which is set to the bubble resonance (2160 Hz). The data was sampled at 10 MHz. The high frequency carrier signal plots so densely as to appear black. The pump signal amplitude (zero-to-peak) is (a) 25 Pa, and (b) 40 Pa [AD Phelps, TG Leighton].

Figure 2.7 shows a mesh plot resulting from insonation of a bubble with an imaging frequency of 1.1 MHz and a pump frequency of amplitude 190 Pa. The pump signal is incremented in 25 Hz steps, and for each setting the high-frequency emissions from the bubble are shown in the frequency window from 1.1332 to 1.1373 MHz. To the right of the constant imaging signal is a broken ridge, corresponding to the $\omega_i+\omega_p$ signal, which is present for all 40 pumping tones. The difference in frequency between the two ridges equals the pumping frequency. The $\omega_i+\omega_p$ signal peaks towards the bubble resonance, but that critical frequency is more clearly indicated by the $\omega_i+\omega_p/2$ and $\omega_i+3\omega_p/2$ signals, which peak sharply when the pumping frequency equals 1850 Hz. In certain circumstances(e.g. when high accuracy is required in the resolution of a bubble radius, for example when a bubble is being exploited to measure pressure changes) therefore the $\omega_i+\omega_p/2$ signal may be a better sizing tool than $\omega_i+\omega_p$, as it is sharper and cannot readily be excited through non-bubble mechanisms, such as direct coupling of the transducers [2.91, 2.92] and turbulence [2.93, 2.94]. However the $\omega_i+\omega_p/2$ signal is parametric†, and

† The critical threshold to generate Faraday waves is the amplitude of meniscus oscillation. The bubble wall pulsation amplitude is greatest near resonance, which is where the $\omega_i+\omega_p/2$ signal is excited at its lowest threshold driving pressure. However as the driving pressure is increased, the bubble pulsation amplitude for a given driving frequency increases, and the threshold for the generation of surface waves is

therefore when less well-controlled bubble populations are present, the $\omega_i+\omega_p$ signal may be preferable. Phelps et al. [2.109, 2.111-2] exploited this signal, and used the Doppler shift imparted by the motion of a wide distribution of bubble sizes in the dense bubble population encountered within the surf zone to separate out the bubble-mediated coupling of the ω_i and ω_p signals from that generated by non-bubble techniques.

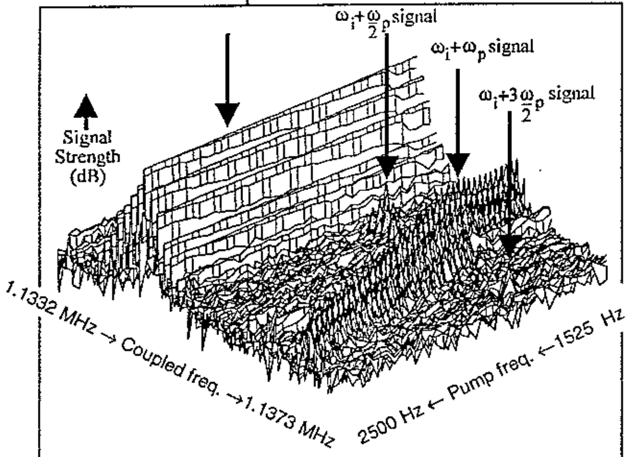

Figure 2.7 Mesh plot of the scattered signal from a single tethered bubble, using the same receiver as in Figure 2.6. The pump signal has an amplitude of 190 Pa 0-peak, and the pumping frequency was incremented in 25 Hz intervals from 1525 to 2500 Hz [AD Phelps, TG Leighton].

Other combination-frequency techniques have been proposed. Strong response at $\omega_1-\omega_0$ and $\omega_1+\omega_0$ may occur when a bubble of breathing-mode resonance ω_0 is excited by a single pump wave of frequency ω_1; and for insonation by two incident signals at ω_1 and ω_2, which excite resonant oscillations in the bubble when $\omega_1-\omega_2=\omega_0$ [2.70]. A third signal, ω_3, incident on the bubble will cause signals at a frequency $\omega_3\pm\omega_0$ to be generated. Providing none of ω_1, ω_2, ω_3 or $(\omega_3\pm\omega_0)$ are close to a bubble resonance, this method could be used to size a population [2.95]. Techniques for the detection of solitary bubbles, based on observing the nonlinear response of a bubble excited by two sound waves, where the difference between the two wave frequencies is equal to the bubble resonance frequency, has been developed [2.96, 2.97]. Naugol'nykh and Rybak [2.98] monitored resonance scattering of bubbles, using a secondary, low-frequency signal (that is, lower than the bubble resonance) to shift the bubble resonance and induce a low-frequency modulation on the scattered signal. The percentage modulation being proportional to the derivative of the bubble-radius distribution function, Naugol'nykh and Rybak predict that the distribution could be reconstructed from the scattered signal.

2.3.4 Characterisation Of Bubbles Using Simultaneous Techniques

Throughout the range of acoustic techniques by which bubble sizing can be achieved, there are inherent limitations as discussed in the preceding sections. Some are appropriate only to relatively high, uniform, bubble population densities [2.66, 2.99], where the inter-bubble spacing is very much less than the acoustic wavelength allowing homogeneous bulk properties to be assigned to the 'bubbly liquid' as a whole. Others may be practicable only at low densities [2.89, 2.101-2]. Several are prone to false triggering, in that some other object (e.g. a solid body, or a cluster of small bubbles [2.103]) may give the same signal as that obtained from a given bubble.

As explained in sections 2.3.2 and 2.3.3, a bubble may be driven by an active acoustic techniques to exploit the acoustic resonance [2.66, 2.99, 2.104] through measurements of sound speed, attenuation, scattering, etc. At a particular frequency the acoustic response

---

exceeded at frequencies increasingly far from resonance. This explanation is supported by experimental observations of the off-resonant threshold [2.89].

of a bubbly liquid is taken to be dominated by bubbles which are resonant with that frequency. The maximum number of different bubble sizes that can be investigated at any one time is determined by the number of different frequencies used, which historically is usually one [2.99, 2.105], but in notable cases has been four [2.66, 2.89] or around nine [2.104] or more [2.33] through the use of well-spaced discrete frequencies (Table 2.1).

Whilst the emission of the second harmonic is a global maximum at resonance, the $2\omega_p$ signal can arise through non-bubble sources of nonlinearity, which must be carefully examined. Such sources do not include solid inhomogeneities. The detection of $\omega_i \pm \omega_p$ [2.106] in the received spectrum has been used to size a bubble spectrum. In converting the acoustic data to bubble population data, a simple assumption is that, bar the presence of resonant bubbles, only ω_i and ω_p are detected. The assumption fails if the pulsation of non-resonant bubbles, or the presence of a quadratic nonlinearity anywhere in the system, is sufficient to generate $\omega_i \pm \omega_p$.

All the techniques outlined in sections 2.3.2 and 2.3.3, which exploit the bubble resonance, suffer in that sources other than resonant bubbles (e.g. off-resonant bubbles, turbulence, transducer effects etc.) can to a greater or lesser extent generate the desired signal, indicating the presence of a resonant bubble when one is not present [2.107]. Such 'false triggering' has not to date been found when signals at $\omega_i \pm \omega_p/2$ are generated if the amplitude component A of the insonating field $P = A\cos\omega_p t + B\cos\omega_i t$ is at the threshold value required to stimulate Faraday waves on the bubble surface [2.102]. However because of its parametric nature this technique is one of the most difficult to employ if the pump sound field amplitude cannot be easily specified accurately at the point of interest.

The less prone a system is to 'false triggering', the more complicated in general it is to deploy. It therefore would be desirable to be able to deploy a range of these techniques to interrogate a given liquid sample, either sequentially or concurrently as defined by the problem. This would enable optimisation of the process of characterising the bubble population in the liquid with respect to minimising the ambiguity of the result and the complexity of the task. The task itself involves first the detection of inhomogeneities in liquids. In certain circumstances it is then necessary to analyse the sample further to distinguish gas bubbles from solid or immiscible liquid-phase inclusions. The final stage of analysis would involve not only the detection, but also the sizing of the gas inclusions, leading to the characterisation of the bubble population. This can be summarised in a four-part *Ideal objective* [2.108]: (i) Detect inhomogeneities in liquids; (ii) Distinguish gas bubbles from solids; (iii) Measure radii of bubbles present; (iv) Measure number of bubbles in each radius class.

A method by which the *ideal objective* might eventually be achieved, uses a range of techniques. The limitations of each can be compensated through the deployment of others. The principle of the Characterisation of Bubbles Using Simultaneous Techniques (COBUST) has been investigated [2.33, 2.109, 2.110] using the methods listed in Table 2.1: Bubble detection is achieved through the geometric scattering of 3.5 MHz ultrasound (using a scanner in both B and M modes simultaneously), and through scattering of signals at ω_p, $2\omega_p$, $\omega_p/2$, $\omega_i \pm \omega_p$, $\omega_i \pm 2\omega_p$, $\omega_i \pm \omega_p/2$ and $\omega_i \pm 3\omega_p/2$. This is done for broadband, and increasing, incremented, tonal 'pump' signals (the former reducing the frequency range, and therefore the duration of the measurement, for the latter test).

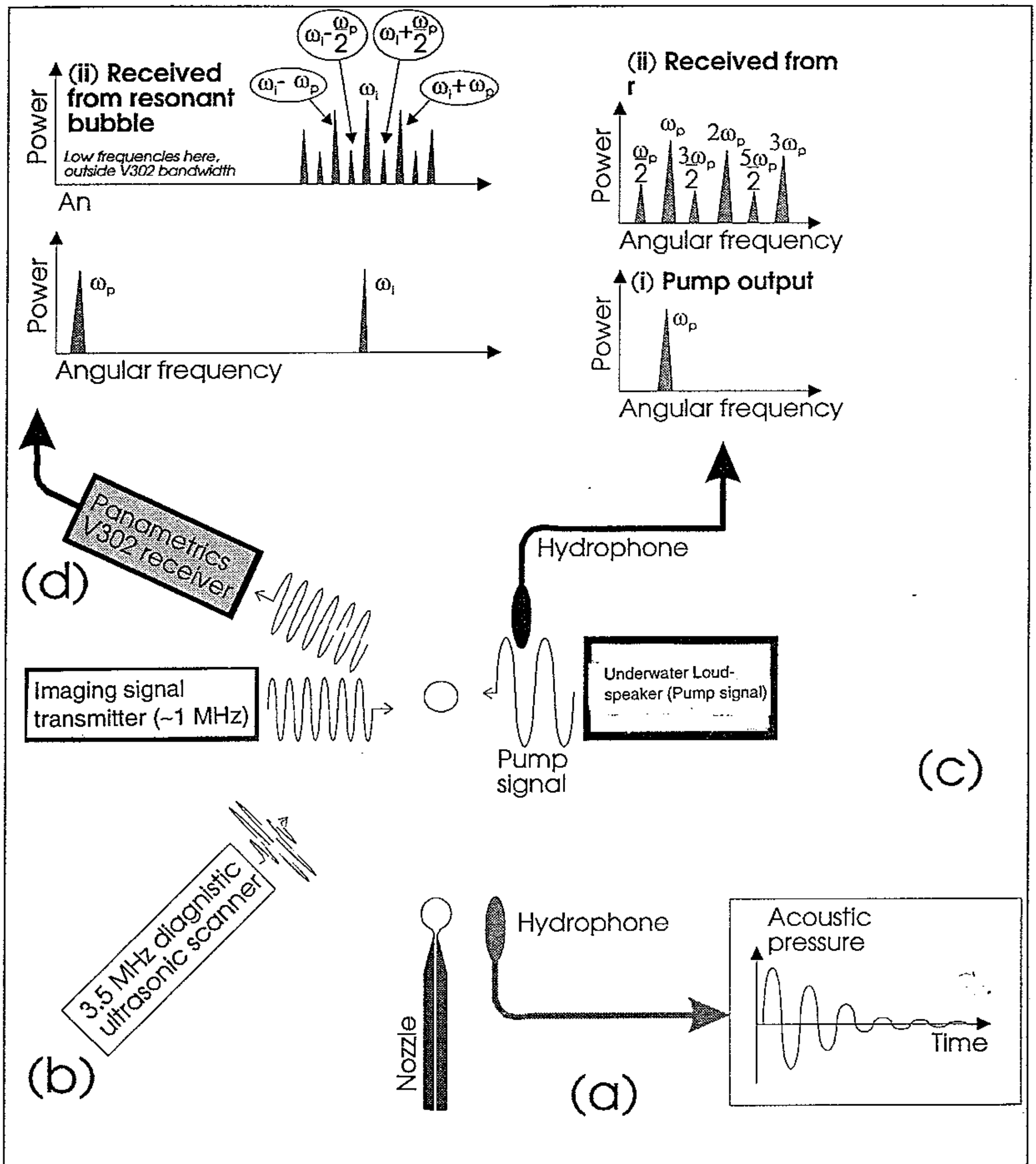

Figure 2.8 Schematic illustration of the apparatus used for COBUST measurements.

The apparatus employed for COBUST is shown schematically in Figure 2.8. Upon injection from a nozzle the bubble is sized from its passive acoustic emissions (an exponentially-decaying sinusoid shown in grey in Figure 2.8a). The pump signal generated at ω_p (by the *Pump signal loudspeaker*) and the scattered spectrum analysed in terms of the first, second, third etc. the subharmonic, and the ultraharmonic (the input and scattered spectra are shown in Figure 2.8c). By additionally introducing the high frequency "imaging" transmitter and receiver, the spectrum of combination frequencies can also be analysed, and the bubble presence inferred through the scattering of signals at $\omega_i \pm \omega_p$, $\omega_i \pm 2\omega_p$, $\omega_i \pm \omega_p/2$, etc. (Figure 2.8d). In addition geometrical scattering using a 3.5 MHz foetal scanning system is shown in Figure 2.8b. Though the wavelength is in general not sufficiently small to obtain good radius resolution directly with geometrical scattering, certain information can be inferred from the rise time as measured in the M-mode of the scanner operation.

The experimental details are summarised in reference [2.33]. The various scattered signals generated when two bubbles are tethered 1 cm apart upon a wire, when the pump frequency is stepped in 50 Hz increments from 2.7 to 4.7 kHz, are seen in figure 2.9. Scattering of the fundamental (ω_p) and of the combination frequencies $\omega_i \pm \omega_p$ broadly show the presence of bubbles (resonant at around 3.2 and 3.9kHz). However the clearest indication is seen through scattering of $\omega_i \pm \omega_p/2$. One technique for identifying the population would be to use $\omega_i \pm \omega_p/2$ to identify the bubble resonances, and $\omega_i \pm \omega_p$ to count the number of bubbles at those resonant frequencies [2.91-2].

However, the great advantage of the combination frequency techniques are seen when the COBUST system is to use to size streams of rising bubbles. First, the region through which the pump frequency is to be incremented is determined using broadband insonation, through examination of the detected scatter around the pump and imaging frequencies (i.e. the spectra detected by the *Hydrophone* and the *High frequency receiver* in Figure 2.8c and 2.8d respectively). Bubble-mediated changes to the spectra occur in the region 3.3 to 4.3 kHz (Figure 2.10) and it is through this range that the pump signal is subsequently incremented (in steps of 100 Hz).

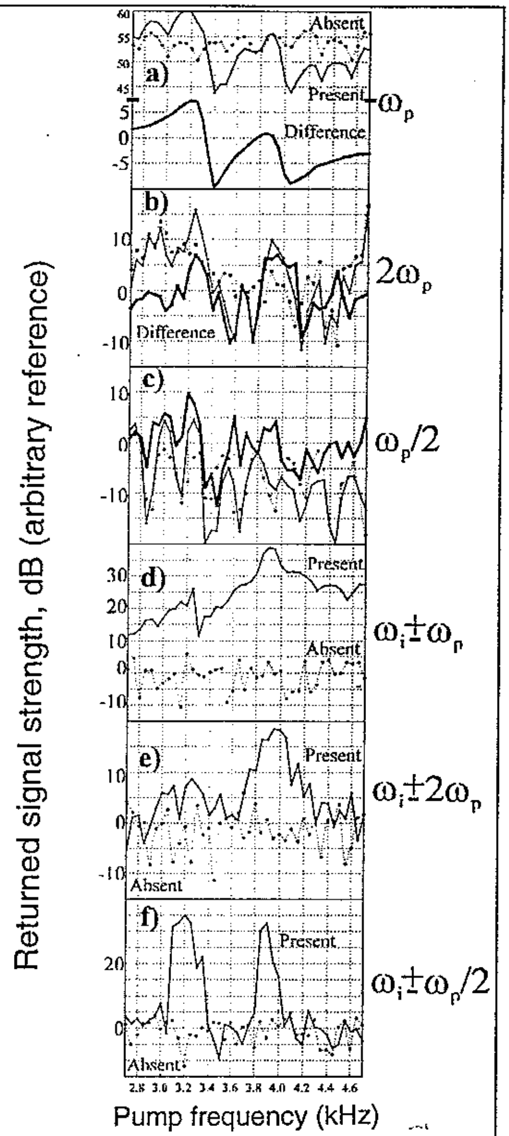

Figure 2.9 Shown as a function of the pump frequency are the scattered signals (dB relative to arbitrary reference such that 0 dB is the average noise floor) at a) ω_p b) $2\omega_p$ c) $\omega_p/2$ d) $\omega_i \pm \omega_p$ e) $\omega_i \pm 2\omega_p$ f) $\omega_i \pm \omega_p/2$ when two tethered bubbles, 1 cm apart, are insonated with incremented pump tones (120 Pa 0-peak amplitude) in 50 Hz ascending steps. The 'bubble absent' (≡dotted line) and 'bubble present' (≡thin solid line) signals are shown, and their ratio (≡the 'bubble mediated amplification', the thick solid line) is shown in parts (a)-(c) only. The signals in 2.9(a)-(c) come from the hydrophone in Fig. 2.8(c), whilst simultaneously the signals in Fig. 2.9(d)-(f) come from the receiver in Fig. 2.8(d).

The scattering at frequencies relating to harmonics, ultra harmonics and subharmonics of the bubble resonance do not in these figures clearly indicate that resonance [2.33]. However the combination-frequency spectra obtained for each setting of the pump frequency are stacked adjacent to one another in a greyscale plot in figure 2.11. The $\omega_i \pm \omega_p$ signal is present at all settings of the pump frequency ω_p. Though it does peak in amplitude at a pump frequency of $\omega_p /2\pi$ = 3.7 kHz, the clearest indication that this is the resonance of the bubbles in the stream is given by this simultaneous additional appearance of structure at $\omega_i \pm \omega_p/2$, $\omega_i \pm 2\omega_p$, $\omega_i \pm 3\omega_p/2$ at a pump frequency setting of 3.7 kHz.

The general COBUST system is adaptable to a range of environs, and has recently been deployed in a pipe of diameter 10 cm [2.102].

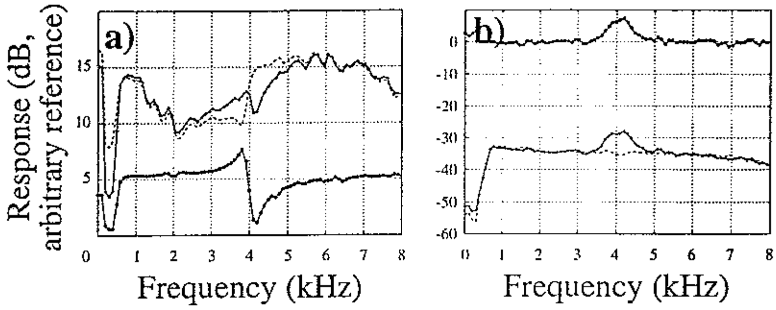

Fig. 2.10 Response (modulus of voltage transfer) for broadband insonation (band limited 1-8 kHz) of rising bubbles, from a) hydrophone, and b) heterodyned high-frequency receiver. Resolution: 98 Hz. Key: Dashed line: No bubbles present. Thin line with cross data points: Bubbles present. Thick line with circle data points: the bubble-mediated amplification.

2.3.5 Relating the scattered signal to the bubble population density

This is clearly a key stage in determining the population of stable bubbles. The details are too involved to report here. However in general the acoustic data is converted to bubble population statistics by employing a model of the response of the bubble to the sound field. As such the conversion algorithm will contain the limitations of the model, though this may be ameliorated somewhat through the use of calibration data or prior knowledge of the expected form of the population to evaluate the optimum values for adjustable parameters [2.77, 2.104, 2.111]. Therefore when any algorithm is considered a number of important issues should be raised to assess its limitations. Two important ones are:

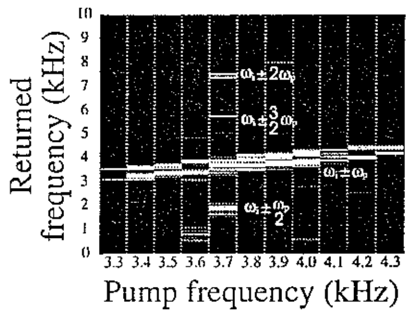

Fig. 2.11 Greyscale histogram showing heterodyned received signal (from V302) for each discrete setting of the pump frequency (100 Hz increments). Light shades indicate strong signal. Signals at $\omega_i \pm \omega_p/2$, $\omega_i \pm \omega_p$, $\omega_i \pm 3\omega_p/2$ and $\omega_i \pm 2\omega_p$ are indicated.

- How accurate is the model of the bubble dynamics?

Even single bubble models can become increasingly involved as such aspects as liquid compressibility, gas dynamics and heat conduction are considered, In general for bubble sizing the emphasis has been on the simpler models. The degree to which the nonlinearity of the bubble is considered is clearly important given the dependence of many models on the spectrum of the sound scattered by the bubble.

- What is limitation on population density? Many techniques are visualised through the dynamics of single bubbles, and to analyse a population the simplest assumption is to superimpose the results/predictions from such single-bubble models. However as the population becomes increasingly dense then the resulting errors increase (because, for example, the resonance of a bubble becomes affected by its neighbours [2.37]). When multiple-scattering or cloud effects (see section 2.7) occur, these must be considered. Alternatively, if the 'bubbly medium' is modelled as having effective bulk properties, is this model valid for wavelengths much smaller than the inter-bubble spacing?

- Are there any other features (solid particles, turbulence etc.) within the medium which can give rise to the acoustic signal which the algorithm will interpret to be bubbles?

Given the complexity of bubble dynamics, ground-truthing and cross-calibration are recommended for all bubble sizing systems.

2.3.6 Invasiveness of acoustic techniques

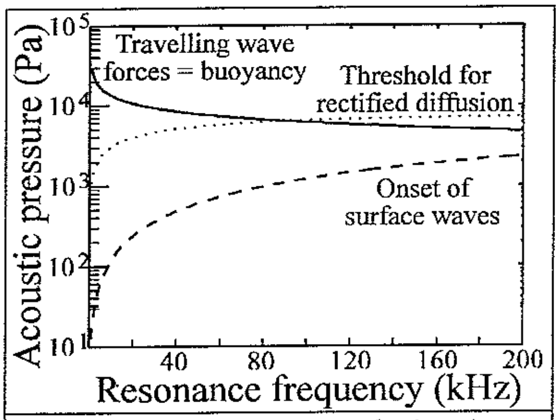

Fig. 2.12. Plot demonstrating the invasiveness of acoustic techniques, showing: thresholds for surface waves (dashed), & rectified diffusion (dotted); and equivalence of radiation force with buoyancy (unbroken) [2.110].

Acoustic detection techniques which rely on the bubble resonance work well because of the excellent coupling between bubbles and the sound fields which drive them into oscillation. However because of this coupling, it is relatively easy for the sound field to alter the bubble population (section 1.2). To be minimally invasive, the pump signal amplitude must be relatively low. To examine this the thresholds for generating the $\omega_i \pm \omega_p/2$ signal (calculated from that for surface wave generation [2.89-90]), and for inducing bubble growth in resonant bubbles by rectified diffusion [2.100] was calculated in the range 0-200 kHz. Though the radiation force from a travelling wave acoustic field, which may induce bubble translations, has no threshold, an estimate of its importance can be found by calculating [2.22, 2.114] that acoustic pressure amplitude at which the force equals that of buoyancy. These are shown in Fig. 2.12. Detection using $\omega_i \pm \omega_p/2$ at the threshold amplitude is unlikely to be invasive in this respect [2.110], but it would be advisable for workers to record the acoustic pressure amplitudes *at the bubble* (if possible) when using any acoustic technique.

2.4 Optical detection techniques

Acoustic signals for bubble detection and sizing are perhaps both the most versatile and the most complicated. Optical techniques are in contrast often readily interpreted, but are unsuitable for small bubbles†, or opaque liquids or containers. Much optical detection does not require either non-inertial or inertial bubble volume change, which is generally prerequisite for erosive and chemical detection (Section 3), and acoustic techniques other than geometrical ultrasonic scattering.

There are broadly speaking two classes of optical technique for the monitoring of non-inertial cavitation. First, light scatter from controlled populations (often single bubbles) can, for example, determine the wall dynamics in detail [2.115-7]. Under such controlled conditions, deviations from sphericity (either oscillatory or in equilibrium shape) common in large bubbles can be overcome [2.118]. However, unless such measures are taken, two-dimensional optical images can often be difficult to relate to the volume‡ of the bubble. Second, the change in opacity when a bubble cloud passes through a sensing volume can give an estimate of the population, though clearly this is insensitive to the type of cavitation occurring.

† In contrast to optical detection, the pulsation resonance frequency reflects the bubble volume, and varies roughly inversely with the equilibrium radius (R_0), making it suitable for sizing small bubbles.

‡ See previous footnote.

Optical techniques which are applied under (usually laboratory) controlled conditions include: exsolution visualisation on pressure reduction above liquids [2.119]; Mie scattering [2.120-24]; and light and electron microscopy [2.125-8] (resolving radii down to 10^{-9} m [2.125-6]). Holograms [2.129], which have resolved down to about 10 μm radius [2.130-1], have been taken at up to 300,000 holograms/s [2.132-4]. Field measurements generally afford less sophisticated techniques. At sea [2.135], photography of bubbles either risen onto a transparent plate [2.136] (though they may dissolve on rising [2.137]) or *in situ* [2.138] may lack the resolution to accurately count the smallest bubbles [2.139] and poor statistics may also have limited observations [2.140]. Image processing has been incorporated to such techniques to obtain bubble size and the distance from the focal plane from the blurring and mean brightness [2.141]. Young discusses a range of techniques [2.142].

There are a variety of methods, including photography and rise-time measurements [2.33], which may be applicable to examine the bubble population generated during high-power ultrasound when the ultrasound, and associated radiation forces has ceased. Techniques relevant to high power insonation are discussed in Section 3.

Given the ability of the optical scattering to follow the wall motion of a bubble which is being driven acoustically, it may be that there is potential to produce an optical technique for deducing the size distribution of bubbles in a cloud by insonating the cloud with sequential tones and correlating the observed modulation of light scatter with the bubbles resonant at that tone (or from the frequency content of the modulation during broadband insonation). Such a technique bears similarities with the two-frequency methods (section 2.3.3(iii)), and could readily be used in conjunction with it, or incorporated into a COBUST system.

In summary therefore optical measurements have use for sizing stable bubbles. However their applicability with respect to quantifying high power ultrasonic fields generating cloud cavitation is more limited, and will be discussed in Section 3. In such clouds the overall transmission loss of a light beam is perhaps one of the most useful quantitative measures, though it cannot readily distinguish between inertial and non-inertial cavitation.

2.5 Electrical detection techniques

As entities having electrical properties differing from those of the liquid they displace, bubbles can give rise to a number of electrical signals which can be used to sense their presence. However many electrical detectors are sensitive neither to bubble radius distribution nor to the type of cavitational activity which is occurring (e.g. inertial or noninertial- see section 3.8). Exceptions include systems where the sensor is coupled to an acoustic technique which drive bubbles to pulsate, so incorporating resonance detection into the envelope signal being monitored (as discussed for optical techniques in the previous section),

(i) Electrical conductivity

Given prior knowledge of the conductivity of the gas and of the liquid involved, observation of the changes in bulk electrical conductivity of a liquid as bubbles are introduced provides a measure of the free-gas volume fraction (void fraction), spatially averaged over the measurement volume [2.143]. The technique is usable in void fractions greater than 1%, where optical and acoustic measurements are complicated by multiple scattering [2.27].

(ii) Coulter counting

The Coulter counter belongs to that range of techniques which, like optical scattering, exploit signals that detect an inhomogeneity in the liquid, and not specifically bubbles. As such, though versatile, these systems must be carefully examined when an unknown sample is tested for bubbles to ensure that a solid or liquid inhomogeneity is not causing an ambiguity. Suspended in an electrolyte, the inhomogeneities should flow one at a time through a smaller aperture between electrodes, across which the resistance is measured. Transient changes in the resistance can be related to the volume of the inhomogeneity, since each homogeneity displaces its own volume of electrolyte. Several thousand inhomogeneities per second can be counted. Bubbles as small as 3.5 μm radius have been detected [3.144]. Comparative bubble detection with optical scattering and Coulter counting has been made [3.142, 3.145].

(iii) Capacitance techniques

The presence of bubbles can be detected through measurement of capacitance, since if a liquid occupies the volume between the plates of a capacitor, then the presence of any bubbles in that liquid will tend to reduce the capacitance (the dielectric constants of liquids being in general higher than those of gases) [2.146]. A measurement of the capacitance is however degenerate, in that more than one bubble population condition can give rise to a given output so that, for example, the measurement can fail to distinguish large bubble from a cloud of smaller ones. It can be adapted to give radius discrimination by driving the bubbles with a pump frequency, and detecting the modulation in the measured capacitance, and assuming that the modulation is due to bubbles resonant with the pump field [2.147].

2.6 Venturi techniques

As discussed in section 1.3.2, a specific pressure drop will cause some, but not all, bubbles to undergo inertial cavitation, depending on the initial size of the bubble. That pressure drop need not be applied acoustically: it may also be generated hydrodynamically. In a Venturi tube a constriction in the flow causes a pressure drop: bubbles of an appropriate size will undergo inertial cavitation and generate rebound pressure pulses [2.48], the detection of which allows inference about the population of bubbles which entered the sensor. A system might use flow rates of 1.5 litres/sec, testing for bubbles larger than ~10 μm radius. The system is clearly invasive in that all bubbles so detected will have undergone substantial growth (involving a degree of exsolution), and rapid collapse (probably involving fragmentation).

2.7 Bubble clouds

Many of the techniques described earlier in this chapter are presented from the physics of a single bubble. When bubbles in clouds are being examined, two issues should be addressed: Account must be taken if such single-bubble signals are modified by the presence of neighbours; The possibility exists of new signals, associated with the cloud, which can be used to characterise the bubble population.

Single bubble signals might be altered because the sensing beam can be multiply scattered (be it optical, acoustical etc. [2.149]). In addition the physics of the interaction of the bubble with the sensor might be altered by the proximity of other bubbles [2.37].

Bubble clouds have in addition resonances peculiar to the cloud itself, the lowest modes of which can be at frequencies much lower than those of the individual bubbles which make up the cloud [2.150-2.155]. Cloud characteristics can be inferred from the scattering at such frequencies [2.156]. In addition there are a range of other acoustic effects to which the cloud can give rise [2.157-2.166]. Given these issues and the availability of new methods for producing controlled bubble clouds [2.167], calibration checks against known, dense populations are recommended.

2.8 Conclusions

There are a variety of methods that may be employed for the detection of stable bubbles. Whilst optical techniques can readily be interpreted (to give, for example, bubble shape) they are difficult to use in opaque environments and most give two-dimensional images. Apart from shadowgraphy, the acoustic techniques described all fundamentally rely on exploitation of the bubble as a resonator. Whilst passive emissions can be used to determine the population upon entrainment, other techniques are required to examine the bubbles at a later time. All have advantages and disadvantages, particularly as regards the possibilities of the desired signal being extractable from bubbles other than resonant size, and even in the absence of any bubbles. Full and complete sizing of a given bubble population may well be achievable only through combination of a range of simultaneous techniques. Advances have been made by combining acoustic techniques (section 2.3.4). There are a number of signals which, on their own, do not give good radius discrimination when applied to a bubble cloud (e.g. ultrasonic geometrical scattering, optical scattering, electrical effects). Monitoring such a signal for modulation at bubble resonances whilst simultaneously driving bubbles to resonate with an acoustic pump field can provide such resolution. Consideration must be given to the invasiveness of finite amplitude acoustic fields when incident on bubbles undergoing non-inertial oscillation. Such fields can alter the distribution and size spectrum of the bubble population through radiation forces, rectified diffusion, and by inducing bubble fragmentation and coalescence [2.22§4]. Other techniques, such as the venturi method, are highly invasive (section 2.3.6).

The aim of this report is to discuss methods of characterising cavitation in a high-power ultrasonic field. The major task has to be to characterise the bubble activity which generates effects associated with high energy acoustic cavitation. These will be discussed in Section 3. Whilst the ability to determine the population of stable bubbles is important (section 1.4), it is of secondary importance. In this section therefore the acoustic detection methods were discussed with emphasis on the associated bubble dynamics, and the non-acoustic effects introduced. However for details of the sizing of stable bubbles the reader is referred to reference [2.27].

References

2.1. Detsch, R.M., Sharma, R.N., The critical angle for gas bubble entrainment by plunging liquid jets. The Chemical Engineering Journal 1990; 44: 157-166.

2.2. Lin, T.J., Donnelly, H.G., Gas bubble entrainment by plunging laminar liquid jets. AIChE J. 1966; 12: 563-571.

2.3. Watkins, R. D., Barrett, L. M., McKnight, J. A. Ultrasonic waveguide for use in the sodium coolant of fast reactors. Nucl. Energy, 1988; 27: 85-89.

2.4. Lions N et al. Special instrumentation for Phenix. Fast reactor power stations. Thomas Telford, London, 1984, pp 525-535.

2.5. Day CK, Smith RW. Undersodium viewing. IEEE Trans 1974; SU-21, No. 3, July.

2.6. McKnight JA et al. The use of ultrasonics for visualising components of the prototype fast reactor whilst immersed in sodium. Ultrasonics Internatioal 83. Butterworth Scientific 1983, pp 135-140

2.7. McKnight JA et al. Recent advances in the technology of under-sodium inspection in LMFBRs. Liquid metal engineering and technology. BNES, London, 1984; 1: 423-430

2.8. Aguilar A, Por G. Monitoring Temperature reactivity corefficient by noise methods in a NPP at full power. Ann. nucl. Energy 1987;14, 521-526

2.9. Apfel, R.E., Methods in Experimental Physics Vol. 19 (Ed. Edmonds, P.D.) Academic Press, New York 1981; 355-413.

2.10. Shankar, P. M., Chapelon, J. Y. and Newhouse, V. L. Fluid pressure measurement using bubbles insonified by two frequencies. Ultrasonics, 1986; 24: 333-336.

2.11. Hulshof, H. J. M., Schurink, F. Continuous ultrasonic waves to detect steam bubbles in water under high pressure. Kema Scientific and Technical Reports, 1985; 3: 61-69.

2.12. Belcher, E. O. Quantification of bubbles formed in animals and man during decompression, IEEE Trans. Biomed. Eng., 1980; 27: 330-338.

2.13. Kisman, H. Spectral analysis of Doppler ultrasonic decompression data. Ultrasonics, 1977; 15: 105-110.

2.14. Tickner, E. G. Precision microbubbles for right side intercardiac pressure and flow measurements. In: Contrast Echocardiography, Meltzer, R. S., Roeland, J. (eds.), (Nijhoff, London). 1982

2.15. Gross DR, Miller DL, Williams AR. A search for ultrasonic cavitation within the cardiovascular system. Ultrasound Med Biol 1985; 11: 85-97

2.16. Dowson D, Unsworth A, Wright V. Proc. Tribology Conv. (London: Inst. Mech. Eng.) 1971; pp. 120-127

2.17. Dowson D, Unsworth A, Wright V. Ann. Rheumatic Dis. 1971; 30: 348-358

2.18. Dowson D, Unsworth A, Wright V. Cracking of human joints - cavitation in metacarpio-phalangeal joint. Ind Lub Tri 1971; 26: 212

2.19. Urick RJ. Principles of underwater sound, 3rd edn. McGraw-Hill, New York 1983; pp. 202-209

2.20. Buckingham MJ. On acoustic transmission in ocean-surface waveguides. Phil. Trans. R. Soc. Lond. A 1991; 335: 513-555

2.21. Buckingham M. Acoustic daylight: Imaging the ocean with ambient noise. Nature 1992; 356: 327-329

2.22. Leighton TG. The Acoustic Bubble. Academic Press, London, 1994

2.23. Anderson I, Bowler S. Oceans spring surprise on climate modellers. New Scientist 1990; 125: 1707

2.24. Woolf, D. K. Bubbles and the air-sea transfer velocity of gases. Atmos.-Ocean 1993; 31: 451-474

2.25. Charlson, R.J., Lovelock, J.E., Andreae, M.O., Warren, S.G. Oceanic phytoplankton, atmospheric sulphur, cloud albedo and climate. Nature 1987; 326: 655-661.

2.26. Watson, A.J., Upstill-Goddard, R.C., Liss, P.S. Air-sea gas exchange in rough and stormy seas measured by a dual-tracer technique. Nature 1991; 349: 145

2.27. Nyborg WL (ed.) Cavitation Detection and Monitoring. Report by Working Group 22 of Accredited Standards Committee S1 of the Acoustical Society of America. in preparation.

2.28. Morriss SL and Hill AD. Ultrasonic imaging and velocimetry in two-phase pipe flow. *Trans. ASME* (1993) **115** 108-116

2.29. Van der Welle R. Void fraction, bubble velocity and bubble size in two phase flow. *Int. J. Multiphase Flow* (1985) **11** 317-45
2.30. Kolbe WF, Turko BT and Leskovar B. Fast ultrasonic imaging in a liquid filled pipe. *IEEE Trans. Nucl. Sci.* (1986) **33** 715-722
2.31. Blackledge JM. B-scan imaging of two phase flows. IEE Colloquium on 'Ultrasound in the process industry', p5/1-17 Sept. 23rd 1993
2.32. Wolf J. Investigation of bubbly flow by ultrasonic tomography. Part. Part. Syst. Charact. 1988; 5: 170-173
2.33. Leighton TG, Ramble DG and Phelps AD. 1995. Comparison of the abilities of multiple acoustic techniques for bubble detection. Proc. Inst. of Acoustics, **17** (8), 149-160
2.34. Minnaert, M. On musical air-bubbles and sounds of running water, Phil. Mag. 1933; 16: 235-248.
2.35. Walton, A.J., Reynolds, G.T. Sonoluminescence. Advances in Physics 1984; 33: 595-660.
2.36. Strasberg M . Gas bubbles as sources of sound in liquids. J Acoust Soc Am 1956 ; 28: 20-26
2.37. Strasberg M. The pulsations frequency of nonspherical bubbles in liquid. J Acoust Soc Am 1953; **25**: 536-537
2.38. Leighton, T. G. and Walton, A. J. An experimental study of the sound emitted from gas bubbles in a liquid. Eur. J. Phys. 1987; 8: 98-104.
2.39. Longuet-Higgins MS, Kerman BR, Lunde K. The release of air bubbles from an underwater nozzle. J Fluid Mech 1991; 230:365-390
2.40. Leighton TG, Schneider MF and White PR. 1995. Study of bubble fragmentation using optical and acoustic techniques. Sea Surface Sound '94. Proc. 3rd Meeting on Natural Physical Processes related to Sea Surface Sound, MJ Buckingham, JR Potter, eds., (World Scientific Publishing Ltd., Singapore) 414-428
2.41. Pumphrey HC, Crum LA, Bjørnø L. Underwater sound produced by individual drop impacts and rainfall. J Acoust Soc Am 1989; 85: 1518-1526
2.42. Pumphrey HC, Elmore PA. The entrainment of bubbles by drop impacts. J Fluid Mech 1990; 220:539-567
2.43. Medwin H, Kurgan A, Nystuen JA. Impact and bubble sound from raindrops at normal and oblique incidence. J Acoust Soc Am 1990; 88: 413-418
2.44. Pumphrey HC, Walton AJ. Experimental study of the sound emitted by water drops impacting on a water surface. Eur J Phys 1988; 9:225-231
2.45. Medwin H, Beaky MW. Bubble sources of the Knudsen sea noise spectra. J Acoust Soc Am 1989; 86:1124-1130
2.46. Updegraff, G.E., Anderson, V.C. Bubble noise and wavelet spills recorded 1 m below the ocean surface. J. Acoust. Soc. Am. 1991; 89: 2264.
2.47. Nishi, RY. Ultrasonic detection of bubbles with Doppler flow transducers. Ultrasonics 1972; 10: 173-179
2.48. Medwin H. Counting bubbles acoustically: a review. Ultrasonics 1977; 15: 7-14
2.49. Thorpe SA, Hall AJ. The characteristics of breaking waves, bubble clouds and near-surface currents observed using side-scan sonar. Continental Shelf Res 1983; 1:353-384
2.50. Farmer DM, Vagle S. Waveguide propagation of ambient sound in the ocean-surface bubble layer. J Acoust Soc Am 1989; 86: 1897-1908
2.51. Daniels, S., Paton, W.D.M., Smith, E.B. An ultrasonic imaging system for the study of decompression induced gas bubbles. *Undersea Biomed. Res.*, 1979; 6: 197.
2.52. Mackay RS, Rubisson JR. Decompression studies using ultrasonic imaging of bubbles. IEEE Trans on Biomed Eng 1978; BME-25: 537-544
2.53. Fry FJ, Goss SA. Further studies of the transkull transmission of an intense focused ultrasonic beam: lesion production at 500 kHz. Ultrasound Med biol 1980; 6; 33-38
2.54. Frizzel LA, Lee CS, Aschenbach PD, Borrelli MJ, Morimoto RS, Dunn F. Involvement of ultrasonically induced cavitation in hind limb paralysi of the mouse neonate. J Acoust Soc Am 1983; 74: 1062-1065
2.55. Watmough DJ, Davies HM, Quan, KM, Wytch R, Williams AR. Imaging microbubbles and tissues using a linear focussed scanner operating at 20 MHz: possible implications for the detection of cavitation thresholds. Ultrasonics 1991; 29: 312
2.56. ter Haar, G.R., Daniels, S., Evidence for ultrasonically induced cavitation *in vivo*. Phys. Med. Biol. 1981; 26: 1145-1149.

2.57. Morton, K.I., ter Haar, G.R., Stratford, I.J., Hill, C.R. The role of cavitation in the interaction of ultrasound with V79 Chinese hamster cells *in vitro*. Br. J. Cancer 1982; 45: Suppl. V. 147.
2.58. ter Haar, G.R., Daniels, S., Morton, K. Evidence for acoustic cavitation *in vivo*: Thresholds for bubble formation with 0.75-MHz continuous-wave and pulsed beams. IEE Trans. UFFC 1986; 33:162-164.
2.59. Beck, T.W., Daniels, D., Paton, W.D.M., Smith, E.B. The detection of bubbles in decompression sickness. Nature 1978; 276: 173.
2.60. Fowlkes JB, Carson PL, Chiang EH, Rubin JM. Acoustic generation of bubbles in excised canine urinary bladders. J Acoust Soc Am 1991;89: 2740-2744
2.61. Fairbank WM, Scully MO. A new non-invasive technique for cardiac pressure measurement: resonant scattering of ultrasound from bubble. IEEE Trans on Biomed Eng 1977; BME-24: 107-110
2.62. Commander KW, Moritz E. Off-resonance contribution to acoustical bubble spectra. J Acoust Soc Am 1989; 85: 2665-266985.
2.63. Commander KW, McDonald RJ. Finite-element solution of the inverse problem in bubble swarm acoustics. J Acoust soc am 1991; 89: 592-597
2.64. Clay CS, Medwin H. Acoustical Oceanography: Principles and Applications. 1977 Wiley, New York
2.65. Breitz N, Medwin H. Intrumentation for in situ acoustical measurements of bubble spectra under breaking waves. J Acoust Soc Am 1989; 86:739-743
2.66. Ye Z and Ding L. Acoustic dispersion and attenuation in bubbly mixture. J Acoustic Soc Am 1995; **98**: 1629-1636
2.67. Bleeker HJ, Shung KK, Barnhart JL. Ultrasonic characterization of Albunex™, a new contrast agent. J Acoust Soc Am 1990; 87: 1792-1797
2.68. Fanelli M, Prosperetti, A Reali M. Shape oscillations of gas-vapour bubbles in liquids. Part 1: Mathematical formulation. Acustica 1984; 55: 213-223
2.69. Donskoi, D.M., Zamolin, S.V., Kustov, L.M., Sutin, A.M., Nonlinear backscattering of acoustic waves in a bubble layer. Acoustics Letters 1984; 7: 131
2.70. Butkovsky, O. Ya., Zabolotskaya, E.A., Kravtsov, Yu. A., Petnikov, V.G., Ryabikin, V.V. Possibilities of active nonlinear spectroscopy of inhomogeneous condensed media. acta physica slovaca 1986; 36: 58
2.71. Tucker DG, Wesby VG. Ultrasonic monitoring of decompression. Lancet 1968; 1: 1253
2.72. Miller DL. Ultrasonic detection of resonant cavitation bubbles in a flow tube by their second harmonic emissions. Ultrasonics 1981; 19; 217-224
2.73. Miller DL, Williams AR, Gross DR. Characterisation of cavitation in a flow-through exposure chamber by means of a resonant bubble detector. Ultrasonics 1984; 22: 224-230
2.74. Vacher M, Giminez G, Gouette R. Nonlinear behaviour of microbubbles: application to their ultrasonic detection. Acustica 1984; 54: 274-283
2.75. Blackstock DT. History of nonlinear acoustics and a survey of Burgers' and related equations. In: Nonlinear Acoustics, Proceedings of the Symposium held at Applied Research Laboratories, The University of Texas at Austin, 1969, ed. Muir TG (AD 719 936), pp. 1-27
2.76. Pfeiler M, Matura E, Ifflä nder H, Seyler G. Lithotripsy of renal and biliary calculi: physics, technology and medical-technical application. Electromedica 1989; 57: 52-63
2.77. Newhouse, V. L., Shankar, P. M. Bubble size measurement using the nonlinear mixing of two frequencies. J. Acoust. Soc. Am., 1984; 75: 1473-1477.
2.78. Chapelon JY, Shankar PM, Newhouse VL. Ultrasonic measurement of bubble cloud size profile. J Acoust Soc Am 1985; 78: 196-201
2.79. Schmitt RM, Schmitt HJ, Siegert J. *In vitro* estimation of bubble diameter distribution with ultrasound. IEEE Eng in Med and Biol Soc 1987; 9th Ann Conf, 13-6
2.80. Siegert J, Schmitt RM, Schmitt HJ, Fritzsch T. Application of a resonance method for measuring the size of bubbles in an echocontrast agent. IEEE Eng in Med and Biol Soc 1987; 9th Ann Conf, 13-6
2.81. Quain RM, Waag RC, Miller MW. The use of frequency mixing to distinguish size distributions of gas-filled micropores. Ultrasound Med Biol 1991; 17: 71-79
2.82. Miller, D.L. Experimental investigation of the response of gas-filled micropores to ultrasound. J. Acoust. Soc. Am. 1982; 71: 471-476.
2.83. Miller, D.L. Theoretical investigation of the response of gas-filled micropores and cavitation nuclei to ultrasound. J. Acoust. Soc. Am. 1983; 73: 1537-1544.

2.84. Miller, D.L. On the oscillation mode of gas-filled micropores. J. Acoust. Soc. Am. 1985; 77(3): 946-953.
2.85. Chapelon JY, Newhouse VL, Cathignol D, Shankar PM. Bubble detection and sizing with a double frequency Doppler system. Ultrasonics 1988; 26: 148-154
2.86. Cathignol D, Chapelon JY, Newhouse VL, Shankar PM. Bubble sizing with high spatial resolution. IEEE Trans. Ultrasonics, Ferroelectrics and freq. Control 1990; 37 : 31
2.87. Ostrovsky LA, Sutin AM. Nonlinear sound scattering from subsurface bubble layers. In: Natural physical sources of underwater sound. Kerman BR, ed. Kluwer academic publishers (Dordrecht, The Netherlands), 1992
2.88. Jordan DW, Smith P. Nonlinear ordinary differential equations. 2nd edition (1987), Oxford University Press, Chapter 7
2.89. Phelps A, Leighton TG. 1996. High resolution bubble sizing through detection of the subharmonic response with a two frequency excitation technique. J. Acoust. Soc. Am. **99**, 1985-1992
2.90. Phelps A, Leighton TG. 1996. The subharmonic oscillations and combination frequency emisisons from a resonant bubble. Acta Acustica. In press
2.91. Phelps AD and Leighton TG. Investigations into the use of two frequency excitation to accurately determine bubble sizes. Proc. IUTAM Conf. on Bubble Dynamics and Interface Phenomena (Birmingham 1993). ed. J. R. Blake et al., 1994, pp.475-483
2.92. Phelps AD and Leighton TG. 1995. Automated bubble sizing using two frequency excitation techniques. Sea Surface Sound '94. Proc. 3rd Meeting on Natural Physical Processes related to Sea Surface Sound, MJ Buckingham, JR Potter, eds., (World Scientific Publishing Ltd., Singapore) 332-341.
2.93. Korman MF, Beyer RT. Nonlinear scattering of crossed ultrasonic beams in the presence of turbulence in water: I Experiment. J Acoust Soc Am 1988; 84: 339-349
2.94. Korman MF, Beyer RT. Nonlinear scattering of crossed ultrasonic beams in the presence of turbulence in water: II Theory. J Acoust Soc Am 1989; 85: 611-620
2.95. Bunkin, F.V., Vlasov, D.V., Zabolotskaya, E.A., Kravstov, Yu. A. Active acoustic spectroscopy of bubbles. Sov. Phys. Acoust. 1983; 29: 99-100
2.96. Ostrovskii L, Sutin A. Nonlinear acoustic methods in diagnostics. In: Ultrasound diagnostics, Grechova ed., Gorky, pp. 139-150 (in Russian).
2.97. Sandler B, Selivanovskii, D, Sokolov A.Measurement of gas bubble concentration on the sea surface. Doklady Akademii Nauk SSSR. 260, 6, 1474-1476 (1981, in Russian)
2.98. Naugol'nykh, K.A., Rybak, S.A. Interaction of sound waves in scattering by bubbles. Sov. Phys. Acoust. 1987; 33: 94
2.99 Medwin H. In situ acoustic measurements of microbubbles at sea. *J Geophys Res* (1977) **82** 971-976
2.100 Eller AI. Growth of bubbles by rectified diffusion. J Acoust. Soc. Am., 1969; **46**: 1246-1250
2.101 Newhouse VL and Shankar PM. Bubble size measurement using the nonlinear mixing of two frequencies. *JASA.* (1984) **75** 1473-1477
2.102 Leighton TG, Ramble DG and Phelps AD. Measurement of bubbles in a pipe using multiple acoustic and ultrasonic techniques. ISVR Technical Report No. , June 1996
2.103 Nishi RY. Ultrasonic detection of bubbles with Doppler flow transducers. *Ultrasonics* 1972; **10** 173-179
2.104 Farmer DM and Vagle S. Waveguide propagation of ambient sound in the ocean-surface bubble layer. *JASA.* (1989) **86** 1897-1908
2.105 Thorpe SA. Measurements with an Automatically Recording Inverted Echo Sounder; ARIES and the Bubble Clouds. *Journal of Physical Oceanography* (1986) **16** 1462-1478
2.106 Koller D, Li Y, Shankar PM and Newhouse VL. High-speed bubble sizing using the double frequency technique for oceanographic applications. *IEEE J. Oceanic Engineering* (1992) **17** 288-291
2.107 Leighton TG. Acoustic Bubble Detection. I. The detection of stable gas bodies *Environmental Engineering* 1994; **7** 9-16
2.108 Leighton TG, Phelps AD, Ramble DG and Sharpe DA. Comparison of the abilities of eight acoustic techniques to detect and size a single bubble. 1996 *Ultrasonics*, in press.
2.109. Leighton TG, Phelps AD, and Ramble. Acoustic bubble sizing: from laboratory to the surf zone trials. Acoustic Bulletin 1996; **21**: 5-12

2.110. Leighton TG, Ramble DG, and Phelps AD. Bubble detection using low amplitude multiple acoustic techniques. Proc. 3rd European Conference on Underwater Acoustics (ed. J. Papadakis; Heraklion, June 1996). 1143-1147

2.111. Phelps AD, Ramble DG and Leighton TG. The use of a combination frequency technique to measure the surf zone bubble population. In preparation.

2.112. Phelps AD, Ramble DG and Leighton TG. Characterisation of the oceanic bubble population using a combination frequency technique. Proc. 3rd European Conference on Underwater Acoustics, (ed. J. Papadakis; Heraklion, June 1996). 1149-1154

2.113. Phelps AD. Characterisation of the subharmonic response of a resonant bubble using a two-frequency technique. PhD thesis, University of Southampton, 1995

2.114. Coakley WT and Nyborg WL. *Chapter II: Cavitation; dynamics of gas bubbles; applications* in F. Fry Ed., *Ultrasound: its applications on medicine and biology* Elsevier, Amsterdam, 1978, Part 1 pp. 77-159

2.115. Gaitan DF, Crum LA. Observation of sonoluminescence from a single cavitation bubble in a water/glycerine mixture. In: Frontiers of Nonlinear Acoustics, 12th ISNA. Hamilton MF, Blackstock DT, eds. (Elsevier, New York) 1990, p. 459

2.116. Gaitan DF, Crum LA, Church CC, Roy RA. An experimental investigation of acoustic cavitation and sonoluminescence from a single bubble. J Acoust Soc Am 1992; 91: 3166-3183

2.117. Holt RG and Crum LA. Acoustically forced oscillations of air bubbles in water: Experimental results. J Acoust Soc Am., 1992; **91**: 1924-1932

2.118. Asaki TJ, Marston PL and Trinh EH. Shape oscillations of bubbles in water driven by modulated ultrasonic radiation pressure: Observations and detection with scattered light. J Acoust Soc Am 1993; **93**: 706-713

2.119. Finkelstein Y, Tamir A. Formation of gas bubbles in supersaturated solutions of gases in water. AIChE J., 1985; 31: 1409

2.120. Marston, P.L. Critical angle scattering by a bubble: physical-optics approximation and observations. J. Opt. Soc. Am. 1979; Vol. 69, No. 9: 1205

2.121. Marston, P.L., Kingsbury, D.L. Scattering by a bubble in water near the critical angle: interference effects. J. Opt. Soc. Am. 1981; Vol. 71, No. 2: 358

2.122. Marston, P.L., Langley, D.S., Kingsbury, D.L. Light scattering by bubbles in liquids: Mie theory, physical-optics approximations, and experiments. Applied Scientific Research 1982; 38: 373-383.

2.123. Langley, D.S., Marston, P.L. Scattering of laser light from bubbles in water at angles from 68 to 85 degrees. SPIE 1984; Vol. 489 Ocean Optics VII: 142

2.124. Langley, D.S., Marston, P.L. Critical-angle scattering of laser light from bubbles in water: measurements, models, and application to sizing of bubbles. Applied Optics 1984; Vol. 23, No. 7: 1044

2.125. Yount DE, Strauss RH. Bubble formation in gelatine: a model for decompression sickness. J Appl Phys 1976; 47: 5081-5088

2.126. Yount DE. Skins of varying permeability: a stabilisation mechanism for gas cavitation nuclei. J Acoust Soc Am 1979; 65: 1429-39

2.127. Yount DE, Yeung CM. Bubble formation in supersaturated gelatine: A further investigation of gas cavitation nuclei. J Acoust Soc Am 1981; 69: 702-715

2.129. Hentschel W, Zarschizsky H, Lauterborn W. Recording and automatical analysis of pulsed off-axis holograms for determination of cavitation nuclei size spectra. Optics Communications 1985; 53: 69-73

2.130. Hüttmann G, Lauterborn W, Schmitz E, Tanger H. Holography with a frequency doubled Nd:YAG laser. SPIE (Holography techniques and applications) 1988; 1026: 14-21

2.131. Nyga R, Schmitz E, Lauterborn W. In-line holography with a frequency doubled Nd:YAG laser for particle size analysis. Applied Optics 1990; 29: 3365-3368

2.132. Hentschel W, Lauterborn W. High speed holographic movie camera. Optical Engineering 1985; 24: 687-691

2.133. Lauterborn, W., Koch, A. Holographic observation of period-doubled and chaotic bubble oscillations in acoustic cavitation. Phys. Rev. 1987; A35: 1974-1976.

2.134. Hentschel W, Merboldt K-D, Ebeling K-J, Lauterborn W. High speed holocinematography with the multiply cavity-dumped argon-ion laser. J Photogr Sci 1982; 30: 75-78

2.135. Blanchard DC, Woodcock AH. Bubble formation and modification in the sea and its meteorological significance. Tellus 1957; 9:145-158

2.136. Kolovayev PA. Investigation of the concentration and statistical size distribution of wind produced bubbles in the near-surface ocean layer. Oceanology 1976; 15: 659-661

2.137. Thorpe S. On the clouds of bubbles formed by breaking wind-waves in deep water, and their role in air-sea gas transfer. Philos. Trans. R Soc London 1982; A 304: 155-210

2.138. Johnson BD, Cooke RC. Bubble populations and spectra in coastal waters: a photographic approach. J. Geophys. Res. 1979; 84, C7: 3761-3766

2.139. Walsh AL, Mulhearn PJ. Photographic measurements of bubble populations from breaking waves at sea. J Geophys Res 1987; 92:14553-14656

2.140. MacIntyre F. On reconciling optical and acoustic bubble spectra in the mixed layer. In: Oceanic whitecaps and their role in air-sea exchange processes. Monanhan EC, O'Muircheartaigh I, eds. D. Reidel Pub. Co., Dordrecht, Holland, 1986; pp. 95-100.

2.141. Jähne B and Geißler P. An imaging optical technique for bubble measurements. Sea Surface Sound '94. Proc. 3rd Meeting on Natural Physical Processes related to Sea Surface Sound, MJ Buckingham, JR Potter, eds., (World Scientific Publishing Ltd., Singapore) 290-303

2.142. Young FR. Cavitation. McGraw-Hill Book Company (London). 1989

2.143. Lamarre E and Melville K. Instrumentation for the measurement of void fraction in breaking waves: Laboratory and field results. IEEE J. Ocean Engineering, 1992; **17**: 204-215

2.144. Pyum JJ, Keller A and Hammitt FG. Fluids Engineering Division, ASME, 1975, Paper 75-FE-15

2.145. Keller A, Yilmaz E and Hammitt FG. Report UMICH 01357-36-T, Dept. Mech. Eng., University of Michigan, Ann Arbor, 1974.

2.146. Cheremisinoff NP (ed.). Encyclopaedia of Fluid Mechanics: Volume 1. Flow Phenomena and Measurement (Houston, TX: Gulf).

2.147. Hardwick AJ and Walton AJ. The acoustic bubble capacitor: a new method for sizing gas bubbles in liquids. Meas. Sci. Technol. 1995; **6**: 202-205

2.148. Trevena DH. Cavitation and Tension in Liquids. Adam Hilger, Bristol and Philadelphia, 1987.

2.149. Skelton, E.A., Fitzgerald, W.J., An invariant imbedding approach to the scattering of sound from a two-phase fluid. J. Acoust. Soc. Am. 1988; 84: 742

2.150. Prosperetti A. Bubble-related ambient noise in the ocean. J Acoust Soc Am Suppl 1 1985; 78: S2

2.151. Carey WM. Low-frequency ocean surface noise sources. J Acoust Soc Am suppl 1985; 78: S1-S2

2.152. Prosperetti A. Bubble dynamics in oceanic ambient noise. In: Sea Surface Sound. Ed Kerman BR, Kluwer Academic, Norwell, MA, 1988, pp.151-172

2.153. Carey WM. Low-frequency noise and bubble plume oscillations. J Acoust Soc Am suppl 1987; 82: S62

2.154. Carey WM, Browning D. Low-frequency ocean ambient noise: measurements and theory. In: Sea surface sound, ed Kerman BR, Kluwer Academic, Norwell MA, 1988

2.155. Prosperetti A. Bubble-related ambient noise in the ocean. J Acoust Soc Am 1988; 84: 1042-1054

2.156. Roy RA, Carey W, Nicholas M, Crum LA. Low-frequency scattering from bubble clouds. Proc. 14th International Congress on Acoustics, Beijing, China, 1992.

2.157. Donskoi, D.M., Zamolin, S.V., Kustov, L.M., Sutin, A.M., Nonlinear backscattering of acoustic waves in a bubble layer. Acoustics Letters 1984; 7: 131

2.158. Kustov LM, Nazarov VE, Ostrovskii LA, et al. Acoust. Lett. 1982; 6:15

2.159. Ostrovsky LA, Sutin AM. Nonlinear sound scattering from subsurface bubble layers. In: Natural physical sources of underwater sound. Kerman BR, ed. Kluwer academic publishers (Dordrecht, The Netherlands), 1992

2.160. Kobelev, Yu., Ostrovsky, L., Sutin, A. Self-illumination effects for acoustic waves in a liquid with gas bubbles. Pis'ma v ZhETF, 1979; 30, 7: 423-425.

2.161. Kobelev, Yu., Ostrovsky, L., Sutin, A. Self-induced transparency and frequency conversion effects for acoustic waves in water containing gas bubbles. In: "Cavitation and inhomogeneities in underwater acoustics". W. Lauterborn (ed.), Springer-Verlag, Berlin-Heidelberg-New York 1980; pp. 151-156.

2.162. Kustov, L., Nazarov, V., Sutin, A. Narrowing of directivity pattern of acoustic radiation in bubble layer. Sov. Phys. Acoustics 1987; 33, 3.

2.163. Omta R. Oscillations of a cloud of bubbles of small and not so small amplitude. J Acoust Soc Am 1987; 82: 1018-1033

2.164. d'Agostino L, Brennen CE. Acoustical absorption and scattering cross sections of spherical bubble clouds. J Acoust Soc Am 1988; 84: 2126-2134

2.165. d'Agostino L, Brennen CE. On the acoustical dynamics of bubble clouds. ASME Cavitation and multiphase forum, American Society of Mechanical Engineers, New York, 1983: 72

2.166. Miksis MJ, Ting L. Effects of bubbly layers on wave propogation. J Acoust Soc Am 1989; 86:2349-2358

2.167. Hwang PA, Roy RA and Crum LA. Artificial bubble cloud targets. Sea Surface Sound '94. Proc. 3rd Meeting on Natural Physical Processes related to Sea Surface Sound, MJ Buckingham, JR Potter, eds., (World Scientific Publishing Ltd., Singapore) 270-289

3. TECHNIQUES FOR THE DETECTION OF INERTIAL CAVITATION

3.1 Cavitation in ultrasonic fields

As discussed in section 1, the characterisation of cavitation in an ultrasonic field is no simple matter, for two reasons. First, non-inertial cavitation alone will occur if one is below the threshold for inertial cavitation. However if one is above the threshold for some bubbles in the population, then both inertial and non-inertial cavitation will occur together (the threshold being dependent both on the initial bubble size and on the acoustic pressure amplitude, which may well vary spatially throughout the liquid sample). Second, one must be clear whether the technique and underlying analysis is appropriate to determining the *threshold* for cavitational activity, or the *degree* of activity, which occurs within a system.

3.2 Acoustic detection techniques

3.2.1 Characterising the degree of cavitational activity through acoustic emissions from a cavitation field

This section will discuss techniques generally applicable to assessing the activity which occurs when ultrasound (generally tone-burst or continuous wave) passes through a population of bubbles. Though not exclusively so, the discussion is relevant to a bubble population containing a broad size in radii[†]. The applicability of the techniques for determining the threshold and degree of cavitational activity will be explored.

As discussed in Section 1, bubble volume changes can cause the emission of acoustic waves [3.1, 3.2]. In Section 2 some of the emissions associated with the nonlinear oscillations of non-inertial bubbles were discussed. Inertial cavitation can also generate acoustic emission. Degeneracy does exist: line spectra and broadband signals, for example, have been detected from both inertial and non-inertial cavitation. In certain circumstances such signals prove to be difficult to use for characterisation of cavitation, since it is not always possible to determine the type of bubble activity responsible for its generation.

In 1980 Neppiras [3.3] summarised the available experimental data as a progression of emissions. If a liquid containing a bubble population is insonated at low power levels, continuous-wave at the fundamental frequency ω_p, the detected acoustic emissions are at ω_p only. At higher intensities, but below the threshold level required to generate inertial cavitation, harmonics are emitted at integer multiples of ω_p up to high order. The $2\omega_p$ emission is prominent, its amplitude being proportional to the square of the fundamental. The physics of the dynamics of single bubbles which relate to such emissions are expounded in Section 2. Low-level broadband continuum noise is present, which becomes very strong as the inertial cavitation threshold is approached. The $\omega_p/2$ subharmonic appears intermittently, the duration of the emission being much shorter than the 'off-times'. Other subharmonics and ultraharmonics can be detected.

[†] After all, if significant cavitation does occur, bubble fragmentation might be expected.

When inertial cavitation occurs, there is an increase in the level of the acoustic emissions (broadband continuum, harmonic, ultraharmonic and subharmonic emissions) above that encountered when non-inertial cavitation only occurs. This phenomenon has the potential for indicating the onset of violent cavitation. The increase in the subharmonic prompted some workers in the past to use it as an indicator of the onset of inertial cavitation. However there are two potential problems.

- First, though the level of subharmonic increases when effects associated with violent cavitation occur, there are a number of bubble-mediated processes, both inertial and non-inertial, which can give rise to a signal at $\omega_p/2$ [3.4§4.3.7]. If conditions allow the assumption that only inertial cavitation is occurring, then subharmonic generation may occur through the prolonged expansion phase and delayed collapse which can occur during inertial cavitation, the bubbles surviving for one, two or three acoustic cycles before collapse [3.5]. Neppiras [3.3] also suggests that a form of periodic unstable oscillation of a bubble driven at twice its resonance near threshold, might emit at subharmonic frequencies. However, as Vaughan and Leeman [3.6] stated in 1986, "the generation of fractional harmonics, in particular the first and third half-harmonic, is a general characteristic of non-linear bubble pulsation and does not specifically indicate the occurrence of transient cavitation".

How such signals can arise from the dynamics of a single bubble is discussed in Section 2. These need re-assessing when a population is being considered. Though they have the lowest amplitude threshold for excitation [3.7], surface waves do not, however, give rise to an emission from single bubbles which propagates to distance. The question of a co-operative effect in a cloud has not been addressed. At a higher threshold, such emission might be the result of the acoustic field acting on a population of bubbles containing, either wholly or in part, bubbles with an equilibrium radius twice the size of the radius which would be the pulsation resonance of the acoustic field [3.8]. Similar mechanisms involving progressively larger bubbles to account for the lower subharmonics were proposed. At high amplitudes the spherical pulsations of single bubbles themselves can contain a subharmonic component [3.4§4.47].

When one has a poorly-characterised sound field acting upon an unknown bubble population, the fact that a signal may arise by more than one mechanism makes it difficult to use as a sizing tool. For a large bubble population in a powerful acoustic field, commonly some bubbles will be undergoing non-inertial, and some inertial, cavitation. All the above mechanisms may operate. In addition broadband contributions may occur. Non-inertial bubbles may contribute to this noise through the emission of microbubbles from large-amplitude surface waves[‡] [3.9], or to reversion of the oscillations of shocked bubbles out of the steady-state, so that their own natural frequencies appear in the spectrum [3.3]. Such 'noise' would then be dependent on the bubble population, and have structure. Random frequencies, unconnected with ω_p, were thought to be the result of the shock excitation of large bubbles which would then oscillate at their own natural pulsation resonances [3.10]. Broadband contributions from inertial cavitation are discussed in the next section.

[‡] See Figure 1.3

• Second, although the increase in the level of acoustic emissions from an insonated sample which is commensurate with the onset of 'violent' cavitation is readily observable, it is no simple matter to interpret from those levels the degree of cavitation activity which is occurring. A far more tractable problem is to attempt to correlate the level of acoustic emission with some other effect (erosion, luminescence, chemical or biological changes). There are two ways of viewing this. It may be seen as an indirect form of characterising the cavitation, inherently limited by our knowledge of how the complex process of cavitation gives rise to the two phenomenon that are being correlated. However, in many aspects of the application of high power ultrasound, it is not the characterisation of cavitation *per se* which is of primary interest, but of the effect (chemical, erosive etc.) which that cavitation might produce. Therefore by introducing a calibration based on the correlation of an effect which is relatively simple to monitor real-time (such as acoustic emission) with the less readily measured effect in which one is interested, the complicated unknown of the characteristics of the cavitation are by-passed. How realistic such a proposition is will be discussed in Section 4. Attempts to correlate acoustic with other indicators of inertial cavitation range from investigations on the relationship between acoustic emission and cavitation erosion [3.11], to attempts to monitor the effect of ultrasound on biological materials. Examples of the latter include the exploitation of subharmonic acoustic emissions [3.12], and additionally broadband acoustic signals [3.13], to relate the acoustic emission to the biological effects and damage induced by the ultrasound in cells suspended *in vitro*. Eastwood and Watmough [3.14] measured the sound produced when human blood plasma was made to sonoluminesce. Attempts to correlate the presence of the half-harmonic with the onset of violent cavitation and sonoluminescence are inconclusive [3.4§4.3.7]. Experiments have shown that the appearance of the half-harmonic is not correlated to the onset of sonoluminescent activity [3.15-3.18] (see section 3.4). Such investigations into the *onset* of activity when a sample is subjected to power ultrasound raise the question of whether one is studying the threshold of cavitation itself, or the threshold for significant activity (section 1), or a detection threshold which is a characteristic of the sensor. These issues are outlined in the following section where the discussion tends not towards tone-burst or continuous-wave power insonation generating a continuously-recycling cavitation field, the main topic of this section. Rather, the following section discusses the detection of the cavitation threshold itself using short pulses of ultrasound and detection systems sensitive to, and interpretable from, the dynamics of single bubbles.

3.2.2 The acoustic detection of short-lived inertial cavitation

Previous sections have employed the concept of a relatively steady-state cavitational response. In Section 2 the bubble, a resonator, could be driven to emit a range of acoustic signals, involving for example pulsations or surface waves. Whilst with rare exceptions [3.19] inertial cavitation of a individual bubble is not a steady state phenomenon, the preceding section discusses the steady state response of a cavitation *field*. In such fields, whilst individual bubbles, whether undergoing either inertial and non-inertial cavitation, often have limited lifetimes because of fragmentation, or coalescence through Bjerknes forces, the dynamics of the population are averaged over many thousands of bubbles, and as such tend to a steady state. Even if the insonation is not continuous-wave but rather tone-burst, then the time average activity tends to a steady state [3.4§5.3].

If however one is discussing the threshold for cavitation, then single events are of importance and a steady-state model is inappropriate. Whilst such experiments can be undertaken with continuous-wave insonation, waiting several minutes for the nucleation of an event, they are in effect not assessing the cavitation threshold one would find if the sample were subdivided into an appropriate number of sub-volumes, each of which was tested independently. Rather, the procedure entails awaiting the occurrence within the sensing volume of the detector of a cavitation nucleus of a type appropriate to the local acoustic pressure and frequency at that site. Such experiments are therefore sparsely nucleated. The liquid might be filtered, or degassed, and the peak acoustic pressure amplitude less than that required to nucleate cavitation throughout most of the liquid; when they occur, the nuclei may be provided by transient cosmic rays or neutron radiation [3.4§2.1.2b].

To determine the threshold for cavitation under controlled conditions, required for the testing of predictive measures such as the Mechanical Index (section 1.3.3), in recent years tests have concentrated on the use of short (μs order) pulses of ultrasound on samples with clearly-defined acoustic focal regions where the acoustic pressure is known, and into which seed nuclei of predetermined properties can be introduced. Such studies allow, for example, the clarification of the detection threshold of different sensors, which can be deployed simultaneously. Such studies have also arisen because of the need to assess the likelihood of cavitation-induced effects during exposure. By the mid 1980's calculations suggested that inertial cavitation could occur in liquids in response to such ultrasonic pulses [3.19-3.23]. Free radical production within the collapsing bubble had also been indicated for microsecond pulses in experiments [3.24-3.27]. Of particular importance for clinical applications are techniques which are minimally invasive beyond the effect caused by the primary cavitating beam. These fall into two broad types: those which detect the pressure wave emitted into the liquid on rebound, and those which exploit the enhanced reverberation of the primary beam which the bubbles cause.

(i) Detection through rebound pressure pulses

In 1968 West and Howlett [3.28] set up a 20.25 kHz (continuous-wave) standing-wave condition in a cylindrical transducer filled with degassed tetrachloroethylene. At certain times, related to the phase of the continuous-wave field, they nucleated the medium using a pulsed neutron source. The shock waves emitted by the collapsing bubbles were used to count the number of cavitation events (up to 25 bubbles per second, compared to about one per minute when no neutron source was used).

The short duration of rebound shocks indicates a broad frequency content. Negishi [3.29] found a continuum in the acoustic spectrum occurred when he detected sonoluminescence. Kuttruff [3.30] confirmed these results by examining the circular shock waves produced by cavities undergoing inertial collapse using Schlieren optics. He showed that the emission of photons was coincident to that of shock waves, and concluded that the luminescence occurred during the final stages of bubble collapse.

Roy et al. [3.31] subjected liquid to a continuous-wave spherically-symmetric stationary acoustic field generated at 61.725 kHz within a spherical resonator. The acoustic pressure amplitude was automatically ramped until cavitation sufficient for the detection of sonoluminescence through photomultiplication just occurred. In addition the operator could listen in on the liquid contained within the spherical cavitation cell via headphones connected to a microphone. Audible 'clicks' or 'pops' were taken to indicate inertial cavitation. They found that the pressure threshold for audible sound emission was always less than or equal to that for sonoluminescence. They deduced that "sound and light emission indicate thresholds for two different types of phenomena associated with inertial cavitation", and concluded that "if one desires a threshold for 'violent' cavitation, then sonoluminescence is a fitting criterion", and that "light emission may serve as an ideal indicator of what Apfel [3.19] calls the 'threshold for transient-violent cavitation'."

The resonant bubble detector (RBD) described in section 2.3.3(i) has been employed in attempts to detect the 'stable' bubble products following shock-induced inertial cavitation downstream from the exposure site of a Dornier System lithotripter [3.32]. Extracorporeal shock wave lithotripsy (ESWL) is a technique by which short pulses of high pressure are focused into the body in order to break kidney or gall stones [3.33]. The 1.65 MHz continuous-wave RBD was sensitive to bubbles of radius $R_0=2\pm0.5$ μm at the detection site. Though bubbles were detected *in vitro* in water and blood, and in blood pumped by the heart through a plastic arterio-venous shunt, cavitation was not detected *in vivo* in the canine abdominal aorta. The RBD effectively detects through the non-inertial oscillations it excites in relatively long-lasting bubbles. Since lithotripter cavitation is characterised by inertial cavitation and rapid changes in bubble size, the stable bubbles being the remnants from collapse, a more direct form of detection would employ the energetic emissions associated with rapid changes in bubble size. Coleman et al. [3.34, 3.35] detected cavitation produced by an electrohydraulic lithotripter using, as a passive remote hydrophone, a focused bowl lead zirconate titanate (PZT) piezoceramic transducer, of 100 mm diameter and 120 mm focal length in water, the focus measuring 5 mm (on axis) by 3 mm wide. This transducer had a 1 MHz resonance: the detection process would therefore correspond to its response to the broadband signal characteristic of the rebound pressure pulse. Coleman et al. [3.34] detected a two-peak structure in the rebound pressures emitted from the cloud of cavitating bubbles at the focus, which correlation with the time-resolved sonoluminescence indicated to be the result of the rebound pressure pulses emitted from the first and second rebounds of the bubble. The interval between these rebounds is weakly dependent on the initial bubble size, suggesting that this technique might potentially be exploited to gain information about cavitation nuclei *in vivo*. By scanning the detector focus over the cavitation field during repeated lithotripter shocks in a water bath, the spatial distribution of the cavitation sources of these emission could be mapped out, and compared with the spatially-resolved sonoluminescence and cell lysis [3.35]. It is interesting to note that a skilled operator can, by listening to the secondary acoustic emissions during clinical lithotripsy, determine whether or not the shock has hit the stone [3.36].

(ii) Passive acoustic detection through reverberation

If an ultrasonic pulse causes inertial cavitation, the sudden extensive bubble growth associated with the event may cause enhanced reverberation of the ultrasonic pulse, both through the presence of the expanded bubbles, and through the increase in gas bodies present after the collapse (the net volume of gas in the fragments may be greater than that contained within the seeds owing to the exsolution of previously-dissolved gas during the expansion). Atchley et al. [3.37] used this enhanced scattering to find acoustic pressure thresholds for the cavitation as a function of pulse duration and pulse repetition frequency at insonation frequencies of 0.98 and 2.30 MHz, for distilled, degassed, deionized water, filtered to 0.2 μm and seeded with hydrophobic carboxyl latex particles (1 μm diameter). Similar experiments [3.31, 3.38, 3.39] used short tone bursts of ultrasound to find the threshold acoustic pressure amplitude for inertial cavitation in a fluid which was carefully prepared to remove uncontrolled seed nuclei (e.g. solid particles) before the introduction of a known nuclei population (including Albunex™ spheres, and hydrophobic polystyrene spheres of nominal radius 0.5 μm).

Figure 3.1 shows the output of the passive detector of Roy et al. [3.40] with and without cavitation. The top trace (a) illustrates the primary pulse from the 757 kHz transducer, followed by a stable low-amplitude background resulting from multiple-path scattering and reverberation in the fluid-filled test chamber. Its stability is testament to the stationary nature of the scattering surfaces. In the lower trace, (b), this scattered background contains a perturbation indicative of a time-varying scatterer, which Roy et al. showed to be at the focal region of the primary transducer. Such signals indicate cavitation. The apparatus used to obtain this result in addition contained an active detection system, and is described in the next section.

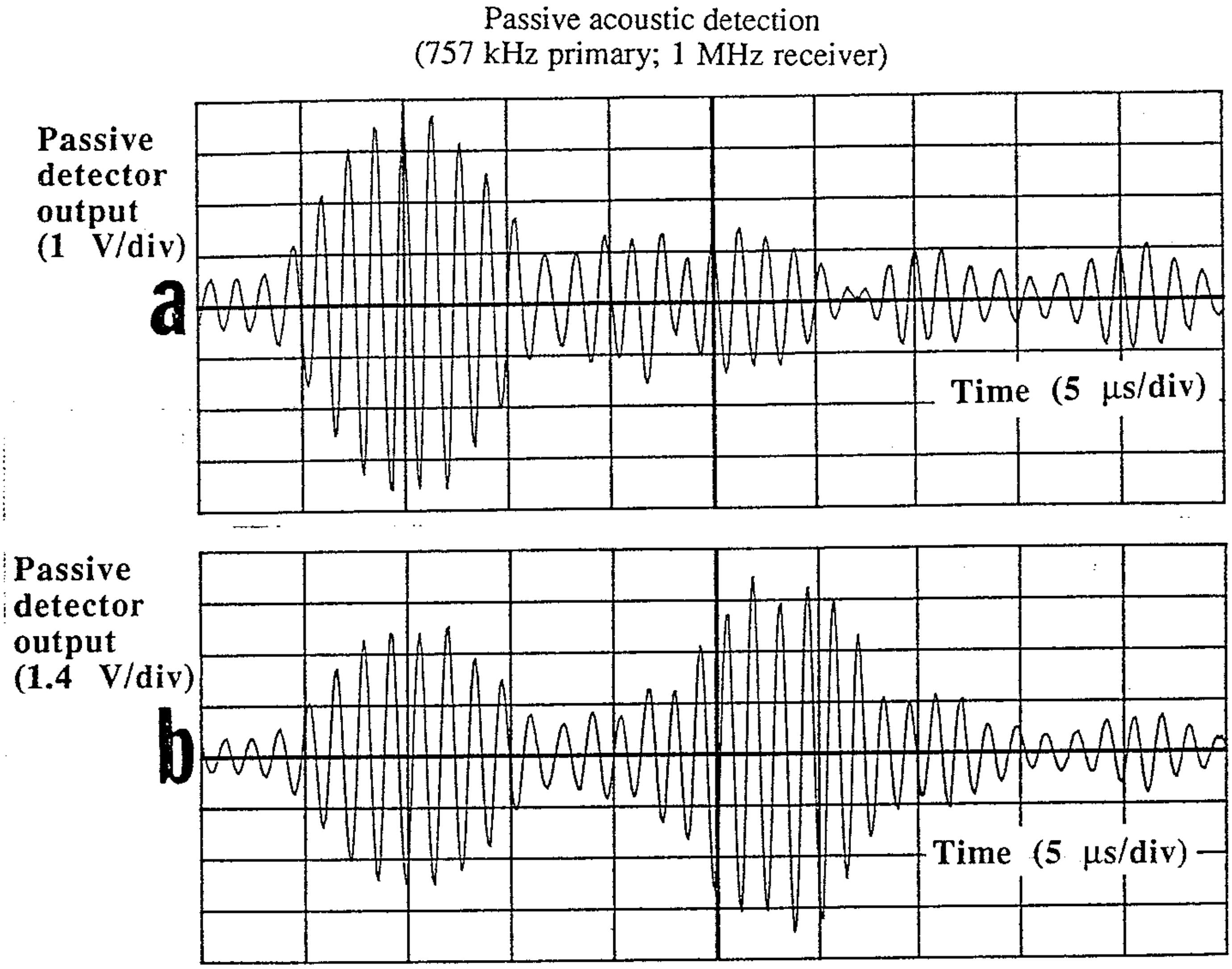

Figure 3.1 The output of the passive detector with and without cavitation. (a) The primary pulse from the 757 kHz transducer, followed by a stable low-amplitude background resulting from the multiple-path scattering and reverberation in the chamber (scale: 1V/div.). (b) The scattered background contains a perturbation indicative of a time-varying scatterer (scale: 1.4 V/div.). Note the difference in vertical scales between the two traces (after Roy et al. [3.40]).

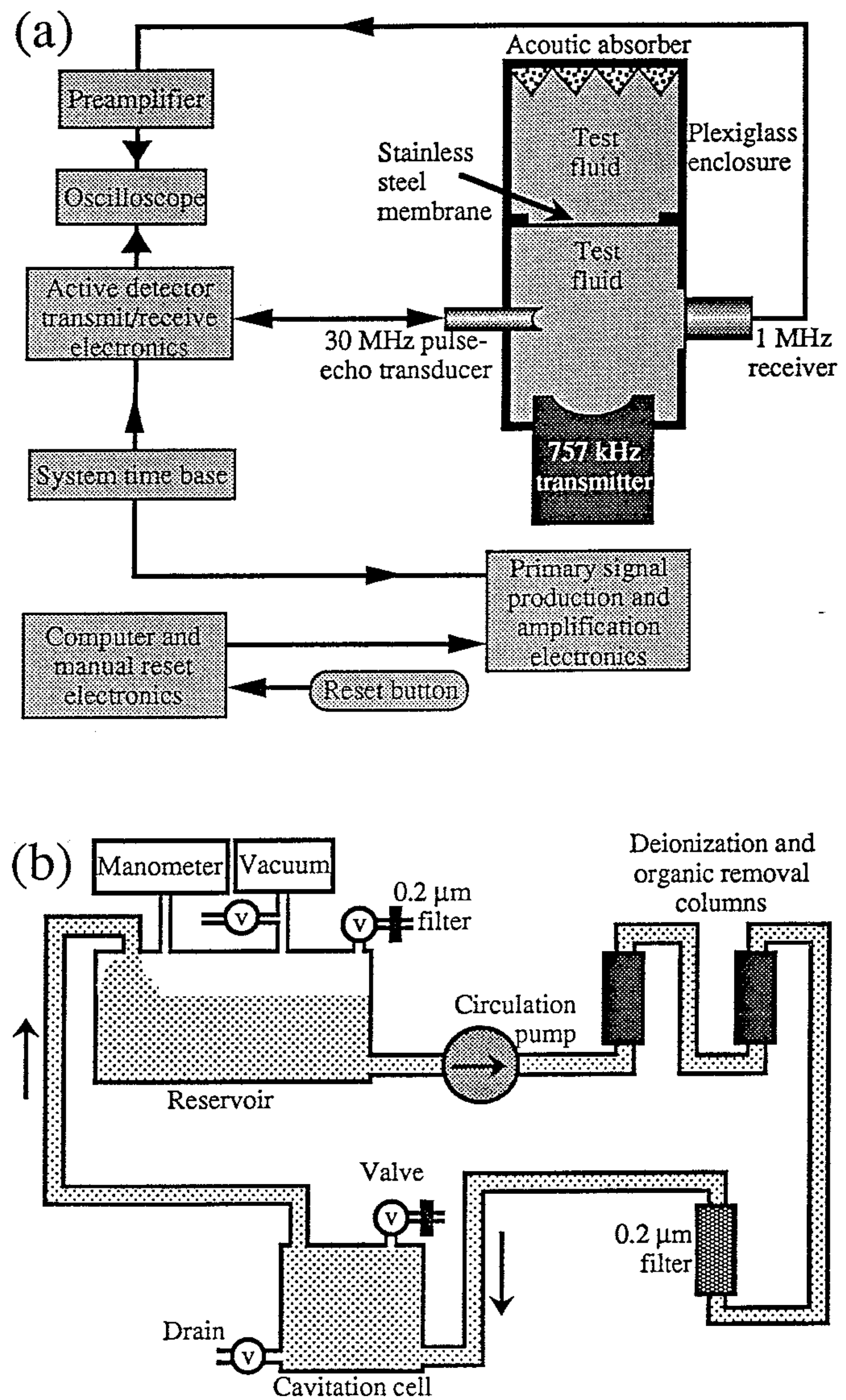

Figure 3.2 A system employing both active and passive acoustic detection. (a) The cavitation cell and associated electronics. (b) The closed-flow circulation system for cleansing and degassing the sample liquid (after Roy et al. [3.40]).

(iii) Active acoustic detection

A system which is more sensitive to bubbles in the micron size range is the active detector described by Roy et al. [3.40]. Subsequent to their production by the pulse from the first transducer (ν=757 kHz; ν_{rep}=1 kHz; τ_p=10 μs), the cavitation bubbles then backscatter high frequency pulses (ν=30 MHz; τ_p=10 μs) from a second transducer. Roy et al. [3.40] in fact deployed both active and passive acoustic detectors in their system, which is illustrated in Figure 3.2. The cavitation cell and the electronics associated with the transducers are shown in a), whilst in b) the fluid management apparatus (a closed-flow system) is illustrated. From the reservoir, where the fluid is degassed using a vacuum pump, it is then sequentially deionized, cleared of organics, and filtered down to 0.2 μm. The fluid is then passed into the cell, which can be flushed of impurities using flow rates up to 5 litres/minutes. Acoustic streaming, generating flows of up to 3 cm/s, could be used convect nuclei into the focal region. The cavitation cell is substantially similar to those employed in the passive detection studies described above. Separated from the test chamber by a 9 μm thick stainless steel acoustic window is a second chamber containing an identical fluid and an absorber of rho-c™ rubber (so-called as it is impedance matched to water). This is done to minimise spurious reflections and inhibit the introduction of standing-waves (the steel window prevents contamination of the test liquid by dirt or small particles from the rubber). The 757 kHz transducer, which generates the cavitation and is therefore labelled the 'primary', is mounted on a two-dimensional translating stage to enable its focus to coincide with that of the 30 MHz pulse-echo detector. The 1 MHz unfocused transducer is coupled with gel to the cell, opposite the 30 MHz active detector.

Figure 3.3 shows (a) the electrical signal which drives the 757 kHz primary transducer, which in turn generates the cavitation. Trace (b) shows the signal from the active detector system in the absence of cavitation, the main pulse representing the interrogating 30 MHz signal. Trace (c) shows the signal from the active detector in the presence of the cavitation generated by the 757 kHz transducer. The reflected signal from the bubbles is clearly evident.

Holland and Apfel [3.38] comment that, when the thresholds measured by the active and passive systems for very similar fluid systems (e.g. having the same polystyrene sphere and gas concentrations) were compared, they were found to be very close, suggesting that the acoustic pressure threshold to cause one bubble to go inertial in this system is the same as that required to make a cloud of bubbles go inertial.

Holland et al. [3.41] used the active detection system alone to investigate *in vitro* inertial cavitation from short-pulse diagnostic ultrasound, both imaging M-mode and Doppler, under conditions comparable to the clinical situation, with ν=2.5 or 5 MHz. Cavitation was detected in water seeded with 0.125 μm mean radius hydrophobic polystyrene spheres at 2.5 MHz, with a threshold peak negative pressure of 1.1 MPa, in both M-mode and Doppler insonations. No cavitation was detected at 5 MHz even at peak negative pressures as high as 1.1 MPa. No cavitation was detected in water seeded with Albunex™ at either frequency.

Active acoustic detection
(757 kHz primary; 30 MHz pulse-echo detector)

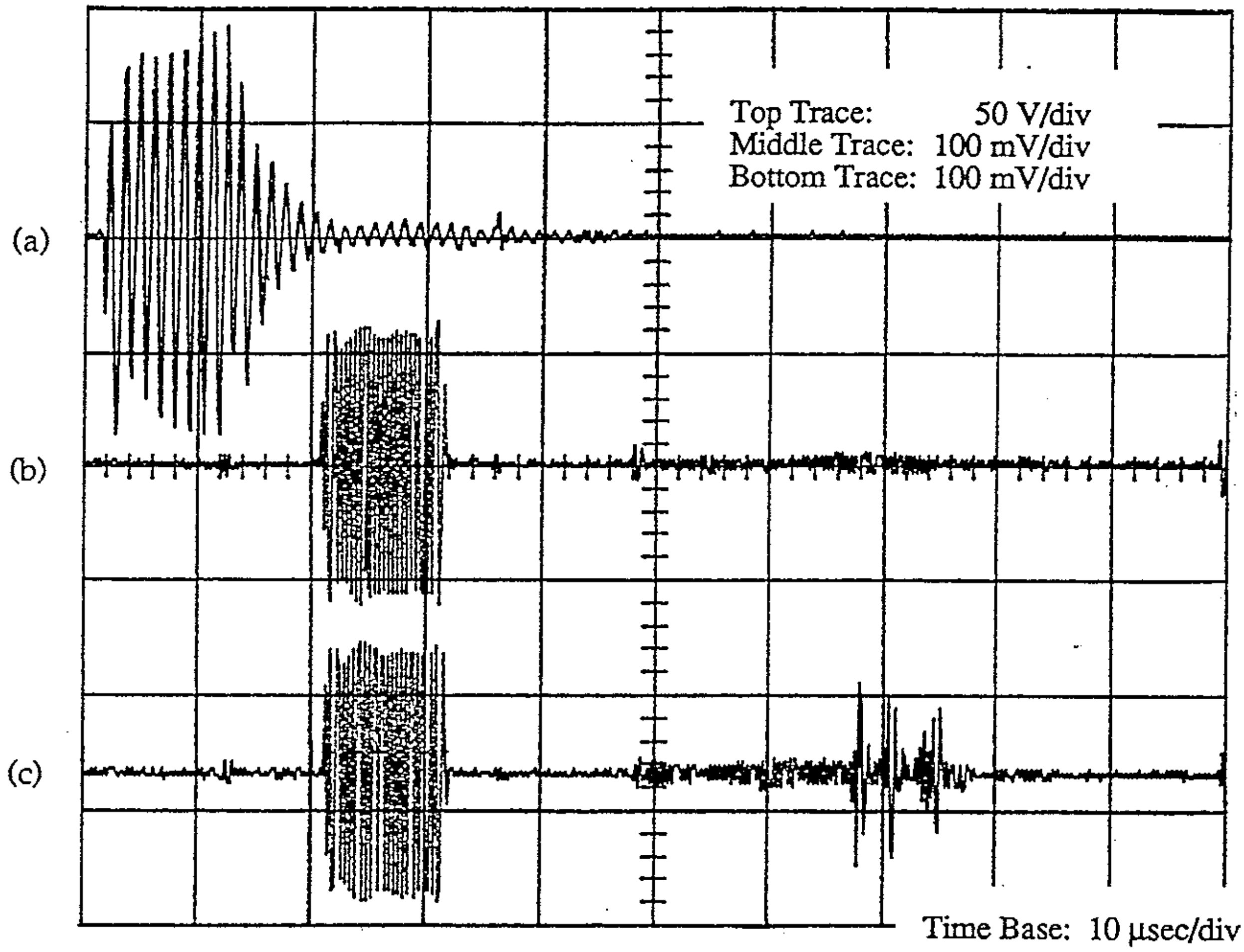

Figure 3.3 The top trace shows the electrical signal which drives the 757 kHz primary transducer (scale: 50 V/div.). The middle trace shows the signal from the active detector system in the absence of cavitation, the main pulse representing the interrogating 30 MHz signal (scale: 100 mV/div.). The bottom trace shows the signal from the active detector in the presence of the cavitation generated by the 757 kHz transducer (scale 100 mV/div.). The reflected signal from the bubbles is clearly evident. The oscilloscope digitising rate was 100 Msamples/s (after Roy et al. [3.40]).

Madanshetty et al. [3.42] discuss the effect of the sensor system on the cavitation threshold for water containing a microparticle suspension. With the active system turned off the passive system detected a cavitation threshold at around 15 bar, with the active system on the latter detected a threshold at only 7 bar. This implies that either the active system is more sensitive, or that it encourages cavitation itself, or both. The fact that the passive system also detects a reduction in threshold (to around 8 bar) suggests that both might be true, and that the cavitational effect of the active system might be considerable. To investigate this Madanshetty et al. [3.42] reduced the peak negative pressure from the active transducer to only 0.5 bar, so that its influence on inertial cavitation should be negligible, and found that the active detector alone at this intensity could not generate cavitation events. They found that the active detector could effect cavitation through the streaming it develops (which is promoted by its high frequency and focused nature). This flow convects nuclei into the cavitation zone. Another possibility suggested by Madanshetty et al. [3.42] is that potential nuclei, which would normally be driven by the 0.75 MHz transducer, would be detained in the region where the fields are strongest by cross-streaming with the flow generated by the active transducer, so enhancing the likelihood of a cavitation event at lower insonating pressures. Citing simulation results of

Church [3.43], Madanshetty et al. [3.42] rule out the possibility of the active detector influencing cavitation through rectified diffusion.

Another mechanism by which the active detector can affect cavitation is through the accelerations it imparts to particles. The combination of these accelerations with the density contrast generate kinetic buoyancy forces. These cause tiny gas pockets on the surface of solid particles to aggregate into gas patches of a size suitable to act as nuclei for cavitation. Madanshetty [3.44] considers smooth. spherical particles of sub-micrometer size, specifically polystyrene latex particles, of 0.984 μm mean diameter and free of surface flaws or crevices down to 50 nm. The 30 MHz field of the active detector causes gas pockets of 50 nm or less to aggregate on the particle surface as the particle oscillates in the sound field, and these aggregates nucleate cavitation.

In comparison with the passive detector, the active detector seems to be more sensitive, may affect cavitation itself, and is sensitive predominantly in its focal region, so may more readily be used to give a degree of spatial information. On the other hand, the passive detector is sensitive to a larger region of space, and remains continually alert for cavitation: for the active detector to operate its interrogating pulse must arrive at its focus at the instant when the inertial bubbles are present. There are implications regarding the strain placed on the user of these systems inherent in the nature and display of the of the detected signals [3.42].

It should be recalled, as discussed in section 2.2, that the report "Cavitation Detection and Monitoring" describes all the above techniques in quantitative detail [3.45].

3.3 Detection through Optical scattering

Whilst optical studies of "inertial cavitation" are not unknown [3.4§4.3.4; 3.46], their implementation can sometimes be difficult. Some drawbacks, such as opacity of media or containers, are common to the detection of both stable and transient† cavitation, and are outlined in Section 2. Others are specific to the nature of transient cavitation. An optical image of a size large enough to encompass the fully-expanded bubble will rarely be able to resolve the initial pre-existing gas pockets which seed this growth. Often the precise location of the event is difficult to determine in advance, depending on the spatial and temporal coincidence of a suitable seed and an appropriate excitation (though focused acoustics and the use of sparks and lasers can influence the siting [3.47, 3.48]).

Some of the problems can be illustrated by Figure 3.4, which shows eight frames from a section of film [3.49]. Insonation begins between frames 1 and 2. Two bubbles of just less than resonance size (labelled A and B, with R_0~0.10 ± 0.05 mm) can be seen quiescent in frame 1. They begin to oscillate in frame 2. In frame 4, further bubbles, which were initially too small to be seen, grow to visible size. These bubbles have collapsed unstably and have all gone by frame 6. The bubbles which undergo non-inertial cavitation, A and B, are driven together once insonation begins, and coalesce in frame 4 to form a single bubble (labelled C). Bubble C exhibits violent surface oscillations which

† The terms transient and stable are in this instance preferable to inertial and noninertial, since as with respect to the scattering of light, there are greater similarities between the characterisation of non-inertial cavitation and the experiments on single-bubble sonoluminescence [3.19], than between the latter and other types of inertial cavitation.

in frame 5 almost break up again. A third bubble (labelled D), also oscillating stably, travels into the depth of field in frame 3. It continues travelling perpendicularly to the picture, and by frame 8 is leaving the optical focus.

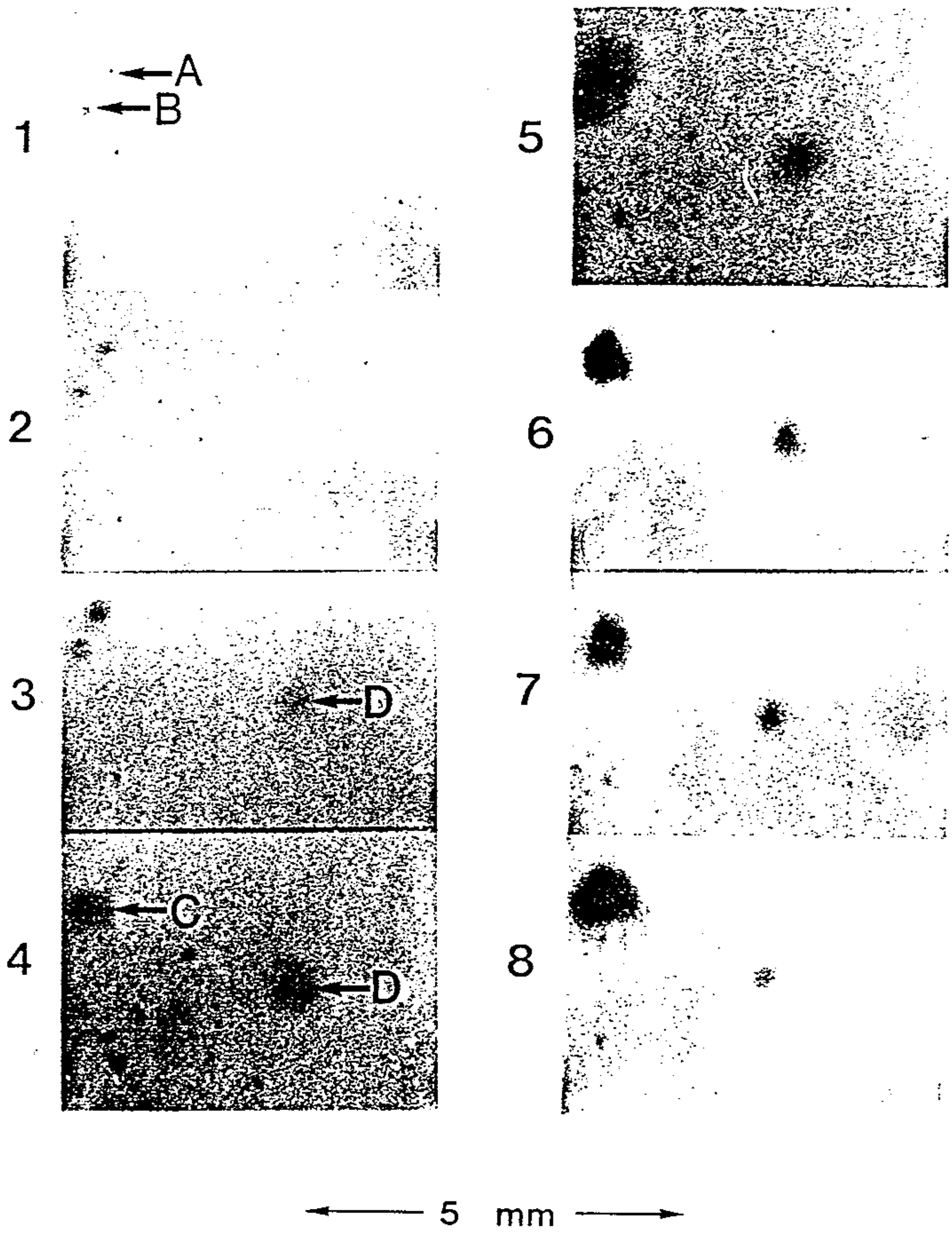

Figure 3.4 Eight consecutive frames selected from a film shot at 8000 f.p.s., showing both inertial and non-inertial cavitation. Insonation (at 10 kHz) begins between frames 1 and 2. Bubbles A, B and D are much too large to nucleate inertial cavitation. A and B coalesce to form bubble C, and D appears as it reaches the depth of focus. Bubbles which were, as seed nuclei, initially too small to be visible in frames 1 and 2, expand to reach maximum size in frame 4, before collapsing to a size too small to be visible (after Leighton et al., [3.49].

In his review paper Neppiras [3.50] cites two visual observations of historical importance. If a sample of aerated water is subjected to a relatively low intensity focused sound field, large bubbles may be seen to levitate. At these pressures the acoustic emissions of such bubbles are small. At higher pressures, surface oscillations may set in, and the bubble surface will appear to shimmer. As the sound pressure amplitude is increased, 'streamers' are generated, with the emission of a hissing sound. These misty, ribbon-like structures consist of stable bubbles travelling at high speed through the liquid to the focus under radiation forces (Figure 3.5). Blake [3.51] observed this only in aerated liquids, and found that there was a threshold acoustic pressure for their generation. He observed a second threshold at higher pressures, where single short-lived bubbles formed and collapsed intermittently. Such events were accompanied by a sharp 'snap' noise. As the pressure increased, the rate of these events increased (though sometimes Blake observed them to disappear completely). This form of cavitation could be observed in completely and partially degassed water. It should be noted that amongst the 'Tests for Cavitation' listed in the "Cavitation Detection and Monitoring" report [3.45] are the application of an overpressure (discussed in section 1.4) and degassing. Both do not simply inhibit or prevent cavitation, as was once a popular belief*. They change the form of the cavitation, and though, for example, a sufficient overpressure will eventually tend to suppress cavitation, there will be a theoretical dynamic tension sufficiently large to generate cavitation [3.4§2.1.2; 3.54]. Appropriate understanding of these processes allows them to be used as tests for cavitation in a range of media [3.45]; as does visual/photographic/holographic‡ observation if the access, transparency, timescales and lengthscales are appropriate to the sensor. Though such optical observations allow a qualitative characterisation of a cavitation field, to obtain quantitative information, for example through the obscuration of a light beam by the cavitation activity, presents difficulties. Not least of these is that accompanying inertial cavitation there will almost always be non-inertial cavitation (the activity in the streamers in Figure 3.5 is likely to be predominantly non-inertial). A range of other optical techniques, such as the use of Schlieren optics [3.30] to visualise rebound pressure pulses, have been used.

---

* It was thought in 1934 that degassed liquids could not sonoluminesce [3.52] though later work showed that it was possible if greater acoustic pressure amplitudes were used, Rosenberg [3.53] requiring twice that needed to obtain sonoluminescence from aerated water.

‡ See section 2.4

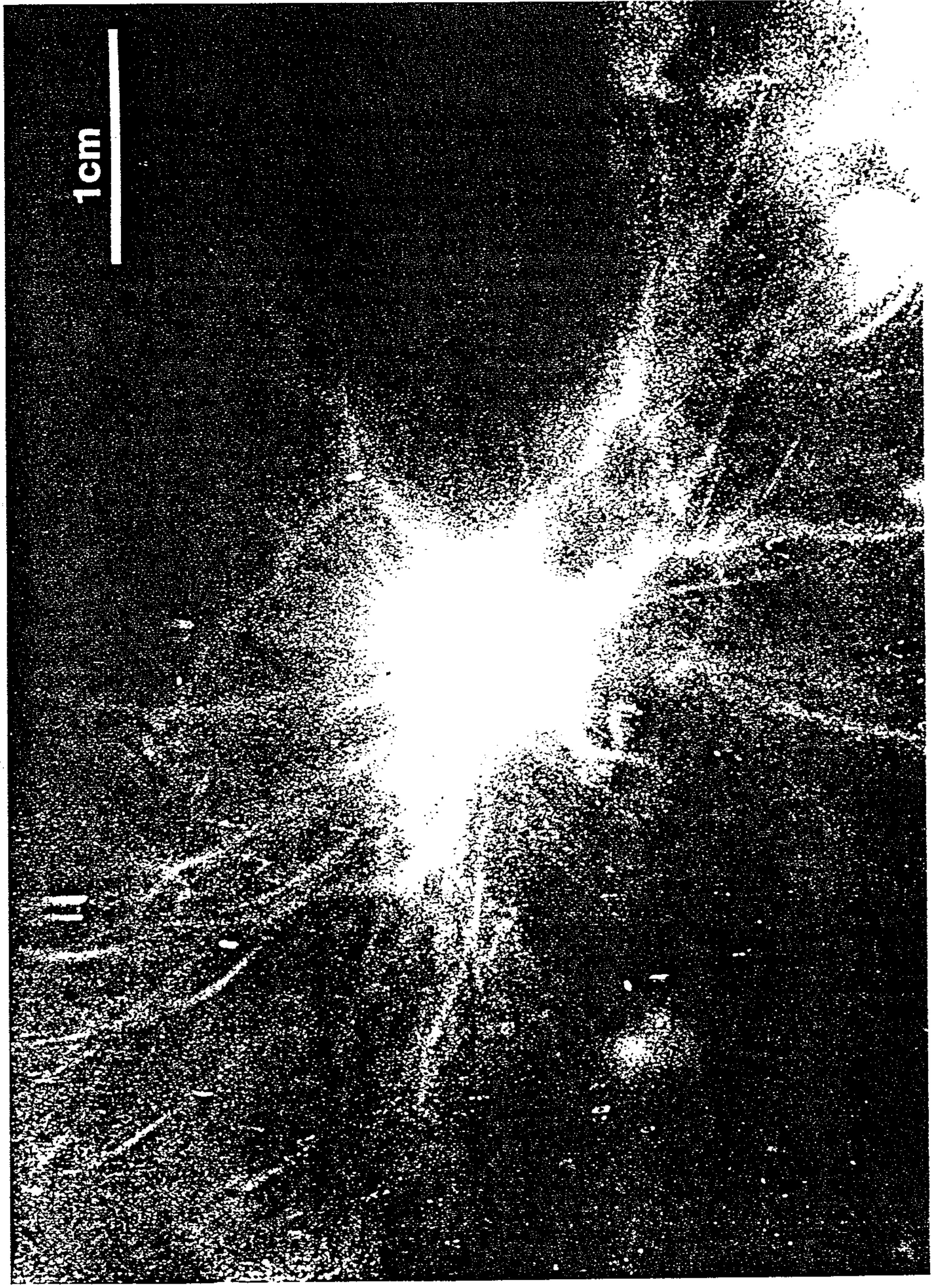

Figure 3.5 A photograph of aerated water cavitating in a cylindrically focused 10 kHz sound field, viewed along the line of the axial focus, where the acoustic pressure amplitude is 0.24 MPa. Exposure time 1/30th second. Streamers are clearly visible, comprising bubble moving rapidly towards the focus (after Leighton [3.4].

3.4 Detection through Sonoluminescence and Chemiluminescence

The overriding advantage of sonoluminescence measurements are that they give spatial‡ and temporal resolution of the cavitation field, and the magnitude of the signal can in broad terms be associated with the 'activity' of the cavitation field.

Apart from its use being limited to transparent media (with rare exceptions [3.55, 3.56]) under blackout conditions, the overriding disadvantage of sonoluminescence is in the uncertainty as to what feature of cavitation if reflects. Since its discovery in the 1930's [3.52], mechanisms for the production of the light have been proposed. Up to 1960 these included: the breakdown of a 'quasi-crystalline structure' in liquids (1936) [3.57]; electrical discharge through balloelectric (1939) [3.58] and charge fluctuation (1940) [3.59] effect; recombination of ions generated mechanically at the nascent surface of the growing bubble (1949) [3.60]; black body emission (1950) [3.61]; chemiluminescent reactions from thermally-generated oxidising agent (1950) [3.62, 3.63]; spherical shocks within the bubble (1960) [3.64]. The three main themes, of thermal, electrical, and mechanochemical processes, have continued since 1960 in a range of proposed mechanisms for sonoluminescence [3.4§5.2.1; 3.65, 3.66]. With such a range from which to chose it is perhaps not unsurprising that there has seldom been a time since 1960 when all workers in the field were not convinced that the true mechanism had been discovered, though there has never been universal agreement as to which that correct mechanism is.

One such period of uncertainty arose following the discovery of the extreme brevity of the flashes of sonoluminescence from a bubble undergoing stable inertial cavitation [3.67, 3.68]. Barber et al. [3.67] used a sufficiently intense 10.736 kHz sound field to generate precise, clock-like regular repetitive bursts of power 0.2 mW and containing 10^6 luminescence photons emitted uniformly in all directions, and measured the burst length to be less than 2.2 ns. The conversion of energy, incident sound to emitted light, is a factor of 10^{11}, with initial conversion efficiencies of 10^{-5}. These bursts are ten times faster than the visible 3-2 hydrogen atom transition. Further investigations, using micro-channel plate photomultipliers with very fast response times and a 30 kHz sound field, revealed that the flash widths were less than 50 ps, with the 'jitter' in time between flashes to be much less than 50 ps [3.68]. The flashes displayed no ringing. Barber et al. [3.68] speculate on the nature of the co-operative/coherent optical (or fluid) phenomena involved in the mechanism. As Crum [3.69] states: "As the phenomenon may be too fast for the establishment of local thermal equilibrium, we may be facing a situation where focusing acoustic stress fields are transduced directly into quantum excitations". Since this discovery a variety of mechanisms for sonoluminescence have been expounded [3.70-3.74].

However the production of sonoluminescence by single bubble may differ† from the generation by a population of bubbles, such as would be found in a high power ultrasonic

‡ see Figure 1.4

† and, speculating, it is not inconceivable that, as with many signals generated by cavitation, more than one mechanism can give rise to the observable, and contribute in differing proportions depending on the conditions. If this is the case, then the process of eliminating rival mechanisms by observing sonoluminescence during conditions which would tend to preclude the action of a specific mechanism, which has been done several times [3.4§5.2.1], is not an absolute test.

field [3.75-3.77]. In such fields it may be more appropriate to note that the detection of sonoluminescence provides unparalleled spatial and temporal resolution, through image intensifier cameras [3.78] and photomultiplier systems, which can be deployed simultaneously. Consider a camera system of 500x500 pixels. It can, within a frame exposure of around 1/25 s, spatially resolve each and every one of the 250,000 pixels in the image: if the frame has dimensions of 1 cm x 1 cm, the pixels measure 20 μm x 20 μm. With a commensurate loss of resolution, the frame size can be increased, sampling as large a volume as required. To this camera system can be added, with minimal spatial resolution of its own, a photomultiplier system of ns (or better) resolution [3.67, 3.68]. Combination of the information afforded by the two systems to infer the nature of the cavitation is dependent on the expertise and experience of the experimenter [3.4§5.2.2a(ii)].

The occurrence of sonoluminescence in space and time frames therefore indicates the presence of bubble activity of a type sufficient to generate the emission. However the question must be asked: how well does the quantity of luminescence reflect the desired quantity (i.e. that process, be it erosion, bioeffect or some other, which the user wishes to assess)? As discussed above, if luminescence is to be used to infer the nature of the cavitation, there are limitations imposed by uncertainties associated with the mechanism for its generation. However in many cases it is not the cavitation *per se* which is of prime interest: it is rather the effects of cavitation, since generally power ultrasound is employed to bring about some chemical, erosive, or biological effect. Interest should then focus on, first, how well the presence of sonoluminescence indicates the generation of the effect (i.e. does the type of cavitation which produces the one also produce the other?); and second, to what extent does the magnitude of the sonoluminescence detected correlate with the degree to which the other effect occurs?

Researchers have studied the relationship between sonoluminescence and bioeffect [3.79]; between chemiluminescence (see later) and bioeffect [3.80]; and between sonoluminescence and acoustic emissions. Negishi [3.29] found a continuum, evidence of rebound emissions, in the acoustic spectrum occurred when he detected sonoluminescence. Kuttruff [3.30] confirmed these results by examining the circular shock waves produced in transient collapse using Schlieren optics. Rebound pressure pulses have also been examined to study temporal [3.34] and spatial [3.35] correlations with sonoluminescence during lithotripsy; and during continuous-wave insonation to examine the threshold for inertial cavitation [3.31] (see section 3.2.2(i)); and in response to microsecond pulses [3.81]. The latter study employed a chemiluminescent phenomenon, whereby free radical species generated within the collapsing bubble can react radiatively# with a chemical dopant (called luminol, also tri-aminophthalic hydrazine; or 5-amino-2,3 dihydro-1,4 phthalazinedione) which is dissolved into the liquid [3.29, 3.82, 3.83]. Isoluminol (6-amino-2,3 dihydro-1,4 phthalazinedione) has also been employed [3.84]. Roy and Fowlkes [3.81] have demonstrated that the sensitivity of the chemiluminescent technique is lower than that of the passive detector. Luminol (0.035 g/l) can be deployed in an aqueous solution (0.1 M KOH-H_2BO_4 buffered at pH 10.9) with a Co(II) ($3x10^{-7}$ M) catalyst [3.83]. The use of luminol is not strictly a process that enhances sonoluminescence, but instead is introduces chemiluminescent reactions excited by the oxidation products of cavitation. After cavitation has ceased, the emission

Indeed the free radicals may themselves be used as an indicator [3.85], as will be discussed in the next section.

persists for around 1/20th of a second [3.66]. There are therefore two considerations which may in certain circumstances make its use inappropriate: (i) It is invasive, in that the cavitating medium must be changed, making it often unsuitable for biological studies of cavitation; (ii) The emission is not the same as sonoluminescence, but a luminescent detector of a specific chemical reaction. How both emissions relate to the cavitation *per se* is not a simple matter. Indeed there could conceivably be a medium, the chemistry of which could generate spurious emission from luminol. This caution having been stated, many careful workers had used luminol to good advantage. The question of chemical tests for the characterisation of cavitation will be discussed in the next section.

Poor correlation has been found between the threshold‡ for sonoluminescence and the onset of another acoustic emission, the half-harmonic. Iernetti and Ceschia [3.15, 3.16], using pulsed 0.7 MHz ultrasound, showed that the appearance of the half-harmonic did not vary with the pulse length, repetition frequency, and gas solubility in the same way as did the threshold for sonoluminescence. In test intervals ranging in duration from 2 to 10 minutes varying the acoustic power for 20 kHz insonation, Margulis and Grundel [3.17, 3.18] showed, by gradually increasing the power of the incident sound, that the sonoluminescent activity did not correlate with the strength of the $\omega/2$ subharmonic. Though in a single study they detected the degradation of DNA, the sonochemical release of free iodine from KI solution, and the generation of $\omega_p/2$ (with good correlation between the threshold for all three), Hill et al. [3.86] failed to detect sonoluminescence. They interpreted this result as indicating that non-inertial cavitation was responsible for the biological and chemical effects they observed. This reflects on the point made earlier, that a given observable may not be unique to a particular type of cavitation. Erosion from dental scalers has been attributed to microstreaming, generated in this case by the instrument rather than cavitation: though some cavitation has also been detected by using spectrophotometry with chemical dosimetry [3.87], Ahmad et al. [3.88] detected no observable sonoluminescence, and inertial cavitation has been deemed to have negligible contribution to the efficacy of ultrasonic files [3.87]. Therefore by equating sonoluminescence to inertial cavitation, it is possible to make negative as well as positive inferences about the role of the types of cavitation in bringing about a specific effect. The studies of Hill et al. [3.86] will be discussed further in the next section.

3.5 Detection through Chemical effects

This section examines the characterisation of cavitation using chemical methods, excluding luminescence (which is covered in section 3.4). Some tests, which have been used specifically for the characterisation of cavitation in cleaning baths, will be discussed in section 3.7.

Techniques which exploit chemical effects of inertial cavitation by definition can interrogate all of the sample which contains cavitation sufficient to cause that effect. This is an advantage over some acoustic methods, though in reality sampling from a larger volume will be necessary: First, if the treated volume is large, so that testing is not inordinately expensive; and second, if one is to achieve some spatial resolution to determine, for example, the effect at an ultrasonic focus. However continuous real-time

‡ though, in all such cases of comparative studies, it should be remembered that a failure to detect a signal may imply that the signal was not generated, or that it was generated below the detection threshold of the sensor.

monitoring by chemical techniques can be difficult, measurements often requiring a cessation of cavitation; and interpretation of such effects in terms of cavitation characteristics may be limited. Opportunities for real-time monitoring of a sample are feasible, for example through various types of spectroscopy, or opacity/colour tests.

The range of sonochemical effects which can be achieved is large [3.89-92]. They are usually taken to result from the chemical effects of the radical species which may be associated with adiabatic heating of gas compressed within the bubbles, the propagation of gas shocks, or electrical effects, much as for the mechanisms of sonoluminescence (see section 3.4). These effects are discussed in chapter 5 of reference [3.4]. Sonoluminescence, and the chemiluminescent reaction of luminol, have already been discussed. Other effects include specific sonochemical reactions [3.85, 3.89-92].

An acoustic field may accelerate chemical reactions that would occur in the absence of sound, or initial reactions that would, to all intents and purposes, not. The latter class are termed "sonochemical" [3.93][†] . These effects were first reported in 1927 by Richards and Loomis [3.95], who had observed both the acceleration of conventional reactions (such as the hydrolysis of dimethyl sulphate) and effects redox reactions in aqueous solution, including what we now know to be due to effects due to the oxidation of sulphite [3.96]. Other classes of reactions which have been observed include the degradation of macromolecules in solution, first reported by Brohult [3.97] in 1937, and the decomposition of pure organic liquids, demonstrated in 1953 by Schulz and Henglein [3.98] despite three decades of dogma to the contrary [3.96]. Sonochemistry does not arise from a direct interaction of sound with molecular species [3.99]. Though bulk heating through the absorption of acoustic energy may affect the rates of conventional reactions, a more dramatic effect would be expected from the high temperatures attained within a collapsing bubble. In 1964 Flynn [3.100] concluded that the correlation between sonochemical yields and the intensity of sonoluminescence justified the assumption that they have a common source. Reviewing the data to that date, he decided that a thermal mechanism was most likely, though it should be noted that by interpreting some of the observations in a different way Prudhomme [3.101] favoured an electrical discharge mechanism as the common source. Indeed electrical discharge theories were those favoured by the first investigators [3.96, 3.99, 3.102-4]. However in recent decades thermochemical mechanisms have been popular, with realisation of the chemical implications of the spatial temperature gradients associated with the collapsing bubble. From the centre of the bubble (where the compressed gas attains a high temperature) to the bulk liquid far from the bubble (which is at ambient temperature), there will be a considerable temperature gradient. Since the type and rate of chemical reaction is strongly dependent on the temperature, difference can be expected in the characteristics of the reactions that can occur within the gas, at the bubble wall, and in the liquid outside the gas bubble [3.105-7]. Mechanical degradation on macrostructures in solution by shear forces close to bubbles define another zone of activity [3.107]. Reviews of sonochemistry are indicated in the references [3.4§5.2.1a, 3.90, 3.91, 3.108-112]. As with other phenomena introduced in this chapter, there is no intention of here surveying the literature, but rather of indicating ways in which sonochemistry can characterise cavitation in an high-power ultrasonic field. This might, for example be done through the

[†] Sonochemical reactions are generally taken to be those initiated or mediated by specieis generated within the bubble, rather than, for example, the triggering of another reaction (such as ignition [3.94]) by the presence of the hot-sopt within the collapsing bubble.

use of spectroscopic techniques to monitor specific chemical reactions. Temperature control, and batch processing subsequent to insonation, are usually undertaken.

Digby et al. [3.113] investigated a technique of characterising inertial cavitation reproducibly using terephthalic acid (TA), which will act as a scavenger for the hydroxy radicals produced during inertial cavitation in water, and had been suggested as a cavitation/free radical dosimeter [3.114-5]. Tests in rotating-tube scenarios (see [3.4§5.3.2]) had investigated a threshold for the effect [3.115-6]. Reaction of the terephthalic acid with all hydroxyl free radicals produces hydroxyterephthalic acid (HTA), the fluorescence from which can be used to calculate the concentration of hydroxyl free radicals [3.114]. HTA is relatively stable, and can be analysed several hours after insonation. Digby et al. [3.113] achieved a degree of spatial and temporal resolution by placing a closed chamber in the ultrasound beam. The chamber initially held 20 ml of TA, covered the -6 dB width of the beam, and was equipped with acoustically transparent windows. From it, at 15 ml intervals, ~3ml aliquots were transferred into a cuvette to be placed in a fluorescence spectrometer. The solution was excited with ultraviolet light of wavelength 310 nm, and the light emitted at 425 nm wavelength was measured. The aliquot was then returned to the chamber, and insonation resumed. Calibration enables the fluorescence to be interpreted in terms of the concentration of hydroxy radicals produced. Digby et al. found that by seeding the sample with polystyrene spheres they could increase both the yield and reproducibility of the experiment. Digby et al. suggest that the use of polystyrene spheres as known cavitation nuclei obviates the need for rotation of the sample (which increases reproducibility by preventing nuclei and cavitation bodies being moved out of the main body of the sample through radiation forces). It should be noted that the use of a self-contained cell containing TA enables the sonochemical reaction *within the cell* to be examined. Thought must be given as to how this relates to the cavitation which would occur in the liquid which would occupy that site in the sound field if the sample cell were absent: the host liquid, the gas content, and the nuclei, may differ. This question will be further explored in Section 4. Miller and Thomas [3.84] have compared the TA dosimeter with the ultrasonic generation of hemolysis. One possible problem with the use of TA is that it is possible to react with more than one hydroxyl free radical to producs polyhydroxyterephthalic acid. Other chemical dosimeters have also been suggested. Fricke solution, the oxidation of $Fe^{2+} \rightarrow Fe^{3+}$ [3.117-119], can be assessed through colour change. The scavenger DPPH (2,2-diphenyl-1-picrylhydrazyl), which decolorises on reaction with a radical, reacts to generate $DPPH_2$ (2,2-diphenyl-1-picrylhydrazine) [3.187], which can be monitored through UV spectrometry. Loss of DPPH can be monitored by loss of signal at 525 nm wavelength. Paranitrophenol (PNP) reacts such that a hydroxyl free radical is added to a benzene ring, producing 4-nitrocatechol (4-NC). The amounts of PNP and 4-NC can be quantified through their absorbancies in alkaline solution at wavelengths of 401 nm and 512 nm respectively [3.188]. Electrochemical effects can also be used to detect cavitation [3.189].The Weissler test is discussed in section 3.7.

Spin-trapping enables highly-reactive free radicals, such as those produced through inertial cavitation, to be detected by electron spin resonance (ESR). Since free radicals are paramagnetic, they can in principle be detected using ESR [3.120-1]. However in practice this is not feasible with radicals such as the hydroxyl, produced by cavitation in aqueous solution, because the hydroxyl lifetime is insufficiently long. To overcome this, a diamagnetic spin trap molecule is used. The procedure is designed to identify the nature of the short-lived free radicals by allowing them to react with the spin trap molecule (usually a nitrone or nitroso compound) to produce a longer-lived radical adduct, which can be identified through electron spin resonance (ESR) spectroscopy. The results can then be interpreted in terms of the original unstable free radical [3.92, 3.121-7]. After insonation, the solution containing the radical adducts can be frozen (e.g. at 77 K [3.26]) and then thawed before ESR measurement. Several workers have, for example, exploited spin trapping with 5,5-dimethyl 1-pyrroline N-oxide (DMPO) in aqueous solution (25 mM [3.26]) to form DMPO-OH and DMPO-H radicals which, being longer-lived than H or OH radicals, could be analysed by ESR [3.121, 3.127-8]. Other radical adducts can, of course, be formed between the spin trap and appropriate alternative free radical species if they are available [3.121, 3.129]. Alternative spin trap agents, such as 4-POBN (α-(4-pyridyl 1-oxide)-N-tert-butylnitrone) in 50 mM solution [3.26], are available. Yields of up to 10^{10} radicals/ml for 1 ms of 1 MHz insonation at an I_{SPTA} of 1-1.5 W/cm^2 have been detected [3.26].

Of particular interest (as will be discussed in section 4) are tests which have correlated the signals generated by several cavitation effects. Erosive and sonochemical studies are discussed in section 3.7. In recent years Miller and Thomas [3.130] compared hemolysis with a TA dosimeter. However two important studies, done nearly three decades ago, illustrate a number of important points regarding such tests, and both incorporated the ultrasonically-induced release of free iodine I_2 from KI [3.86, 3.131-2] or NaI [3.133] solution as a detector of sonochemical activity. In 1969 Hill et al. [3.86] published an investigation into the effect of changing the pulse length on three ultrasonically-stimulated processes, one a bioeffect, one an acoustic effect, and one a sonochemical effect. The bioeffect was the degradation of deoxyribonucleic acid macromolecules (commercially prepared polydisperse calf thymus and salmon sperm DNA, with effective molecular weights of 10^7 and 5.5×10^6 respectively). The acoustic effect was the generation of the first subharmonic harmonic of the driving frequency (which was investigated as a possible measure of cavitational activity). The sonochemical effect was the release of free iodine from a KI solution. Working at 1 MHz, in far-field travelling wave conditions and with duty cycles of 1:1, 1:2 and 1:10, Hill et al. [3.86] rotated the sample cell about a vertical axis within the sound field and water bath. This rotation technique was originally devised for a different experiment, in which the need to stir cell suspensions had been anticipated. The fortuitous incorporation of rotation generated the remarkable observation (mentioned earlier) that a rotation of 0.3 to 3 revs sec^{-1} induced an 'all or nothing' response in all three effects investigated. The positive results discussed below are for rotated samples.

The initial experiments studied the decrease in molecular weight as the DNA was degraded, as a function of insonation time (≤20 minutes) and acoustic intensity (≤8 W cm^{-2} spatial average for 3 minutes) for continuous-wave. In the latter, a threshold of $I_{SA}\approx0.4$ W cm^{-2} was observed, below which no effect was observed. The effect increased rapidly to a maximum at around 3 W cm^{-2} with a gentle decrease up to intensities of 8 W cm^{-2}. In similar conditions the release of free iodine was found to threshold $I_{SA}\approx0.5$ W cm^{-2} ($I_{SP}\approx1.5$ W cm^{-2}), with a maximum effect at $I_{SA}\approx2.25$ W cm^{-2}. No sonoluminescence could be detected with their equipment. Subharmonic emission increased sharply to a maximum at $I_{SA}\approx2$ W cm^{-2}. The similarities in these continuous-wave observations is clear, as expected if the effects have, directly or indirectly, a common source (i.e. cavitation). The authors used this system to study the enhancement of a cavitational effect when ultrasound is pulsed, over and above that when continuous-wave. There have since been extensive studies of this phenomenon, with several mechanisms proposed, and as these are reviewed in the literature [3.4§5.3] there will be no attempt to study 'pulse-enhancement' here. However the study by Hill et al. demonstrates a number of important points for the characterisation of cavitation. Sonochemical, acoustic, and biological cavitation effects were studied together to investigate the cavitation in an ultrasound field. In addition the failure to detect sonoluminescence was interpreted at the time by to mean that inertial cavitation did not occur. This would logically imply that the observed effects are the result of non-inertial cavitation. This can only be safely deduced if the different *detection* thresholds of the acoustic, bioeffect, sonochemical, and sonoluminescent sensors have been established, and distinguished from the threshold for inertial cavitation.

In a similar experiment Clarke and Hill [3.131] in 1970 examined the ultrasonically-induced release of free iodine from KI solution, DNA degradation and the disruption of mouse lymphoma cells in a rotating sample. The apparatus was similar to that employed by Hill et al. [3.86], and a pulse enhancement effect was demonstrated. From a biological viewpoint, Clarke and Hill concluded from their results that cell death and iodine release both resulted from cavitation effects. In an analogous manner to Hill et al. [3.86], they proposed that non-inertial, rather than inertial, cavitation was the cause. The mechanism of damage was the result of microstreaming, which occurs maximally at one particular bubble size (i.e. when the bubble pulsation frequency is resonant with the acoustic field). They suggested that high amplitude of radial pulsation generating maximum microstreaming results in high hydrodynamic shear and tensile stresses in the region of the bubble, which could disrupt cells. It is perhaps less clear how the sonochemical effect could have arisen through non-inertial cavitation: Clarke and Hill speculated that the large amplitude of bubble pulsation at resonance might well cause any free radical production to be maximised, though current thinking would tend to suggest free radical production is more likely to indicate inertial cavitation (discussions of sonochemical activity from non-inertial cavitation can be found in references [3.134]). How such uncertainties might influence the choice of signal for the characterisation of cavitation is discussed in Section 4.

3.6 Detection through Biological effects

Of the interesting features regarding the use of a biological effect to characterise ultrasound, two immediately appear to be of prime importance. First, there are a wide range of possible bioeffects that can be induced. Second, bioeffects can be generated through more than one cavitation-mediated mechanism. Contributing to both these facts is the given the complexity of biological systems. These facts had wide-ranging implications. Whilst a very wide range of bioeffects can be generated by ultrasonic cavitation, interpreting these effects in terms of the characteristics of that cavitation is not simple. Biological effects of cavitation may be related to either the sonochemical [3.131] or physical [3.135] mechanisms [3.4§5.4.2]. Cavitation can produce a great many effects which have proven to be so complicated in mechanism as to make them as yet unsuitable for use in measurement beyond the most rudimentary indication of the type of cavitation occurring. Examples of these include the bioeffects associated with gas depletion when bubbles grow by rectified diffusion [3.136], microstreaming [3.137] and with the high-speed translation of bubbles under radiation forces [3.138]. These are in addition to bioeffect resulting from the known phenomena associated with inertial cavitation, such as rebound pressure pulses and free radical generation, and jetting.

This being said, it is logical to chose a simple biological system to attempt to characterise cavitation. Several systems were introduced in section 3.6 [3.86, 3.130]. One of the most studied has been hemolysis [3.130, 3.139]. However as this effect can be brought about by a range of bubble-mediated mechanisms, both inertial and non-inertial, on its own it does not test for a specific type of cavitation. The deduction that can be made when such a test is used in combination with another is discussed in Section 4, where particular attention is paid to tests which correlate bioeffect with some other observable. Two notable correlations with acoustic emission were introduced in section 3.2.1. Morton et al. [3.12] showed that the detection threshold for the emission of the time-integrated subharmonic from suspended cultures of V79 cells exposed to 1 MHz ultrasound, coincided with that for cell death. Edmonds and Ross [3.13] monitored the rms values of the combined subharmonic and noise components of the acoustic emission. Cell viability and survival correlated with acoustic emission, but not with cell growth. Correlations between bioeffect and sonochemical yield were discussed in the previous section.

3.7 Detection through Erosive effects

Techniques which exploit erosive effects of inertial cavitation will interrogate that part of the sample which contains cavitation sufficient to cause that effect, and which is adjacent to a structure the erosion of which can be measured (Figure 3.6). Over the duration of the test, bubbles and cavitation clouds are likely to migrate under Bjerknes forces, which may bring them adjacent to the test sample surface. Inclusion of a test sample itself can: introduce nucleation sites into the medium; potentially alter the sonochemistry [3.140]; and alter the sound field within the volume it is testing, both directly (through the reflection of sound off its surface etc.) and indirectly (by altering the pattern of the cavitation field, and changing its influences on the sound field [3.75]).

Continuous real-time monitoring by these techniques can sometimes be difficult, measurements often requiring a cessation of cavitation; and interpretation of such effects in terms of cavitation characteristics may be limited. Such techniques usually involve the detection of effects associated with jet impact [3.141] (Figure 1.1 row 10) and rebound pressures (either from single or cloud cavitation events [3.142]).

Figure 3.6 A back-lighted sample of aluminised mylar sheet, which had been subjected for around 1 minute to a cylindrical sound field which, at the axial focus, had an acoustic pressure amplitude of 0.24 MPa. In the dark regions the aluminium has remained adhering to the sheet. However it has been eroded away, such that the light shines through the transparent mylar, in large, roughly circular regions (after Leighton [3.4]).

Much research on the rebound pressures has been done since the early work of Rayleigh [3.143], and is reviewed by Plesset and Prosperetti [3.144] and Mørch [3.145]. The emitted spherical shock wave may have an amplitude of up to 1 GPa. Cavitation events and shock wave propagation can be recorded using holography and Schlieren photography [3.146]. However when an isolated bubble collapses, this shock is so rapidly attenuated that only surfaces within about the initial bubble radius of the centre of collapse may be damaged [3.147-8]. On the other hand in a concentrated mass of bubbles, the collapse of one may initiate the collapse of a neighbour, and under certain circumstances the combined shocks from this 'cloud cavitation' can cause damage at much greater distances [3.149-50]. This was observed experimentally by Brunton [3.151] when cavitation occurred near a solid surface. The model proposed for this effect is of a large hemisphere of cavities collapsing inwards as consecutive shells; the collapse of each shell releases the hydrostatic pressure onto the adjacent inner neighbour shell. The energy of each collapsing shell is passed on to the next shell, so that cavitation in the centre of the cloud is an order of magnitude more energetic than the collapses in the outermost shell. This model was formulated by Mørch [3.145], Hansson and Mørch [3.152], and by Hansson et al. [3.153], and supported by the experimental observations of Ellis [3.154]. Noting the reported variability in the pressures generated even by laser- and spark-induced single-bubble collapses, where the bubbles all initially attained the same maximum size, Zhang et al. [3.155] employed a statistical model for erosion by multi-bubble collapses.

The other mechanism for cavitation erosion is through liquid jets formed by bubble involution. Neppiras [3.156] describes the collapse of an initially-spherical bubble generated by laser action a distance of 2.3 mm from a boundary. Jetting first occurs towards the solid surface, and on rebound a counter-jet is generated. After that, the bubble invariably disintegrates [3.156]. Benjamin and Ellis [3.157] predicted that a ring vortex would emerge from the jet flow, and Lauterborn [3.158] and Olson and Hammit [3.159] observed how jetting may lead to the formation of a "bubble cavitation ring" from the toroidal shape enforced on the bubble by the jet. The torus itself can then expand and collapse violently, leaving behind a ring-shaped cloud of small bubbles. Naudé and Ellis [3.160] and Tomita and Shima [3.161] showed that the dynamics of the asymmetric collapse depend strongly on the ratio of the distance between the point of bubble formation and the wall, to the maximum radius attained by the bubble on expansion. Over a wide range of values of the ratio, a vortex ring is found to emerge from the jet flow. Impact jet speeds of up to 400 m/s have been measured [3.161-2], and the highest pressure amplitudes measured at the solid boundary were found for bubbles attached to the boundary, when there is no cushioning liquid film between bubble and boundary. However for most of the detailed observations of individual bubbles or of small bubble populations, the collapses are usually not ultrasonically-induced but instead are brought about through incident shock waves or lasers, so that the jetting will occur near to the boundary and the detectors [3.4§5.4.1].

In contrast measurements of bulk erosion often exploit ultrasonically-activated bubble clouds. Crawford [3.163] describes how the weighing of a lead block before and after ultrasonic treatment can be used to indicate what erosive cavitation activity has occurred over its surface. This technique is clearly limited: it is not real-time, though could no doubt be made so by incorporating the weight into an active inertial resonator system which could track the mechanical resonance during cavitation. However in such a deployment it nevertheless detects only the cavitational activity which will remove material from the test block, as opposed to simply deforming it. Crawford cites reports of weight losses of order 0.4 g/hour have been reported [3.164]. Erosion of particles may also be used, as measured by mass loss or particle size reduction*. However there may be contributions from particle-particle interactions. Polymer degradation [@] through the mechanical effects, in contrast, is generally less simple to measure, but the chain length reduction is thought to result only from cavitation.

It should also be noted that non-inertial cavitation can bring about erosive effects through, for example, microstreaming [3.165] and rapid bubble motions induced by radiation forces [3.4§5.3.2c; 3.166]. Chemical species in the liquid can contribute to the effect and cause corrosion [3.167-8]. Given that, as with many of the effects of cavitation, a single observable can be brought about through a variety of mechanisms, the exploitation of erosion as a method of characterising cavitation is not simple. Other factors also contribute to the complexity of any scheme designed to monitor cavitation through erosion. The time-history of the material changes may not be linear, many materials demonstrating an 'incubation period' in tests, prior to the onset of cavitation erosion [3.54, 3.167-8]. The type of erosion seen (plastic deformation, mass loss etc.) depends on the material chosen, and the rate depends on the properties of the material, its surface finish, and the liquid and its gas content. Most relationships arising from studies of cavitation erosion have been empirical, characterising the material resistance to erosion [3.54, 3.112], rather than the cavitation *per se* [3.163, 3.169-70].

A number of authors have attempted to characterise cavitation in cleaning baths, using erosion and other techniques. Since cleaning baths represent an important application of erosive cavitation, such chemical tests will be discussed in this section. Indeed as early as 1964 standard chemical procedures for cleaning baths were documented [3.171-2]. Weissler [3.173] discusses the use of a colour measure of the sonochemical liberation of chlorine from carbon tetrachloride as a method of characterising ultrasonic cleaning baths. Recognising the role of cavitation in both the operation of such baths and in the sonochemical test he describes, Weissler [3.173] attempted to formulate the cleaning ability of, say, an ultrasonic bath, in terms of a summation $\Sigma_i a_i n_i$ over all classes i of cavitation event, with a weighting a_i appropriate to the cleaning effectiveness of that event, with n_i being the number of events in class i per second per unit volume. Weissler recognised that the n's are functions of temperature, frequency, dissolved gas content , treatment time, location of the test site within the cleaning tank etc., and suggested that a double integral of $\Sigma_i a_i n_i$ over the time of treatment and the specified volume constitute an improved expression. Weissler [3.173] introduced a similar expression $\Sigma_i b_i n_i$ for the sonochemical effect of the cavitation, where b_i is the coefficient of the relative sonochemical effectiveness of each class of cavitation. Weissler proposed measuring the sonochemical activity of the cleaning bath and then, by assuming that the ratio a_i / b_i is constant at least for a particular cleaning bath at a particular frequency, extrapolating to determine the cleaning effectiveness of the bath. Such an approach may be of limited value given the range of possible cavitation effects, not just involving the various activities a single bubble can undertake [3.4§4.3.2, 3.4§4.4.8], but also cloud effects (acoustic shielding, local degassing etc. [3.174]). In addition, though it should be possible to detect individual events at low levels of cavitation (section 3.2.2(i)), it would be very

* Though systems exist to rapidly characterise the size distribution of partciles in a population (see, for example, sections 2.4 and 2.5), a standard dilution technique may be required to make the population used in the field amenable to such size characterisation.

difficult to do this during intense cavitation, and is no simple matter to assign an efficacy to each event.

Citing a presentation of the above formulations by Weissler [3.175], Crawford [3.163] proposes, as a standard material for erosion, aluminium foil. He describes how, when immersed in a cavitation field, the foil first dimples (dimples are closely packed and of 0.1 mm diameter), then is punctured at the dimples form 'pinholes'. With erosion commencing from the ragged edges, the pinholes then expand and may coalesce. In a cleaning bath this stage can be reached in 15-20 s for a foil thickness of ~10 μm. Sections of the foil detach as the coalescence continues. In a 500 W cleaning bath, operating at 20 kHz, Crawford recorded the 'destroyed area' (measured using light transmission) as a function of the exposure time, and observed that generally up to 35% of the area of the foil was destroyed before coalescence caused larger pieces of foil to detach. He proposes an index found by obtaining the product of the proportion of the area eroded and a constant reflecting the thickness and type of the foil, and dividing this product by the time of insonation. Crawford considers it to be a first-order solution to allow, for example, a comparison between baths, or a day-to-day check on the operation of an individual bath.

Another suggestion [3.176] separates out Type A cavitation activity measures, which are based on physical effects such as radiated sound, whose value at a point in the liquid depends on events scattered throughout the cavitation field; from Type B, which arise from physical effects (e.g. a chemical reaction) that are localised at or near to the event which give rise to the effect. The authors suggest that if statistical averages can only be measured, then for example Type B measures of cavitation activity indicate the 'average violence of cavitation events occurring within a small volume in a specified time interval'.

Boucher and Kreuter [3.177-8], also examining techniques for the measurement of the efficacy of cleaning baths, discuss sonochemical [3.173, 3.179], erosive, and the integration of cavitation noise* after elimination from the data of the transducer signal‡, the technique they favour. They propose a unit of cavitation, the CAVIT [3.177-8], quoted as follows: "The CAVIT is the one hundred seventy fifth of the amount of cavitational energy released in a tank (5½" wide by 9⅜" long by 4" deep) filled with 2½ litres of partially degassed water when irradiating 18 W of acoustic energy [*sic*] in the liquid at a frequency comprised between 35 and 37 kcps and within a temperature range of 26° and 27°C. Under the above stated conditions a pure lead sheet (4" wide by 8" long by 1/16" high) placed in horizontal position inside one of the maximum erosion zones will lose 0.44% of its initial weight after one hour of insonation starting at a temperature of 26°C. Also under the above stated condition 2½ litres of the Weissler reagent poured directly into the tank will give a light transmittance of 50% after 1190 seconds of irradiation" (the Weissler reagent test involves the release of chlorine gas upon insonation of carbon tetrachloride solution [3.173, 3.178]).

The same range of techniques are discussed in a 1966 report of the American Standards Association [3.715] with respect to standardisation of cleaning baths. Whilst recognising

* See also reference [3.11].

‡ Attempts have been made to formalise the distinction between driver and cavitation-related noise in erosive devices can [3.186].

the importance of spatial resolution, it recommends quantitative soil removal rate as a primary standard, with chemical or physical phenomena being selected as secondary standards "for reasons of simplicity or cost", provided that the activity measured for the secondary standard should bear a consistent quantitative relationship with the primary. Two tests are discussed from each category: the removal of soils consisting of radiative isotope, and of dyed grease (which is, after insonation, removed from the test piece by solvent, which in turn becomes coloured by a degree dependent on the amount of soil remaining); chemical reactions consisting of bromine and chlorine release; and the physical effects of lead erosion (rejected as a primary standard because of poor reproducibility at the time) and foil rupture (discussed in the context of a qualitative, rather than quantitative, indicator). Finally cavitation noise is investigated. The preferred measure in the report is soil removal, partly because it is a direct measure of the quantity of interest to users of cleaning baths. In the event that a good soil cannot be found, the authors recommend that a chemical test be the primary standard. One suggests trial solution for a standard soil, the removal of which would provide a measure of the 'cavitation' that has occurred, was graphite pencil lines on ground glass; however this proved to be extremely difficult to standardise [3.163].

Cavitation erosion measurements, by their nature, tend to require complicated ultrasound field, with bubble clouds containing both inertial and non-inertial cavitation. Such systems are typified by the cleaning bath. This represents one extreme of the cavitation field studied, where the investigations have concentrated on macroscopic effects which are amenable to measurement, and which reflect the phenomena of interest to the end user. This topic will be further explored in Section 4.

3.8 Characterisation of cavitation through electrical effects

Electrical sensors for bubble presence were discussed in section 2.5. Of the three examples given, bulk conductivity sensors provide the best opportunity for examining a cavitation field during power ultrasound exposure. However the system is intrinsically insensitive to the type of cavitation, other than the inferences that can be made through the transiency or otherwise of any features. In section 2.5 the displacement by the bubble of liquid of differing properties gave rise to the signal. Huang et al. [3.181] instead discuss the effect on conductivity of species produced by sonochemical action during inertial cavitation. They specify the chemical reaction within the cavitation hot-spot between nitrogen and oxygen, present in aqueous solution because of dissolved air, leading to NO, NO_2, HNO_3 and HNO_2. Clearly the relative contributions to a given electrical signal from various sources needs consideration[†].

3.9 Characterisation through the input impedance

The generation of bubbles in a liquid will alter its acoustic properties and therefore its coupling to the acoustic driver. Neppiras and Coakley observed the electrical signals across the insonating transducer to measure the acoustic impedance of the sample [3.182]. The use of filters allows monitoring at specific harmonics and subharmonics [3.183].

[†] The effect on electrical properties due to the production of such species need not be considered when no sonochemical activity is present, as is the case for the studies cited in Part 2. Huang et al. [3.181] do not incorporate the effect on the conductivity of any increase in void fraction which may result from exsolution over the 3 minute insonation period.

3.10 Conclusions

Inertial cavitation is not simple to characterise experimentally. Large expansion ratios, rapid wall motions, and a range of emissions for many of which the mechanism of generation is not unique, are just a few of the complicating factors. In addition, in key applications of interest the manifestations of inertial cavitation range from sparse, spatially-confined transient events relevant to microsecond pulses of biomedical ultrasound, to sizeable, sustained cavitation fields driven by continuous-wave ultrasound in cleaning baths. It is no wonder that the approaches to characterising inertial cavitation vary from field to field.

Whilst sufficiently energetic cavitation may be detected through the a range of effects (such as erosion and bioeffect), the process of relating such observations to gain information about the bubble field can be difficult, as the mechanisms by which these effects can arise are complicated (particularly, as is often the case, when many bubbles are involved) [3.174, 3.184]. The volume changes associated with inertial cavitation may be coupled to acoustic fields, and provide a more readily interpretable signal for sparse bubble populations: however in cavitation clouds both inertial and non-inertial cavitation are acoustically active. With the possible (but by no means certain) exceptions of sonochemical and sonoluminescent signals, it is possible for all the observables discussed in Section 3 to be generated, in a cavitating multi-bubble field, by more than one type of cavitation event. Therefore to infer the range of cavitation which occurs in a high power ultrasound field from such acoustic, biological, or erosive indicators is no simple task. In addition, since a range of cavitation will occur, those signals which are generated uniquely by a specific type of cavitation, though they may therefore be good measures of that phenomenon, will be unable to give information about the wider range of cavitation types that occur. Not only might a range of single bubble behaviours (listed in Figure 1.1) go undetected, but so too might population effects [3.174], such as acoustic shielding. The logical conclusion of this process, of characterising the cavitation, is to deploy a range of sensors to analyse the range of signals from the whole population. This becomes unnecessarily complicated, as complete characterisation of the cavitation is rarely required in many practical applications.

References

3.1. Esche, R. Untersuchung der schwingungskavitation in flüssigkeiten. Acustica, 1952; 2: (Akust. Beih.) AB208-AB218.

3.2. Bohn, L. Acoustic pressure variation and the spectrum in oscillatory cavitation. Acustica 1957; 7: 201-216.

3.3. Neppiras, E. A. Acoustic cavitation. Phys. Rep. 1980; 61: 159-251.

3.4 Leighton, T. G. *The Acoustic Bubble* (Academic Press, London) 1994

3.5. Apfel, R.E., Methods in Experimental Physics Vol. 19 (Ed. Edmonds, P.D.) Academic Press, New York 1981; 355-413.

3.6. Vaughan, P.W., Leeman, S. Some comments on mechanisms of sonoluminescence. Acustica 1986; 59: 279-281

3.7. Phelps A, Leighton TG. 1996. The subharmonic oscillations and combination frequency emisisons from a resonant bubble. Acta Acustica. In press

3.8. Güth, W. Nichtlineare Schwingungen von Luftblasen in Wasser. Acustica 1956; 6: 532-538.

3.9. Neppiras EA, Fill EE. A cyclic cavitation process. J Acoust Soc Am 1969; 46: 1264-1271

3.10. Neppiras, EA. Subharmonic and other low-frequency emission from bubbles in sound-irradiated liquids. J. Acoust. Soc. Am. 1969; 46: 587-601.

3.11. Basu S. Accelerated cavitation screening of organic coatings using acoustic emission technique. Trans. ASME, J. of Vibration, Stress, and Reliability of Design, 1984; 106: 560-564

3.12. Morton KI, ter Haar GR, Stratford IJ, Hill CR. Subharmonic emission as an indicator of ultrasonically-induced biological damage. Ultrasound Med Biol 1983; 9: 629-633

3.13. Edmonds, P.D., Ross, P., Acoustic emission as a measure of exposure of suspended cells *in vitro*. Ultrasound in Med. & Biol. 1986; 12: 297-305.

3.14. Eastwood, L.M., Watmough, D.J., Sonoluminescence, in water and in human blood plasma, generated using ultrasonic therapy equipment. Ultrasound in Med. & Biol. 1976; 2: 319-323.

3.15. Iernetti G. Pulsed ultrasonic cavitation. Part I: Cavitation noise, luminescence thresholds, nuclei distribution. Acustica 1970; 23: 189-207

3.16. Ceschia M, Iernetti G. Cavitation threshold model verified through pulsed sound cavitation in water. Acustica 1973; 29: 127-137

3.17. Margulis MA, Grundel LM. The ultrasonic luminescence of a liquid near the cavitation threshold. 1. The development of the pre-threshold luminescence of a liquid in an ultrasonic field. Russ. J. phys. Chem. 1981; 55: 386-389

3.18. Margulis MA, Grundel LM. Irradiation of a liquid with ultrasound near the cavitation threshold. 2. Fundamental irregularities of sonoluminescence at low ultrasound intensities. Russ. J. phys. Chem., 1981; 55: 989-991

3.19 Gaitan DF, Crum LA, Church CC, Roy RA. An experimental investigation of acoustic cavitation and sonoluminescence from a single bubble. J Acoust Soc Am 1992; 91: 3166-3183

3.20. Apfel, R.E. Acoustic cavitation prediction. J. Acoust. Soc. Am. 1981; 69: 1624-1633.

3.21. Apfel, R.E. Possibility of microcavitation from diagnostic ultrasound. IEEE Trans Ultrasonics, Ferroelectrics, Freq Control 1986; UFFC-33: 139-142.

3.22. Flynn, H.G. Generation of transient cavities in liquids by microsecond pulses of ultrasound. J. Acoust. Soc. Am. 1982; 72: 1926-2932.

3.23. Carstensen, E.L., Flynn, H.G. The potential for transient cavitation with microsecond pulses of ultrasound. Ultrasound Med. Biol. 1982; 8: L720-L724.

3.24. Crum, L.A., Fowlkes, J.B., Cavitation produced by short acoustic pulses. Ultrasonics Intl. Proc. 1985; 1: 237-242.

3.25. Fowlkes, J.B., Crum, L.A. Cavitation threshold measurements for microsecond pulses of ultrasound. J. Acoust. Soc. Am. 1988; 83: 2190-2201.

3.26. Carmichael, A.J., Massoba, M.M., Reisz, P., Christman, C.L. Free radical production in aqueous solutions exposed to simulated ultrasonic diagnostic conditions. IEEE Trans Ultrasonics, Ferro-electrics, Freq Control 1986; UFFC-33: 148-155.

3.27. Christman, C.L., Carmichael, A.J., Mossoba, M.M., Riesz, P., Evidence for free radicals produced in aqueous solutions by diagnostic ultrasound. Ultrasonics 1987; 25: 31-34.

3.28. West, C., Howlett, R. Some experiments on ultrasonic cavitation using a pulsed neutron source. Brit. J. Appl. Phys (J. Phys. D) 1968; Ser. 2, Vol. 1: 247

3.29. Negishi, K. Experimental studies on sonoluminescence and ultrasonic cavitation. Journal of the Physical Society of Japan 1961; 16: 1450-1465

3.30. Kuttruff, H. Über den zusammerhang zwischen der sonolumineszcenz und der schwingungskavitation in flüssigkeiten. Akustica 1962; 12: 230-254 (in German)

3.31. Roy, R.A., Atchley, A.A., Crum, L.A., Fowlkes, J.B., Reidy, J.J. A precise technique for the measurement of acoustic cavitation thresholds and some preliminary results. J. Acoust. Soc. Am. 1985; 78: 1799-1805.

3.32. Williams, A.R., Delius, M., Miller, D.L., Schwarze, W., Investigation of cavitation in flowing media by lithotripter shock waves both *in vitro* and *in vivo*. Ultrasound Med. Biol. 1989; 15: 53-60.

3.33. Sturtevant B. The physics of shock wave focusing in the context of extracorporeal shock wave lithotripsy. Intl. Workshop on Shock Wave Focusing. March 1989, Sendai, Japan, pp. 39-64

3.34. Coleman A J, Choi M J, Saunders J E and Leighton T G. 1992. Acoustic emission and sonoluminescence due to cavitation at the beam focus of an electrohydraulic shock wave lithotripter. Ultrasound Med. Biol., 18, 267-281.

3.35. Coleman AJ, Whitlock M, Leighton TG and Saunders JE. 1993. The spatial distribution of cavitation induced acoustic emission, sonoluminescence and cell lysis in the field of a shock wave lithotripter. Phys. Med. Biol. , **38**, 1545-1560

3.36. Olsson L, Almquist L-O, Grennberg A, Holmer N-G. Analysis and classification of secondary sounds from the disintegration of kidney stones with acoustic shock waves. Ultrasound Med Biol 1991; 17: 491-495

3.37. Atchley, A.A., Frizzell, L.A., Apfel, R.E., Holland, C.K., Madanshetty, S., Roy, R.A. Thresholds for cavitation produced in water by pulsed ultrasound. Ultrasonics 1988; 26: 280-285.
3.38. Holland, C.K., Apfel, R.E. Thresholds for transient cavitation produced by pulsed ultrasound in a controlled nuclei environment. J. Acoust. Soc. Am. 1990; 88: 2059-2069.
3.39. Roy RA, Church CC, Calabrese A. Cavitation produced by short pulses of ultrasound. Fronntiers of Nonlinear Acoustics, 12 ISNA, ed. Hamilton MF, Blackstock DT. Elsevier Applied Science, 476-491, 1990
3.40. Roy, R.A., Madanshetty, S., Apfel, R.E. An acoustic backscattering technique for the detection of transient cavitation produced by microsecond pulses of ultrasound. J. Acoust. Soc. Am. 1990; 87: 2451-2455.
3.41. Holland CK, Roy RA, Apfel RE, Crum LA. *In-vitro* detection of cavitation induced by a diagnostic ultrasound system. IEEE Trans on UFFC1992; 39: 95-101
3.42. Madanshetty SI, Roy RA, Apfel RE. Acoustic microcavitation: its active and passive detection. J Acoust Soc Am 1991; 90: 1515-1526
3.43. Church, CC. A method to account for acoustic microstreaming when predicting bubble growth rates produced by rectified diffusion. J. Acoust. Soc. Am. 1988; 84: 1758-1764.
3.44. Madanshtty SI. A conceptual model for acoustic microcavitation. J. Acoust. Soc. Am. 1995; **98**: 2681-2689
3.45 Nyborg WL (ed.). Cavitation Detection and Monitoring. Report by Working Group 22 of Accredited Standards Committee S1 of the Acoustical Society of America. In preparation.
3.46. Olson HG, Hammitt FG. High-speed photographic studies of ultrasonically induced cavitation. J Acoust Soc Am 1969; 46: 1272-1283
3.47. Tomita, Y., Shima, A. Mechanisms of impulsive pressure generation and damage pit formation by bubble collapse. J. Fluid Mech. 1986; 169: 535-564.
3.48. Vogel, A., Lauterborn, W., Timm, R. Optical and acoustic investigations of the dynamics of laser-produced cavitation bubbles near a solid boundary. J. Fluid Mech. 1989; 206: 299-338.
3.49. Leighton, T.G., Walton AJ, Field JE. "The high-speed photography of transient excitation". Ultrasonics 1989; 27: 370-373.
3.50. Neppiras, E. A. Acoustic cavitation. Phys. Rep. 1980; 61: 159-251.
3.51. Blake FG, Jr. Technical Memo No. 12, Acoustics Research Laboratory, Harvard University, Cambridge, Massachusetts, USA. (September 1949) 1949
3.52. Frenzel, J., Schultes, H. Luminescenz im ultraschall beschickten wasser. Kurze mitteilung. Zeit. für Phys. Chem. 1934; B27: 421-424
3.53. Rosenberg MD. La generation et l'etude des vibrations ultra-sonores de tres grande intensité. Acustica, 1962; 12: 40-49
3.54. Trevena DH. Cavitation and Tension in Liquids. Adam Hilger, Bristol and Philadelphia, 1987.
3.55 Leighton T G, Pickworth M J W Tudor J and Dendy P P. 1990. Studies of the cavitational effects of clinical ultrasound by sonoluminescence: 5. Search for sonoluminescence in vivo in the human cheek. Ultrasonics, **28**, 181-184
3.56 Smith RT, Webber GMB, Young FR, Stephens RWB. Sound propagation in liquid metals. Adv. Phys., 1967; 16: 515-522
3.57. Chambers, L.A., Phys. Rev. 1936; 49: 881.
3.58. Harvey, E.N. Sonoluminescence and Sonic Chemiluminescence . J. Am. Chem. Soc. 1939; 61: 2392-2398.
3.59. Frenkel, Ya.I., Acta Phisiochemica URSS 1940; 12: 317-323 (in Russian).
3.60. Weyl WA, Marboe EC. Research, 1949; 2: 19
3.61. Noltingk BE, Neppiras EA. Cavitation produced by ultrasonics. 1950. Proc. Phys. Soc. 1950; B, 63: 674-685
3.62. Griffing V. Theoretical explanation of the chemical effects of ultrasonics. J. chem. Phys., 1950; 18: 997-998
3.63. Griffing V. The chemical effects of ultrasonics. J. chem. Phys., 1952; 20, 939-942
3.64. Jarman, P.D., J. Acoust. Soc. Amer. 1960; 32: 1459-1463.
3.65. Walton, A.J., Reynolds, G.T. Sonoluminescence. Advances in Physics 1984; 33: 595-660.
3.66. Finch, R.D. Sonoluminescence. Ultrasonics 1963; 1: 87-98
3.67. Barber, B.P., Putterman, S.J. Observation of synchronous nanosecond sonoluminescence. Nature 1991; 352: 318
3.68. Barber, B.P., Hiller, R., Arisaka, K., Fetterman, H., Putterman, S. Resolving the picosecond characteristics of synchronous sonoluminescence. J Acoust Soc Am 1992; 91: 3061-3063
3.69. Crum LA. Sonoluminescence. J Acoust Soc Am 1992; 91: 517

3.70 Kamath V, Prosperetti A and Egolfopoulos FN. A theoretical study of sonoluminescence. J. Acoust. Soc. Am. 1993; **94**: 248-260

3.71 Wu, C.C. and Roberts, P. H. Shock-wave propagation in a sonoluminescing gas bubble. Phys. Rev. Lett. 1993; **70**(22): 3424-3427

3.72 Lepoint, T., Voglet, N., Faille, L. and Mullie, F. Bubbles deformation and interface distortion as a source of sonochemical and sonoluminescent activity. Proc. IUTAM Symposium on *Bubble Dynamics and Interface Phenomena* (Birmingham, UK, 6-9 Sept. 1993), Blake, J.R., Boulton-Stone, J.M. and Thomas, N.H. eds. Kluwer Academic Publishers, pp. 321-333

3.73 Crum, L.A. and Cordry, S. Single-bubble sonoluminescence. Proc. IUTAM Symposium on *Bubble Dynamics and Interface Phenomena* (Birmingham, UK, 6-9 Sept. 1993), Blake, J.R., Boulton-Stone, J.M. and Thomas, N.H. eds. Kluwer Academic Publishers, pp. 287-297

3.74 Eberlein C. Theory of quantum radiation observed as sonoluminescence. Physics Review Letters 1996; **76**: 3842

3.75. Leighton TG. Bubble population phenomena in acoustic cavitation. Ultrasonics Sonochemistry 1995; **2**: S123-136

3.76 Crum LA. Comments on the evolving field of sonochemistry by a cavitation physicist. Ultrasonics Sonochemistry, 1995; **2**: S147-S152

3.77 Roy RA. Acoustic detection of inertial activation from ultrasound. J. Acoust. Soc. Am. 1995; **98**: 2921 (abstract).

3.78. Reynolds, G.T., Walton, A.J., Gruner, S. Observations of sonoluminescence using image intensification. Rev. scient. Instrum., 1982; 53: 1673-1676

3.79 Pickworth M J W, Dendy P P, Twentyman P R and Leighton T G. 1989. Studies of the cavitational effects of clinical ultrasound by sonoluminescence: 4. The effect of therapeutic ultrasound on cells in monolayer culture in a standing wave field. Phys. Med. Biol., **34** (11), 1553-1560.

3.80. Suhr D, Brümmer F, Hülser DF. Cavitation-generated free radicals during shock wave exposure: investigations with cell-free solutions and suspended cells. Ultrasound Med Biol 1991; 17: 761-768

3.81. Roy, R.A., Fowlkes, J.B. A comparison of the thresholds for free-radical generation and transient cavitation activity induced by short pulses of ultrasound. J. Acoust. Soc. Am. Suppl. 1. 1988; 84: S36.

3.82. Crum, L.A., Fowlkes, J.B. Acoustic cavitation generated by microsecond pulses of ultrasound. Nature 1986; 319: 52-54.

3.83. Fowlkes, J.B. and Crum, L.A. An examination of cavitation due to short pulses of megahertz ultrasound. Tech. Rep. No. NCPA LC.01 for NIH (University of Mississippi, University, MS, 1988).

3.84. Miller DL and Thomas RM A comparison of hemolytic and sonochemical activity of ultrasonic cavitation in a rotating tube. Ultrasound Med. Biol. 1993; **19**: 83-90.

3.85. Suslick, K.S., Hammerton, D.A., Cline, R.E., Jr. The sonochemical hot spot. J. Am. Chem. Soc. 1986; 108: 5641-5642.

3.86. Hill CR, Clarke PR, Crowe MR, Hannick JW. 1969 Ultrasonics for Industry Conference Papers 26-30

3.87. Lumley, P.J., Walmsley, A.D., Laird, W.R.E. An investigation into the occurrence of cavitational activity during endosonic instrumentation. J. Dent. 1988; 16: 120-122.

3.88. Ahmad, M., Pitt Ford, T.R., Crum, L.A. Ultrasonic debridement of root canals: An insight into the mechanisms involved. J. Endodont 1987; 13: 93-101.

3.89. Mason TJ. Practical Sonochemistry (Ellis Horwood, Chichester, UK), 1991.

3.90. Suslick, K.S., ed. Ultrasound : Its Chemical, Physical, and Biological Effects VCH Publishers, New York 1988

3.91. Hill CR (ed.). Physical principles of Medical Ultrasonics. Ellis Horwood Ltd, Chichester (for John Wiley and Sons, New York), 1986

3.92. Mason TJ, Lorimer JP (eds.). Sonochemistry: Theory, Applications and Uses of Ultrasound in Chemistry (Ellis Horwood, Chichester, UK), 1989.

3.93. Coakley WT, Nyborg WL. Chapter II: Cavitation; Dynamics of gas bubbles; Applications. In: *Ultrasound: Its applications on medicine and biology*, Fry, F, ed. New York: Elsevier, Part 1, 1978, pp. 77-159

3.94. Chaudhri MM, Field JE. The role of rapidly compressed gas pockets in the initiation of condensed explosives. Proc Roy Soc Lond 1974; A340: 113-128
3.95. Richards, W.T., Loomis, A.L. The chemical effects of high frequency sound waves I. A preliminary survey. J. Amer. Chem. Soc., 1927; 49: 3086-3100
3.96. Henglein, A. Sonochemistry: historical developments and modern aspects. Ultrasonics 1987; 25: 6-16
3.97. Brohult, S. Splitting of the Hæmocyanin molecule by ultra-sonic waves. Nature 1937; 140: 805
3.98. Schulz, R., Henglein, A. Über den Nachweis von freien Radikalen, die unter dem Einfluβ von Ultraschallwelen gebildet werden, mit Hilfe von Radikal-Kettenpolymerisation und Diphenyl-pikryl-hydrazyl. Z. Naturforsch 1953; 8b: 160-161
3.99. Suslick, K.S., Doktycz, S.J., Flint, E.B. On the origin of sonoluminescence and sonochemistry. Ultrasonics 1990; 28: 280-290
3.100. Flynn HG. *Physics of acoustic cavitation in liquids.* In: Physical Acoustics. Mason WP, ed. (New York: Academic Press) 1964; vol 1 part B: 57-172
3.101. Prudhomme, R.D. Vijnana Parishad Anusandhan Patrika 1972; 15: p. 3
3.102. Frenzel, J., Schultes, H. Luminescenz im ultraschall beschickten wasser. Kurze mitteilung. Zeit. für Phys. Chem. 1934; B27: 421-424
3.103. Frenkel, Ya.I., Acta Phisiochemica URSS 1940; 12: 317-323 (in Russian).
3.104. Bresler, S. Acta Physicochim (USSR) 1940; 12: 323
3.105. Suslick KS, Hammerton DA. The site of sonochemical reactions. IEEE Trans Ultrasonics Ferroelec Freq Contr 1986; 33: 143-147
3.106. Fischer, Ch.-H., Hart, E.J., Henglein, A. Ultrasonic irradiation of water in the presence of $^{18,18}O_2$: Isotope exchange and isotopic distrubution of H_2O_2. J. phys. Chem., 1986; 90: 1954-1956
3.107. Henglein A. Chemical effects of continuous and pulsed ultrasound in aqueous solutions. Ultrasonics Sonochemistry 1995: **2**: S115-121.
3.108. Bergmann, L., Der Ultraschall S. Hirzel Verlag, Stuttgart, FRG 1954
3.109. El' Piner, I., Ultrasound: Physical, Chemical and Biological Effects Consultants Bureau, New York, USA 1964
3.110. Weissler, A., Encyclopedia of Chemical Technology Vol. 15 (Eds Kirk, R.E. and Othmer, D.F.) Wiley Interscience, New York, USA 1981; 773
3.111. Boudjouk, P., Nachr Chem Techn Lab 1983; 31: 797
3.112. Young FR. Cavitation. McGraw-Hill Book Company (London). 1989
3.113. Digby M, Duck FA, Lenz EJ and Price GJ. Technical note: Measurement of collapse cavitation in ultrasound fields. Brit. J. Radiol. 1995; **68**: 1244-1248
3.114. Price GJ and Lenz EJ. The use of dosimeters to measure radical production in aqueous sonochemical sytems. Ultrasonics 1993; **31**: 451-456
3.115. McLean JR and Mortimer AJ. A cavitation and free radical dosimeter formultrasound. Ultrasoundd med. Biol. 1988; **14**: 59-64
3.116. Miller DL and Thomas RM. Frequency dependence of cavitation activity in a rotating tube exposure system compared to the mechanical index. J. Acoust. Soc. Am. 1993; **93**: 3475-3480.
3.117. Spinks JWT and Woods R. An Introduction to Radiation Chemistry. Second edition (Wiley, New York), 1976
3.118. Kondo T, Kirschenbaum LJ, Kim H and Riesz P. Sonolysis of dimethyl sulfoxide-water mixtures: a spin-trapping study. J Phys. Chem. 1993; **97**: 522-527.
3.119. Jana AK and Chatterjee SN. Estimation of hydroxyl free radicals produced by ultrasound in Fricke solution used as a chemical dosimaeter. Ultrasonics Sonochemistry 1995; **2**: S87-S91
3.120. Mason RP. Free radical metabolites of foreign compounds and their toxological significance. In: Reviews in Biochemical Toxicology (Hodgson E, Bend JR and Philpot RN, eds.) Elsevier/North-Holland, Amsterdam 1979, p. 151
3.121. Edmonds PD and Sancier KM. Evidence for free radical production by ultrasonic cavitation in biological media. Ultrasound Med. Biol. 1983; **9**: 635-639
3.122. McCay PB, Noguchi T, Fong K-L, Lai EK, and Power JL. Production of radicals from enzyme systems and the use of spin traps. In: Free Radicals in Biology (Pryor WA, ed.) Academic Press, New York, 1980; **4**: 155-184
3.123. Finkelstein E, Rosen GM and Raukman EJ. Spin trapping of superoxide and hydroxyl radical: practical aspects. Arcives Biochemistry and Biophysics, 1980; **200**: 1-16

3.124. Janzen EG. A critical review of spin trapping in biological systems. In: Free Radicals in Biology (Pryor WA, ed.) Academic Press, New York, 1980; **4**: 116-150
3.125. Kalyanaraman B. Detection of Toxic Free Radicals in Biology and Medicine. In: Reviews in Biochemical Toxicology (Hodgson E, Bend JR and Philpot RN, eds.) Elsevier, New York, 1982; Vol. IV.
3.126. Makino K, Mossoba MM and Riesz P. Chemical effects of ultrasound on aqueous solutions. J. Am. Chem. Soc. 1982; 104: 3537-359
3.127. Makino K, Mossoba MM and Riesz P. Chemical effects of ultrasound on aqueous solutions. Formation of hydroxyl radicals and hydrogen atoms. J. Phys. Chem. 1983; 104: 1369-1377
3.128. Kondo T, Gamson J, Mitchell JB and Riesz P. Free radical formation and cell lysis induced by ultrasound in the presence of different rare gases. Int. J. Radiat. Biol., 1988; **54**: 955-962
3.129. Kondo T, Krishna CM and Riesz P. Pyrolysis radicals formed by ultrasound in aqueous solutions of nucleotides: A spin-trapping study. Int. J. Radiat. Biol. 1990; **57**: 23-33
3.130. Miller DL and Thomas RM A comparison of hemolytic and sonochemical activity of ultrasonic cavitation in a rotating tube. Ultrasound Med. Biol. 1993; **19**: 83-90
3.131. Clarke, P.R., Hill, C.R. Physical and chemical aspects of ultrasonic disruption of cells. J. Acoust. Soc. Am. 1970; **47**: 649-653
3.132. Weissler A, Cooper HW, Snyder S. Chemical effects of ultrasonic waves: oxidation of KI solution by CCl_4. Journal of the American Chemical Society, 1950; **72**: 1769
3.133. Ciaravino V, Flynn HG, Miller MW Carstensen EL. Pulsed enhancement of acoustic cavitation: a postulated model. Ultrasound Med. Biol. 1981; 7: 159-166
3.134. Riesz P. Free radical generation by ultrasound in aqueous solutions of volatile and non-volatile solutes. Adv. Sonochem., 1991; **2**: 23-64
3.135. Carstensen, E.L., Campbell, D.S., Hoffman, D., Child, S.Z., Aymé-Bellegarda, E.J. Killing of *drosophila* larvae by the fields of an electrohydraulic lithotripter. Ultrasound in Med. & Biol. 1990; Vol 16, No. 7: pp.687-698.
3.136. Watmough, D.J., Dendy, P.P., Eastwood, L.M., Gregory, D.W., Gordon, F.C.A., Wheatley, D.N. The biophysical effects of therapeutic ultrasound on HeLa cells. Ultrasound Med. Biol. 1977; Vol. 3: pp. 205-219.
3.137. Rooney, J.A. Shear as a mechanism for sonically induced biological effects. J. Acoust. Soc. Am. 1972; 52: 1718.
3.138. Miller DL, Williams AR. Bubble cycling as the explanation of the promotion of ultrasonic cxavitation in a rotating tube exposure system. Ultrasound Med Biol 1989; 15: 641-648
3.139. Miller DL, Thomas RM, Williams AR. Mechanisms for hemolysis by ultrasonic cavitation in the rotating exposure system. Ultrasound Med Biol 1991; 17: 171-178
3.140. Tomlinson WJ and Chapman D. Effect of amplitude on the erosion and corrosion of copper by 20 kHz ultrasound. Wear 1989; **130**: 381-384
3.141. Lush PA, Sanada N, Takayama K. 1987. Proc. 7th. Int. Conf. on Erosion by Liquid and Solid Impact (ed. J. E. Field and J. P. Dear). Cavendish Laboratory, Cambridge, UK, paper 24
3.142. Hansson I, Mørch KA, Preece CM. 1978. Ultrasonics International IPC Science and Technology Press Ltd., Guildford, United Kingdom 77, p. 267
3.143. Rayleigh, Lord. On the pressure developed in a liquid during the collapse of a spherical cavity. Phil. Mag.1917; 34: 94-98.
3.144. Plesset MS, Prosperetti A. Bubble dynamics and cavitation. Ann Rev Fluid Mech, 1977; 9: 145-185
3.145. Mørch KA. 1979. Erosion, (ed. C. M. Preece), pp. 309-353. Academic
3.146. Dmitriev, A.P., Dreiden, G.V., Ostrovskii, Yu. I., É tinberg, M.I. Profile of a shock wave produced by collapse of a spherical bubble in a liquid. Sov. Phys. Tech. Phys. 1985; 30: 224
3.147. Hickling R, Plesset MS. Collapse and rebound of a spherical bubble in water. Phys. Fluids, 1964; 7: 7-14
3.148. Ivany RD. 1965. Univ. of Michigan, Dept. of Nuclear Eng., Tech. Rep. No. 15
3.149. Vyas B, Preece CM. Stress produced in a solid by cavitation. J. Appl. Phys., 1976; 47: 5133-5138
3.150. Mørch KA. 1977. Euromech. Colloq. 98, Eindhoven, Netherlands.
3.151. Brunton JH. 1967. Proc. Int. Conf. Rain Eros., 2nd (A. A. Fyall and R. B. King, ed.), p. 291. Royal Aircraft Establishment, Farnborough, United Kingdom.
3.152. Hansson I, Mørch KA. The dynamics of cavity clusters in ultrasonic (vibratory) cavitation erosion. J. Appl. Phys., 1980; 51: 4651-4658

3.153. Hansson I, Kendrinskii V, Mørch KA. On the dynamics of cavity clusters. J. Phys. D:Appl. Phys. 1982; 15: 1726-1734
3.154. Ellis AT. 1966. Proc. 6th Symp. on Naval Hydrodyn., Washington DC, pp. 137-161
3.155. Zhang, Y.J., Li, S.C., Hammitt, F.G. Statistical investigation of bubble collapse and cavitation erosion effect. Wear 1989; 133: 257-265
3.156. Neppiras, E. A. Acoustic cavitation. Phys. Rep. 1980; 61: 159-251.
3.157. Benjamin, T.B., Ellis, A.T. The collapse of cavitation bubbles and the pressures thereby produced against solid boundaries. Phil. Trans. R. Soc. Lond. 1966; A 260: 221-240.
3.159. Olson HG, Hammitt FG. High-speed photographic studies of ultrasonically induced cavitation. J Acoust Soc Am 1969; 46: 1272-1283
3.160. Naudé, C.F., Ellis, A.T. On the mechanism of cavitation damage by nonhemispherical cavities collapsing in contact with a solid boundary. Trans. ASME D: J. Basic Engng 1961; 83: 648-656.
3.161. Tomita, Y., Shima, A. Mechanisms of impulsive pressure generation and damage pit formation by bubble collapse. J. Fluid Mech. 1986; 169: 535-564.
3.162. Dear, J.P., Field, J.E. A study of the collapse of arrays of cavities. J. Fluid Mech. 1988; 190: 409-425.
3.163. Crawford AE. The measurement of cavitation. Ultrasonics 1964; **2**: 120-123
3.164. Brown B. British Communication and Electronics (December 1962), 918.
3.165. Walmsley AD, Walsh TF, Laird WRE et al. Effects of cavitational activity on the root surface of
3.166. Miller DL, Thomas RM, Williams AR. Mechanisms for hemolysis by ultrasonic cavitation in the rotating exposure system. Ultrasound Med Biol 1991; 17: 171-178
3.167. Tomlinson WJ, Moule RT and Blount GN. Cavitation erosion of pure iron in distilled water containing chloride and chromates. Tribology International 1988; **21**: 21-25
3.168. Tomlinson WJ and Talks MG. Cavitation erosion of grey cast irons containing 0.2 and 1.0% phosphorus in corrosive waters. Tribology International 1989; **22**: 195-204
3.169. Rosenberg LD. On the physics of ultrasonic cleaning, Ultrasonic News, October 1960, vol. IV No. 4, pp. 16-20
3.170. Anthony OA. Technical aspects of ultrasonic cleaning, Ultrasonics, 1963; 1: 194-198
3.171 Cavitation activity measuring procedure. Report from the Ultrasonic Manufacturers Association Inc., © 1964.
3.172. Ultrasonic cleaning equipment standard. Report from the Ultrasonic Manufaturers Association Inc., August 8, 1964.
3.173. Weissler A. A chemical method for measuring relative amounts of cavitation in an ultrasonic cleaner. IRE International Convention Record, 1962, part 6, pp. 24-30
3.174. Leighton TG. 1995. Bubble population phenomena in acoustic cavitation. Ultrasonics Sonochemistry, **2**, S123-136
3.175. Weissler A. Paper presented at the Institute of Radio Engineers' Symposium on Sonics and Ultrasonics (1962).
3.176. Specification for sonic cleaning equipment. Writing Group S1-W-31, American Standards Association, 1963.
3.177. Boucher RMG and Kreuter J. Measurement of cavitation activity in ultrasonic cleaners. Contamination Control, March 1967, pp. 16-18
3.178. Boucher RMG and Kreuter J. The measurement of cavitation activity in ultrasonic cleaners. Macrosonics Corporation, Internal Report, 1966.
3.179. Weissler A. Ultrasonic cavitation measurements by chemical methods. Fourth International Congress on Acoustics, Copenhagen, 1961, J.32, pp. 21-29
3.180. Comments on standardization of methods for evaluating ultrasonic cleaners. Writing Group S1-W-31, American Standards Association, 1966.
3.182. Neppiras EA and Coakley WT. Acoustic cavitation in a focused field in water at 1 MHz. J Sound Vib. 1976; **45**: 341-373
3.183. ter Haar GR. Ultrasonic Biophysics. Chapter 12 in: Hill CR (ed.). Physical principles of Medical Ultrasonics. Ellis Horwood Ltd, Chichester (for John Wiley and Sons, New York), 1986
3.184. Leighton TG. 1994. Acoustic Bubble Detection. I. The detection of stable gas bodies. Environmental Engineering, **7**, 9-16
3.185. Leighton TG. 1995. Bubble population phenomena in acoustic cavitation. Ultrasonics Sonochemistry, **2**, S123-136
3.186. Schafer ME and Broadwin A. Acoustical characterization of ultrasonic surgical devices. Ultrasonics Symposium 1994, pp. 1903-1906.

3.187. Sehgal C, Yu TJ, Sutherland RG and Verrall RE. Use of 2,2-Diphenyl-1-picrylhydrazl to investigate the chemical behaviour of free radicals induced by ultrasonic cavitation. J. Phys. Chem., 1982; **86**: 2982-2986

3.188. Kontronarou A, Mills G, Hoffmann MR. Ultrasonic irradiation of *p*-Nitrophenol in aqueous solution. J. Physical Chem., 1991; **95**: 3630-3638

3.189. Klima J, Bernard C, Degrand C. J. Electroanal. Chem., 1995; **399**: 147-155

4. DISCUSSION OF THE POSSIBILITY OF A STANDARD FOR CAVITATION

4.1 Can cavitation be standardised?

Can cavitation be standardised? In an absolute sense, this would seem to be an impossibility. Though by no means an exact analogy, the question is rather akin to asking if fire can be standardised. Fire is familiar to many, readily produced, and can be controlled sufficiently to produce a wide range of beneficial effects. It can appear in unwanted situations and be hazardous. It is easier to visualise a typical flame, and to exploit the effects it can produce (e.g. light emission, heat production, oxidisation, fluid circulation, etc.), than it is to comprehend in detail what occurs within the flame. Such details exhibit fine spatial and temporal variations, though the averages are readily measurable. The effects produced by the phenomenon (listed above) can be measured and compared against standard units. All these are characteristics of cavitation.

It is possible, however, to examine in isolation the elements which can contribute to a complex bubble field. When examining stable bubbles in sparse population, acoustic techniques are often the most useful; and of these those which exploit the resonance are the most powerful way of obtaining bubble size information. As the population density increases, their reliabilities must be compared with those of other techniques, both acoustic and otherwise. Geometrical scattering of high frequency ultrasound or light tend to be insensitive to the bubble size, as do most non-acoustic techniques (e.g. electrical conductivity). These can be made sensitive to bubble size by pulsating the bubble acoustically and detecting the modulated signal, as discussed in Part 2. With the detection of inertial cavitation it is neither the bubble pulsation nor the resonance which is important, nor indeed to most users any primary cavitation measure, but rather the effects of cavitation (cleaning, erosive, chemical, biological).

These arguments would tend to suggest that for cavitation fields, containing many bubbles and, for the most part, designed to produce some desired effect, standardising that effect would be the easier option. However not all applications generate the same degree of cavitation. Figure 4.1 illustrates just some of the range of applications of cavitating field, shown as a function of the pulse length and of the pressure amplitude. The range is very broad, in these parameters and also in the acoustic frequency and duty cycle. Continuous-wave applications (to the right of the figure) can generate self-sustaining clouds in which both inertial and non-inertial cavitation will occur. Of the continuous-wave applications shown, only physiotherapeutic ultrasound is not explicitly designed to generate cavitation, and as such it uses lower pressure amplitudes and, broadly speaking, higher frequencies. Cavitation should also be less likely in clinical physiotherapy because nuclei are likely to be less abundant *in vivo* than in the other continuous-wave applications shown on the figure. A similar scarcity of nuclei is relevant to the microsecond-pulse applications shown to the left of the figure, so that lithotripsy (which can cause cavitation *in vivo*) is seen to exploit higher pressure amplitudes.

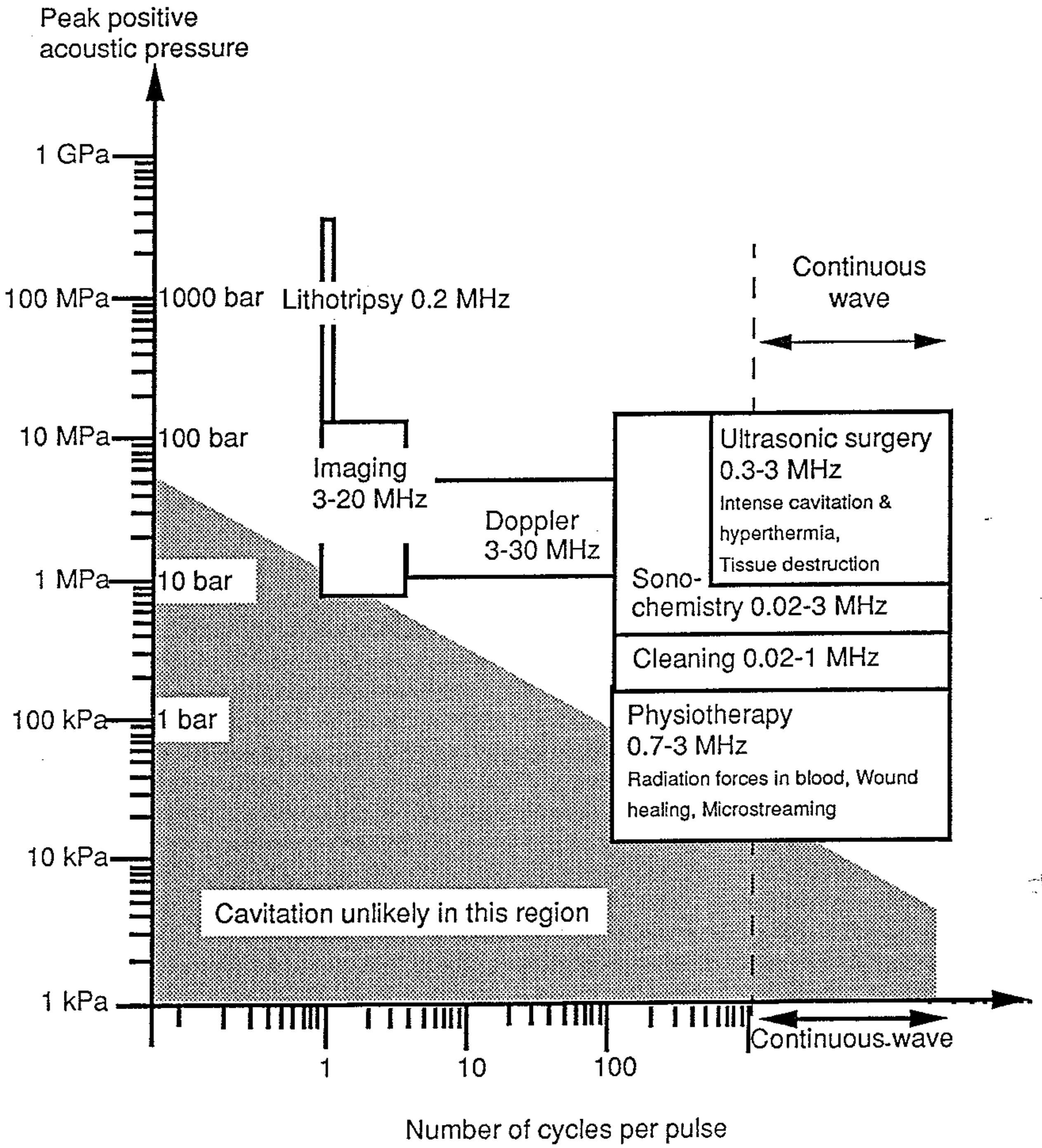

Figure 4.1 A rough schematic of the acoustic pressures and pulse lengths employed in some of the applications of ultrasound. Parameters are meant as a rough guide only . If an application lies outside the zone where 'cavitation is unlikely', this by no means indicates that cavitation may occur in that application: this would depend on a number of factors, not least the likelihood of nucleation in the liquid sample in question.

Reference	Luminescence SL/CL	Sonochem-istry	Bioeffect	Mech. damage	Optical	Acoust. impedance	Emit broadband/transient acoustics	Subharmonic emission	End-point	Correlation
Negishi '61 [3.29]	×						×		onset	3
Kuttruff '62 [3.30]	×				×		×		temporal	3 Optical (Schlieren) detection of rebound pulses coincident with SL
de Santis et al '67 [4.1]					×			×	onset	2 subharmonic appears just before bubble seen
Neppiras '68 [3.10]					×			×	onset	2 subharmonic appears just before bubble seen
Neppiras '68 [3.10]					×		×		onset	3
Hill et al. '69 [3.86]	×	×	×					×	onset	1 for SL with all others 3 for sonochemistry, bioeffect & subharmonic
Clarke & Hill '70 [3.131]		×	×	×					onset & maxima	2 Authors conclude that bioeffect is from mechanical, rather than chemical, effects.
Saksena & Nyborg '70 [4.2]	×						×		onset	3
Iernetti '70 [3.15]	×							×	onset	1
Ceschia & Iernetti '73 [3.16]	×							×	onset	1
Coakley & Saunders '73 [4.3]		×				×			onset	3
Neppiras & Coakley '76 [3.182]					×		×		onset	3
Eastwood & Watmough '76 [4.4]	×							×	onset	2 sporadic subharmonic before SL is seen, but reaches constant level when SL level crossed
Eastwood & Watmough '76 [4.4]	×						×		onset	3
Hedges et al. '77 [4.5]		×						×	onset	3 for subharmonic and Iodine release 1 for subharmonic and Ferric sulphate reaction
Graham et al '80 [4.6]	×	×	×					×	onset	3 for SL and I_2 release (activity correlates too), with subharmonic threshold slightly lower (2) 2 for subharmonic and plant root growth rate 3 for subharmonic and *E. coli* survival 1 for subharmonic and lymphocyte pyknosis
Margulis & Grundel '81 [3.17, 3.18]	×							×	onset	1
Morton et al '82 [4.7]			×					×	activity	3
Morton et al '83 [3.12]			×					×	onset	3
Basu '84 [3.11]				×			×		activity	3
Roy et al. '85 [3.31]	×						×		onset	1
Edmonds & Ross '86 [3.13]			×				×	×	activity	2 Combined rms acoustic emissions correlated well with cell viability and survival, but not with growth.
Roy & Fowlkes '88 [3.81]	×						×		onset	2
Coleman et al. '92 [3.34]	×						×		temporal	3
Coleman et al. '93 [3.35]	×		×				×		spatial	3 for cell lysis and rebound emissions 2 for SL and rebound emissions
Miller & Thomas '93 [3.130, 4.9]	×	×	×						activity	2 (Bio with CL & with TA); 3 (CL & TA) Able to distinguish between mechanical (cell lysis) and sonochemical effects (Isoluminol used to quantify residual H_2O_2 not provide space/time resolution; correlates well with free radical detection using TA)
Miller & Thomas '95 [4.10]	×		×						activity	1 Suggests DNA strand breaks not caused by residual H_2O_2 only (Isoluminol used to quantify H_2O_2 not provide space/time resolution)
Fuciarelli et al. '95 [4.11]	×		×						activity	1 Suggests DNA base damage products not caused by residual H_2O_2 (Isoluminol used quantify H_2O_2 only).

Table 4.1. Historical correlations of cavitation effects (sono- or chemi-luminescence; sonochemistry; bioeffect; mechanical damage (including erosion); optical (visual/Schlieren, i.e. excluding luminescence); acoustic impedance, noise, or subharmonic): 3≡good correlation; 2≡some correlation, but differences found; 1≡poor correlation. Scores arise from the subjective impression from the author. The individual experiments are discussed in Part 3.

The most common industrial ultrasonic systems exploit high power continuous-wave or tone-burst waveforms to generate cavitation fields containing a complex population of bubbles, some of which undergo inertial cavitation and others, not doing so. A proportion of bubbles will be capable of achieving the desired industrial effect, others will indirectly influence that effect, and a proportion will be capable of generating the signal exploited by the *in situ* detector. How the latter population overlaps with the other two is an important issue. Such cavitation fields are probably the most difficult to characterise, and much of section 4.2 is aimed, at least in the first instance, at them.

Given this wide range in acoustic fields and in the desired effect (which ranges from a desire for no cavitation to one for intense chemical or physical change), two approaches to characterising a cavitating fields suggest themselves. The first is to characterise the bubble activity in the field (through measurement of some effect it produces), and relate it back to basic characteristics elucidated, for example, through correlation between theory and experiment of the dynamics of controlled bubble populations. Given the range of behaviour which can occur, this could be very difficult. The second approach would be to say that, in the application in question, it is a given effect that the cavitation produces which is of prime importance. As a result it may be more desirable to correlate that effect (e.g. chemical, erosive, bioeffect) with a signal that can be more readily be monitored (acoustic emissions or sonoluminescence, both of which allow remote, minimally-invasive, real-time sensing). Attempts to investigate such correlations are recorded in Table 4.1 (the individual experiments are discussed in Part 3). This second, more utilitarian approach does not involve the basic bubble dynamics, and in by-passing them does not consider the mechanisms which produce the effect. The two approaches amount, first, to a standardisation of cavitation, and, second, to a calibration of effects. Both require as a primary and necessary stage, the measurement of the effects of cavitation in some standard manner. This process will be discussed in section 4.2.

Before doing so, it is useful to clarify certain aspects of the correlation studies listed in Table 4.1 since, if the second approach is to be followed, a coherent programme of such studies on controlled cavitation fields will be necessary. Initial examination of the scoring patterns of the correlations from Table 4.1, shown in matrix form in Table 4.2, shows that the implementation of the second approach will require some care.

	Luminescence SL/CL	Sonochemistry	Bioeffect	Mechanical damage	Optical	Acoustic impedance	Emit broad-band/transient acoustics	Subharmonic emission
Luminescence SL/CL		1,3,3,3 [2.5]	1,2,2,1,1 [1.4]		3		3,3,3,3,1,2,3,2 [2.5]	1,1,1,2,2,1 [1.3]
Sonochemistry	1,3,3,3 [2.5]		3,2,2,2 [2.3]	2		3		3,3,1,2 [2.3]
Bioeffect	1,2,2,1,1 [1.4]	3,2,2,2 [2.3]		2			2,3 [2.5]	3,2,3,1,3,3,2 [2.4]
Mechanical damage		2	2				3	
Optical	3						3,3 [3]	2,2 [2]
Acoustic impedance		3						
Emit broad-band/transient acoustics	3,3,3,3,1,2,3,2 [2.5]		2,3 [2.5]	3	3,3 [3]			
Subharmonic emission	1,1,1,2,2,1 [1.3]	3,3,1,2 [2.3]	3,2,3,1,3,3,2 [2.4]		2,2 [2]			
AVERAGE	2.1	2.4	2.1	2.3	2.7	3	2.8	2

Table 4.2. Summary and averages of the correlations awarded to the tests shown in Table 4.1.

The scores from Table 4.1 are recorded at the relevant matrix position in Table 4.2. If a given correlation has only been tested once, the score is entered in bold. If there are more than one test for a given correlation, their scores are averaged to produce the figures in bold square brackets. Such a scoring system is necessarily crude, and with so few tests involved the validity of averaging in this way is questionable. In addition a low score might either indicate that two effects, which arise from different bubble dynamics, are uncorrelated; or alternatively that the sensor is sensitive and highly discriminative. If two different signals do arise from two different forms of cavitational behaviour, the best correlation which can be expected between the signals will reflect the degree to which the generation mechanisms correlate; and therefore, a high correlation may indicate that a technique is unable to discriminate such differences. Finally, the average score for each column is calculated at the base, though the author warns that such a procedure (averaging across the correlations with a range of other techniques) has some interest but little justification. However the Table 4.2 provides a useful starting point for noting trends.

The overall averages at the base of the columns give some interesting scores. Those for signals relevant to processing (sonochemistry, bioeffect and mechanical damage) are promising (higher scores exist for optical and impedance measurements, but these are biased by the small number of tests incorporated in the study). The lowest of these is for bioeffect, which is physically reasonable since some bioeffects can arise through relatively low-energy cavitation, and be brought about through chemical and mechanical effects (Section 3.6). Broadband/transient acoustic emission scores highly (though again, with the exception of the studies with luminescence, the tests are few). This is promising since this acoustic technique is simple to use, minimally invasive, and applicable to a wide range of media (opaque, hostile etc.).

Within the body of the matrix, good correlations tend to exist between sono- or chemi-luminescence and both sonochemical tests and broadband/transient acoustic emissions. However the author has found no tests of the correlation between sonochemistry and broadband emission to incorporate in this table in order to reinforce this positive observation. Correlation of luminescence with bioeffect and subharmonic emission is poor. This creates an apparent paradox, since sonochemical tests tend to score highly against a range of other sensors, including bioeffect and subharmonic emission. This can only be resolved, if the scorings are taken to be reliable, by the recognition that the luminescence and chemical tests used have been fundamentally different. Indeed they have been, and the role of a single indicator between tests can change dramatically. For example, the earliest tests used luminescence and sonochemistry to detect the cavitation threshold, the luminescence being employed as a real-time indicator; in contrast, in the later tests [3.130, 4.9-4.11] the luminescence of isoluminol is used to quantify the residual hydrogen peroxide. The fact that a given correlation can score 3 in one instance and 1 in another (compare, for example, luminescence and sonochemistry) proves that individual experiments vary widely.

Whilst it is possible to comment at length on Table 4.2, the main conclusion must be that the tests done to date were not designed to produce a standard for cavitation, as the variation in testing procedure indicates. In addition the majority of the studies has examined the onset, and not the activity, of an effect, which is necessary if the second approach is to be successfully adopted. Throughout the course of the historical studies listed, knowledge of the underlying cavitation mechanisms which generate such signals, and how they relate to bubble dynamics, has improved. This not only means that experimental design has changed, but so has the interpretation of results. For example, the failure to see a correlation in the earlier studies may have in those days been interpreted as indicating a technique to be unreliable. However an alternative explanation is that the various sensors respond to different forms of bubble activity, and certain authors (e.g. Clarke and Hill [3.131]) recognised this. In the studies of Miller and Thomas [3.130, 4.9] this fact is recognised and exploited to differentiate the activity of the mechanical effects (hemolysis) from the production of free radicals (as detected by terephthalic acid) and residual hydrogen peroxide (as quantified through the use of isoluminol). Therefore rather than viewing the data in Table 4.1 as a whole, it is important to interpret it as a progression, where the later researchers benefited not only from knowledge of the prior one, but also worked in a community where the underlying bubble dynamics were better understood, and with, of course, the facility for improved sensors and data handling. To simply add up the score for each technique over more these four decades of experimentation would therefore be misleading. This is particularly so when it is remembered that some workers used concentrated, and others sparse, cavitation fields; focused, travelling wave, and rotating tube conditions, and a wide frequency range have been employed. A standardisation of cavitation conditions, sensors, and of endpoint is required. These issues are approached in section 4.2.

4.2 The measurement of the effects of cavitation in a standard manner

If the cavitation field associated with a certain application, for example in the industrial workplace, is to be characterised, then it is the cavitation field that is fixed and the option presented is in the choice of the detection method. Since such characterisation has proved difficult to achieve to date, it is therefore in this choice that the problems arise.

The choice encompasses two parts: The choice of the signal(s) to be used, and the definition of the endpoint of the measurement. The signals will be discussed in section 4.2.4.

4.2.1 Choice of endpoint

As can been seen from Table 4.1 it is important to define the endpoint if one is to compare two detection systems. Most industrial systems which exploit cavitation need a measure of the 'activity' as it occurs in their system. They exploit ultrasound in conditions above the threshold for inertial cavitation, the issues being ones of linearity/calibration, dynamic range etc.. The question of measurement of the threshold itself is, to a certain extent, irrelevant. However historically the endpoint has often been the threshold conditions (usually acoustic pressure) required to detect an effect associated with inertial cavitation, for a number of reasons. First, a threshold is the simplest of measurements: a simple 'yes' or 'no' answer is required of the detector. Second, knowledge of the threshold conditions, and verification of theories which might be extrapolated to *in vivo* conditions, were required to assess the potential for cavitation during diagnostic medical ultrasound examinations. Last, and perhaps most importantly, inertial cavitation is a threshold phenomenon, although what is meant by that needs thought: certain thresholds have been artificially defined [3.6, 3.38], though reliable formulation to indicate that such a threshold should exist. However such formulation is based upon the assumption that there is initially a free-floating spherical bubble nucleus available to seed the cavitation. If this is not available, the measured threshold might refer to the conditions required to seed the sample with such nuclei (as discussed in sections 1.3.2). It might refer to the threshold to first nucleate inertial cavitation, or the threshold for 'enhanced activity' (Calabrese[1.77] insonated at the former threshold for 10 minutes to ensure observing the cavitation event which indicated that he was at that threshold as exposures become more brief the likelihood increases that cavitation will not be induced until the 'enhanced activity' threshold is exceeded). Indeed the measured threshold will refer to the threshold for the detector system itself, if this lies above that for inertial cavitation or for seeding (whichever is relevant). These ambiguities indicate the need to test the detector systems against defined endpoints for cavitation fields of reproducible properties.

The threshold may be a suitable endpoint for obtaining useful sensitivity information about the detectors, but relies upon the generation of sub-threshold and super-threshold conditions. This facility is, in many practical applications, either not available, or not useful. This is the measure of interest *in situ* is usually the cavitation caused by the field which is already set up; and because for the purpose of calibration or cross-calibration of detectors, it gives effectively only a single data point. What is required is a measure of the 'activity'.

4.2.2 A Suggested approach

Consider a user who has a cavitation field in a power ultrasound application and requires a detector which can measure cavitation *in situ*. The range of available detectors is discussed in section 4.2.4. To relate the signal from the detector to the ability of the cavitation field to produce a given effect, the detector must be calibrated against a standard detector which ideally measures that effect directly. In practice some effects may not be amenable to this type of test (erosion, for example, is invasive with respect to both the sound field and the test liquid - see section 4.2.3).

To work in practice the detectors clearly have to be observing a controllable cavitation field. Such a field might be set up in a spherically or cylindrically symmetric sound field, containing a standard test liquid. The conditions‡ required to produce a given standard signal (e.g. sonochemical yield) at the focus are noted, and that signal is used to provide the unit of calibration for the detector to be deployed *in situ*. The options for the standard system as discussed below.

4.2.3 Choice of test sample

Having chosen the endpoint, the detector must be calibrated against standard cavitating fields. Ideally a range of known 'amounts' of cavitation are required, so that from an appropriate range of measurement in such fields the signal obtained from the detector when used in the unknown field can be interpreted in terms of a 'level of cavitation' through interpolation. This method has the problems associated with the first approach outlined in section 4.1, that of defining a 'level of cavitation'. A simpler alternative is, as discussed in section 4.2.1, to use the second approach, and to provide reproducible cavitation fields in which the extent of some key effect (e.g. sonochemical reaction) is known, and against which the detector signal has been calibrated.

The cavitating sample, against which the detectors are calibrated, must have well-controlled properties. Standardising the liquid and its gas content is relatively simple. Far

‡ See section 4.2.3

more difficult is the question of nucleation. It is tempting to suggest the single stable bubble, undergoing inertial cavitation, as devised by Gaitan et al. [3.19], because the stability and reproducibility of the system exceed those of most other manifestations of inertial cavitation; and also because the nucleation of a single stable bubble is simple. However two factors which argue against its use are: first, that the type of cavitation undertaken by such bubbles might differ markedly from that cavitation encountered during many applications; and second, that the dynamic range of effects generated may not encompass the region of interest required for a calibration to cover many common applications. A better solution will be to generate a cavitation cloud at the focus of a sound field which, in non-cavitating conditions, is well-defined. Spherical [3.31] or cylindrical [3.19] systems driven at specific modes satisfy this criterion. Stability is an important consideration*.

To provide a standard cavitation field, the issue of nucleation is key. Since cavitation changes the nuclei distribution, usually increasing the population of nuclei through exsolution and bubble fragmentation, then standardisation requires a number of procedures. The measurement should only be made once the system has reached steady state†. The nuclei supply should be plentiful, to remove the vagaries which occur if nuclei are so sparse that the chance of a nucleus entering the focus is a significant factor in determining the signal which is detected [3.42]. There are several options for achieving this plentiful supply of nuclei. Gas-filled contrast agents provide a population which is well-characterised initially, but after the first few acoustic cycles those bodies which have nucleated inertial cavitation have disintegrated, and the liquid is contaminated with the stabilising products from their walls: the steady-state cavitation will be nucleated by some population other than the initial contrast agent bodies. Latex spheres represent a more stable seed [3.44]. Gassy seeds could be supplied without the addition of such bodies into the sample through the use of radioactive sources [3.28]. Clearly uncontrolled seeds, as might be provided by solid particles in the liquid [1.56] or hydrophobic material [1.64] should be removed. To maintain distributed nuclei, sample rotation might be necessary in certain geometries of sound field (less so in others). To maximise the nucleation a lower frequency (e.g. tens of kHz) is recommended, where the question of whether a free-floating gas body can nucleate inertial cavitation is less dependent on its initial size (section 1.3.2). There are questions regarding the control of the conditions to produce steady state. It would be difficult to correct for any gas exsolution that will occur without causing greater interference in the test. However temperature control may be necessary to standardise the sonochemical effect. This means that the measure of the 'conditions#' discussed earlier, which will be monitored to ensure repeatability, cannot be thermometric, but must instead refer to the power supplied to the transducer. Finally, the choice of a sonochemical test for the standard detector, and the options available for *in situ* tests, will be discussed in the next section.

* 'Tweaking' of the sound field, by slightly altering the frequency or shifting the relative positions of the transducer and the sample, can for example cause transient increases in sonoluminescence [3.49, 4.8] and subharmonic [4.6] emissions.

† Achieving steady-state not only assists in reproducibility, but has ramifications with respect to the varying time resolutions of detectors.

See section 4.2.2

4.2.4 Choice of detector

There are wide implications regarding the choice of detector. There are a range of issues common to the detection of a variety of phenomenon, such as sensitivity, spatial and temporal resolution, noise, stability, optical/acoustical opacity, expense, availability, the degree of expertise required for sensor deployment and signal interpretation. Some aspects of invasiveness are obvious, such as the effect free radical scavengers might have on a biological system, or the disturbance of the sound field by a lead block in a erosion test. Other effects might be more subtle, such as an indirect influence on the cavitation by causing a change in, for example, surface tension, gas diffusion, and internal circulation. One feature which should be clear from the discussions in Parts 2 and 3 is the question of propriety and versatility e.g. the choice of Active Cavitation Detector (section 3.2.2iii) is good for investigating cavitation thresholds from microsecond pulses, but poor for investigation of cleaning baths.

In addition, in complex cavitation fields many of the signals used for detection can arise from a variety of mechanisms. If the range of bubble-related activities which can generate the signal in question is narrow (as is the case with sonochemical techniques), the detector may fail to characterise the behaviour of a proportion of the bubble population which has considerable implications to their exploitation of the sound field (e.g. sonoluminescence will not allow identification of large bubbles which do not cavitate inertially, but which can scatter the sound field and shield those bubbles which do section 1.3.1). If the range of bubble-related phenomenon which can give rise to a signal is large, then ambiguities will occur (light scatter from a cavitation cloud will occur from both inertial and non-inertial bubbles, and so not reflect the potential for erosion). Phenomenon other than cavitation can generate in some detectors signals which can be misinterpreted as bubble-related (e.g. cosmic rays passing through sonoluminescence detectors; turbulence for combination-frequency detectors; particles perhaps generated through cavitation erosion in light-scatter systems).

As described in Part 3, a wide range of indicators have historically been exploited. Some of these are potentially complicated: bioeffects can arise from both inertial and non-inertial cavitation on, and erosion of sizeable masses both disturbs the sound field and contaminates the liquid with extra nuclei. Nevertheless they have proven very popular. Clearly an important feature to users is how well the feature utilised to characterise a field matches the effect which that field is designed to generate (e.g. bioeffect, cleaning). If the performance of an individual type of equipment is the main objective, and versatility not an issue, then if the sensor system used to 'characterise the cavitation' matches the operational endpoint, then the system will function extremely well without the problematic issue of how the system actually characterises the cavitation *per se* ever arising. General observations on cavitation detectors discussed in Part 3 follow.

Biological indicators: Biological effects generated through exposure to ultrasound can be brought about through a wide range of mechanisms, cavitational (both inertial and non-inertial) and non-cavitational (hyperthermia, radiation forces, microstreaming). As a measure the detector can match the operational endpoint.

Erosion: There are strong arguments for and against the use of erosion as an indicator of cavitation. It will find favour in several industrial applications of power ultrasound because the signal can match the operational endpoint, because the method is uncomplicated and low cost, and because the measured parameter (mass loss) is simple to calculate and can be done so without having to understand the complexities of a cavitation field. Against these significant advantages are weighed the three issues of: invasiveness; the usefulness and reliability of the measurement; and of its versatility. This last feature can be illustrated by fact that, though an erosion measurement indicates the ability of the cavitation to generate erosion (a major advantage to some applications), it indicates less well the nature of the cavitation. As such it might be of less use where some other operational endpoint is important.

Significant damage is produced only by high energy cavitation (inertial, jetting), though cleaning and the removal of surface material can be brought about through microstreaming (sections 3.4 and 3.7). Mass loss measurements (which could be made real-time through incorporation of a mechanical resonance into the sample) will not detect deformation. The effect of microstructure and finish on the erosion is still being researched. Though the disturbance to the sound field varies with the sample (e.g. much greater for lead blocks than for aluminised mylar), if the liquid is to contain a standard nuclei content then erosion is unsuitable since the liquid becomes contaminated as erosion occurs. Unless a protocol can be designed which overcomes these difficulties, erosion could not be used as the primary standard.

Acoustic emission: This system can be deployed using local or remote (minimally invasive) sensors, and with broadband hydrophones can simultaneously monitor a range of signals (broadband emission, subharmonics, the fundamental[†]). It has correlated well in several tests (Table 4.1), particularly with respect to broadband/transient acoustic emissions. Not only is the technique successful in the continuous-wave fields favoured in power ultrasound applications (Section 3.2.1), it is perhaps the only[‡] method of undertaking non-invasive measurements of inertial cavitation *in vivo* resulting from microsecond pulses of ultrasound [3.345].

Electrical and optical effects: Both general[*] types of sensor respond to changes in spatially-averaged properties of the liquid (translucency, conductivity). Both sense bubble presence rather than inertial (or any particular type) of cavitation, but to characterise bubbles in the absence of an intense cavitating sound field they could both be made sensitive to bubble resonances by monitoring the signal modulation as the sample is acoustically excited.

Sonochemistry: In the various applications of cavitating ultrasonic fields illustrated in Table 4.1, the opinion of what constitutes the key factor for measurement will be application specific, depending on the operational endpoint. For cleaning baths it will erosive; for chemical reactors, sonochemical. However for all these applications, if it is not the first choice, a sonochemical measure would likely be the second choice, since it

---

[†] First, during intense cavitation the amplitude of the fundamental as measured by such a sensor cannot simply be taken to be the amplitude of the driving field. Second, though the subharmonic can be generated by non-inertial cavitation and non-cavitational processes, an increase in amplitude does correlate well with the onset of inertial cavitation (see Table 4.1), so that the magnitude of the signal at this frequency should relate to a certain extent to the level of inertial cavitation 'activity'.

[‡] Though images relating to bubble activity have been detected during diagnostic ultrasound scanning during lithotripsy, this detection is more likely to give strong signals for stable bubbles (e.g. post-cavitation fragments).

[*] Clearly if used with isolated bubbles (e.g. Mie scattering [2.115-6, 2.120-4]) there are exceptions.

can readily be quantified and designed to occur as a result of inertial cavitation[#]. In all such tests a knowledge of the absolute number of free radicals generated is a valuable measure.

Sonoluminescence and chemiluminescence: Light emission is probably the most powerful technique for the characterisation of cavitation fields. It can instantaneously provide fine spatial resolution with sufficient pixels and temporal resolution to form a video image. No other technique can do this. Sub-nanosecond temporal resolution can be readily obtained, though without significant spatial resolution. There are two main problems. First, although the luminescence can be quantified, its generation mechanism is still not proven and it is therefore less easy to interpret a photon count in terms of a given operational endpoint (cleaning, bioeffect, chemical yield) than is a sonochemical test. The second problem arises through the need for blackout conditions, making the technique difficult to use on industrial sites. Regardless of this fact, its use would be extremely valuable in complex, cavitating, fields since it is by far the most time-efficient, minimally invasive test for the identification of the regions of strongest cavitation: Such identification should be the first phase in attempts to characterise the cavitation in any situation other than far-field travelling wave conditions.

4.3 Conclusions

The proposed primary standard might consist of a spherically-symmetric sound field which is capable of producing a reproducible range (from sub-threshold to intense) of cavitation conditions, as determined by a 'primary technique', for which there are four candidates: sonoluminesence, sonochemistry, chemiluminescence, and acoustic emission. Of the first three, sonoluminescence is the only non-invasive, real-time technique. The others require the addition of chemical agents to the test liquid. Latex spheres might also have to be added to seed cavitation if the frequency is sufficiently high to cause problems with nucleation, though this could also be achieved less invasively (for example through the use of neutron sources[†]). The entire contents of the sphere could be doped with chemicals, and its contents sampled to give a spatially averaged effect. It would be better to isolate a test sample in some acoustically-transparent test chamber at the focus of the sphere, if the degree of invasiveness could be minimised satisfactorily.

Against the primary measure (photon count, chemical yield) a secondary technique could be calibrated. There are a range of these, and those which are simple to apply on site (such as acoustic emission), or which reflect the ability of the system to deliver its operational endpoint (chemical), are preferable. Erosion possesses certain characteristics desirable in a secondary measure, but for good quality measurements, and certainly for cross-calibration with the standard, it would need to deployed with an appropriate designed protocol, as massive test bodies would disturb the sound field in the sphere during calibration, and even thin films would soil the test liquid.

The site at which the secondary measure interrogates the ultrasound field in the workplace should be chosen with care, as thought must be given to the spatial variability of the cavitational activity. This can be examined using a technique which can afford

[#] Sonochemistry from non-inertial cavitation [3.134] or macromolecule shear [3.107] can occur, but with control sonochemistry can be specific to inertial cavitation far more readily than optical or electrical tests.
[†] ensuring this does not interfere with the photon detectors

sufficient spatial resolution. Of these sonoluminescence or chemiluminescence are best, though blackout must be achieved.

As a first step to achieving the establishment of a standard system, it is recommended that a trial spherical (or cylindrical) test vessel be set up. It should be equipped with a removable, acoustically-transparent sample chamber which can be centred on the acoustic pressure maximum, and into which samples for sonochemical or biological tests can be placed. The vessel should be equipped with photon detectors and broadband acoustic sensors, both of which can be remote and non-invasive. The signal processing from the acoustic sensor should be sufficient to simultaneously quantify the broadband and spectral components. A fluid management system needs to be set in place. Using this system, trials should be undertaken to test how well, to first order, sonoluminescence and sonochemical quantities correlate, as a function of the (continuous-wave) 'power' to the system, and what degree of repeatability can be achieved. In the second stage, variation of the acoustic frequency, and comparison with hemolysis measurements, may be undertaken. The objective will be to design a reproducible cavitation field for calibration purposes, and to determine whether the primary test should be acoustic, chemical, luminescent, or a combination of these.

References

4.1. de Santis P, Sette D and Wanderlingh F. Cavitation detection: The use of subharmonics. J. Acoust. Soc. Am. 1967; **42**: 514516

4.2. Saksena TK and Nyborg WL. Sonoluminescence from stable cavitation. J. Chem. Phys. 1970; **53**: 17221734

4.3. Coakley WT and Sanders MF. Sonochemical yields of cavitation centres at 1 Mhz. J Sound and Vib. 1973; **28**: 7385

4.4. Eastwood LM and Watmough DJ. Sonoluminescence, in water and in human blood plasma, generated using ultrasonic therapy equipment.Ultrasound Med. Biol., 1976; **2**: 319323

4.5. Hedges HJ, Leeman S and Vaughan P. Acoustic cavitation. Proc. Underwater Acoustics Group, Inst. of Acoustics, 1977, No. 5, p. 19

4.6. Graham E, Hedges HJ, Leeman S and Vaughan P. Cavitational bioeffects at 1.5 MHz. Ultrasonics 1980; **18**: 224228

4.7. Morton KI, ter Haar GR, Stratford IJ and Hill CR. The role of cavitation in the interaction of ultrasound with V79 Chinese hamster cells *in vitro*. Br. J. Cancer 1983; **9**: 629633

4.8. Leighton T G, Pickworth M J W, Walton AJ and Dendy P P. Studies of the cavitational effects of clinical ultrasound by sonoluminescence: 1. Correlation of sonoluminescence with the standing wave pattern in an acoustic field produced by a therapeutic unit. Phys. Med. Biol. 1988, **33**, 1239-1248.

4.9. Miller DL and Thomas RM. Frequency dependence of cavitation activity in a rotating tube exposure system compared to the mechanical index. J. Acoust. Soc. Am. 1993; **93**: 3475-3480

4.10. Miller DL, Thomas RM and Buschbom RL. Comet assay reveals DNA strand breaks induced by Ultrasound cavitation *in vitro*. Ultrasound Med. Biol., 1995; **21**: 841-848

4.11. Fuciarelli AF, Sisk EC, Thomas RM and Miller DL. Induction of bae damage in DNA solutions by ultrasonic cavitation. Free Radical Biology and Medicine 1995; **18**: 231-238